A population approach to systems of Izhikevich neurons: can neuron interaction cause bursting?

by

Rongzheng Xie
B.Sc., Swansea University, 2014

A Thesis Submitted in Partial Fulfillment of the
Requirements for the Degree of

MASTER OF SCIENCE

in the Department of Mathematics and Statistics

A population approach to systems of Izhikevich neurons: can neuron interaction cause bursting?

by

Rongzheng Xie
B.Sc., Swansea University, 2014

Supervisory Committee

Dr. Rod Edwards, Co-supervisor
(Department of Mathematics and Statistics)

Dr. Slim Ibrahim, Co-supervisor
(Department of Mathematics and Statistics)

Supervisory Committee

Dr. Rod Edwards, Co-supervisor
(Department of Mathematics and Statistics)

Dr. Slim Ibrahim, Co-supervisor
(Department of Mathematics and Statistics)

ABSTRACT

In 2007, Modolo and colleagues derived a population density equation for a population of Izhekevich neurons. This population density equation can describe oscillations in the brain that occur in Parkinson's disease. Numerical simulations of the population density equation showed bursting behaviour even though the individual neurons had parameters that put them in the tonic firing regime. The bursting comes from neuron interactions but the mechanism producing this behaviour was not clear. In this thesis we study numerical behaviour of the population density equation and then use a combination of analysis and numerical simulation to analyze the basic qualitative behaviour of the population model by means of a simplifying assumption: that the initial density is a Dirac function and all neurons are identical, including the number of inputs they receive, so they remain as a point mass over time. This leads to a new ODE model for the population. For the new ODE system, we define a Poincaré map and then to describe and analyze it under conditions on model parameters that are met by the typical values adopted by Modolo and colleagues. We show that there is a unique fixed point for this map and that under changes in a bifurcation parameter, the system transitions from fast tonic firing, through an interval where bursting occurs, the number of spikes decreasing as the bifurcation parameter increases, and finally to slow tonic firing.

Table of Contents

List of Tables

List of Figures

Acknowledgements

I would like to thank:

my family, for all their love and encouragement,

Dr. Rod Edwards and Dr. Slim Ibrahim, for mentoring, support, encouragement, and patience, and

The University of Victoria, for academic and financial support.

Chapter 1

Introduction

Parkinson's disease (PD) is a common neurological degenerative disease. Tremor in hands, arms, legs, jaw, or head is one of the main symptoms of Parkinson's disease. Most people with Parkinson's disease are treated with medication, ablation or deep brain stimulation (DBS). Compared to ablation, DBS is less invasive, reversible, and has adjustable features and is now utilized for an increasing number of brain disorders[20]. However, the physiological mechanisms of electrical stimulation are still unclear. In order to understand the effects of treatments, it is first necessary to understand the origin of Parkinsonian tremor oscillations in the brain. In this thesis, the focus is on understanding how bursting behaviour arises in a model for Parkinsonian tremor oscillations proposed by Modolo, et al.

In order to study the mechanisms of interacting populations of neurons with or without electrical stimulation, a mathematical model is a reasonable method to investigate dynamics of a large populations of neurons. However, direct simulations of hundreds of thousands of neurons based on a single neuron model such as the Izhikevich model take a huge amount of computing time. Fortunately, the population density approach (PDA) was introduced by Knight, Manin and Sirovich in 1996[5] and modified by Omurtag, Knight and Sirovich in 2000[2] and by Nykamp and Tranchina in

2000[6]. The PDA describes a neural population with only one equation: a conservation law. Omurtag, Knight and Sirovich[2] and Nykamp and Tranchina[6] derived a population density equation for the leaky integrate-and-fire (LIF) model and Huertas and Smith[14] and Casti[4] have similar derivations for the integrate-and-fire-or-burst (IFB) model. However, these models can only reproduce tonic spiking (LIF) or tonic spiking and bursting (IFB).

In 2007, Modolo, Garenne, Henry and Beuter[10] derived a population density equation for the Izhikevich model, which is a two-dimensional hybrid model that combines continuous dynamics with an instantaneous reset, reviewed in[8]. The comparison between the simulations for the population density equation and direct simulations suggests that this simple and phenomenological model can help explore mechanisms of Parkinsonian tremor oscillations and network modulation associated with chronic electrical stimulation of the brain. Also in 2007, Modolo, Mosekilde and Beuter[15] explained that the main advantage of this approach is that it provides a global description of a large number of neurons (virtually an infinite number) with only a single equation (a conservation law) and therefore requires a significantly shorter computing time than the usual discrete simulations. In 2008, Modolo, Henry and Beuter[11] have similar research goals (comparison between simulations of the population density equation and direct simulation using the subthalamo-pallidal dynamical model of Gillies and Willshaw[1]). It is of course necessary to discretize the PDE in order to carry out simulations, but the resulting set of ODEs can be much smaller than what is required for realistic direct stimulation. A comparison of the two models indicated that the population-based model was more biologically realistic and more appropriate for exploring DBS mechanisms.

Although Modolo, Garenne, Henry and Beuter have compared direct simulations and simulations for the population density equation with a Dirac distribution as an ini-

tial condition, the pattern of the evolution of the population density equation is still unclear from the density picture in[10]. The density picture from[10] shows that the population of neurons at a later time is spatially distributed. Actually, if the neurons are identical and identically connected and concentrated in a true Delta function they should leave and arrive together from one grid cell to another grid cell. The non-zero size of the grid cells used in the numerical method causes numerical diffusion. Without numerical approximation, however, and assuming identical neurons with identical numbers of afferents (inputs), we can analytically treat the population of neurons as a single neuron. This leads to a new ODE system to discribe the population dynamics. Furthermore, we can define a Poincaré map, call it Φ, for the new ODE system reduced from the population density equation. Touboul and Brette[12] studied the adaptation map (Poincaré map Φ) for subthreshold neural dynamics in 2008. Touboul and Brette[13] suggest that this map is a generalization of Poincaré maps that are used in continuous dynamical systems to understand cycle properties. Depending on the initial condition, the system can either fire infinitely many spikes (tonic spiking) or finitely many spikes (phasic spiking) and it can also have chaotic dynamics under certain circumstances. Foxall, Edwards, Ibrahim and van den Driessche[7] used a similar idea to study the global asymptotic stability of a fixed point for the Φ map of the single-neuron Izhikevich model in 2012. Sufficient conditions are given on the parameters of the model for Φ to be nonexpansive (for regular spiking to be globally asymptotically stable). Rubin, Signerska-Rynkowska, Touboul and Vidal[17][18] published a pair of papers in 2017 using the same Poincaré map in a class of nonlinear dynamical systems with resets modeling the voltage and adaptation of neurons. In the first paper, Rubin and colleagues use the fact that bursting patterns correspond to periodic orbits of the adaptation map that governs the sequence of values of the adaptation variable at the resets. Rubin and colleagues not only investigate the be-

havior of the system at the bifurcations between bursts of different periods but also analyze the emergence of different forms of chaos and establish the presence of period doubling events. In the second paper, a form of mixed-mode oscillations (MMOs) for a class of bidimensional nonlinear hybrid dynamical systems was studied by Rubin and colleagues. A particular structure of the Φ map ensures that any type of transient MMO can be generated by these neuron models and discontinuous rotation theory was used to develop a precise description of the dynamics in the case where the adaptation map admits one discontinuity in its invariant interval.

Our new ODE system is not exactly the Izhikevich model but is similar to the Izhikevich model because it is reduced from the population density equation for the Izhikevich model with a Dirac distribution as an initial condition in the phase space. Therefore, we can also apply the Poincaré map Φ to our new ODE system.

The thesis is organized as follows. We start in chapter 2 by describing the Izhikevich model, summarizing the population density approach (i.e., the conservation law) and deriving the population density equation for the Izhikevich model by the conservation law.

In chapter 3, we apply the finite volume method (Godunov's method in $\mathbb{R}^2$) to the population density equation for the Izhikevich Model. In particular, we focus on simulations showing the evolution of the population density equation for the Izhikevich model with a Dirac distribution as an initial condition in the phase space. These show that the time evolution of the population density equation for the Izhikevich model has a bursting pattern.

In chapter 4, we show that, at least when the population density is a Dirac distribution, interaction within the population can induce bursting behaviour. Without numerical approximation, we consider analytically the population of neurons with a Dirac distribution as a single neuron so that we can use a new ODE system to

describe the population dynamics. This ODE behavior is different from the single-neuron Izhikevich model because the single cell that represents the whole population receives an impulse following a spike and reset after a small delay time (1ms). The impulse causes a "jump" in membrane potential, v[10]. Since the impulse size is fixed and the v-nullcline becomes arbitrarily wide as the adaptation variable, u, increases, the single neuron (i.e. Dirac distribution of the population of neurons) cannot cross the right branch of the v-nullcline by neuron interaction for large u. This leads to the question: can neuron interaction cause bursting behavior? In order to answer this question, we first define a Poincaré map, Φ, on the reset line, that describes the Izhikevich model with impulse ϵG in the v direction following a spike after a delay time τ=1ms, where $G > 0$ is the mean number of synaptic afferents per neuron and $\epsilon > 0$ is the distance of the "jump" for a single spike. By investigating the behaviour in different parameter ranges of the Φ map we show that it has a unique fixed point u_{fp} and the stability of the fixed point depends on which range u_{fp} is in. Φ has a tonic firing behavior if the fixed point is stable ($-1 < \Phi'(u_{fp}) < 1$) and Φ has a bursting behavior if the fixed point is unstable ($\Phi'(u_{fp}) < -1$). A combination of analysis and numerical simulation shows that the unique fixed point u_{fp} changes from stable (a fast tonic firing with an infinite number of spikes per burst, i.e., no recovery phase) to unstable (a bursting with k spikes per burst, where $1 < k < \infty$) and then returns to stable (a slow tonic firing with one spike per "burst") again as u_{fp} increases. A flip bifurcation occurs when $\Phi'(u_{fp}) = -1$. This signals a period doubling of Φ, and possibly a period-doubling cascade, but all in a minute interval of the parameter d before bursting emerges. The number of spikes per burst increases as d decreases, where d is a nonphysical parameter in the Izhikevich model.

In chapter 5, we summarize all results and give possible options for further work.

Chapter 2

Derivation of the Population Density Model for Izhekevich neurons

In this chapter, we will introduce the Izhikevich model [8], the population density approach [2] and the derivation of population density equation for the Izhikevich model [10].

2.1 The Izhikevich model for a single neuron

The Izhikevich model [8] is:

$$\begin{cases} \dfrac{dv}{dt} = 0.04v^2 + 5v + 140 - u + I(t) \\ \dfrac{du}{dt} = a(bv - u) \end{cases} \tag{2.1}$$

$$v(t^-) = s \rightarrow v(t^+) = c, \quad u(t^+) = u(t^-) + d, \tag{2.2}$$

where v is the membrane potential and u is the recovery variable that describes the effects of all ionic channel dynamics, both expressed in $[mV]$. $\{a, b, c, d\}$ are non-physical parameters, $I(t)$ is the applied current expressed in $[pA]$ and $s = 30\ mV$ corresponding to the spike apex. A small a reflects the fact that the recovery variable

operates on a slower time scale than the membrane potential. c is the reset value of the membrane potential after a spike. b is the slope of the u-nullcline ($u = bv$). This sort of hybrid 2-dimensional model is a reduction of a smooth higher-dimensional model that retains a wide variety of behaviours with appropriate parameter choices. This single neuron model allows various neuron behaviours (see Figure 2.1).

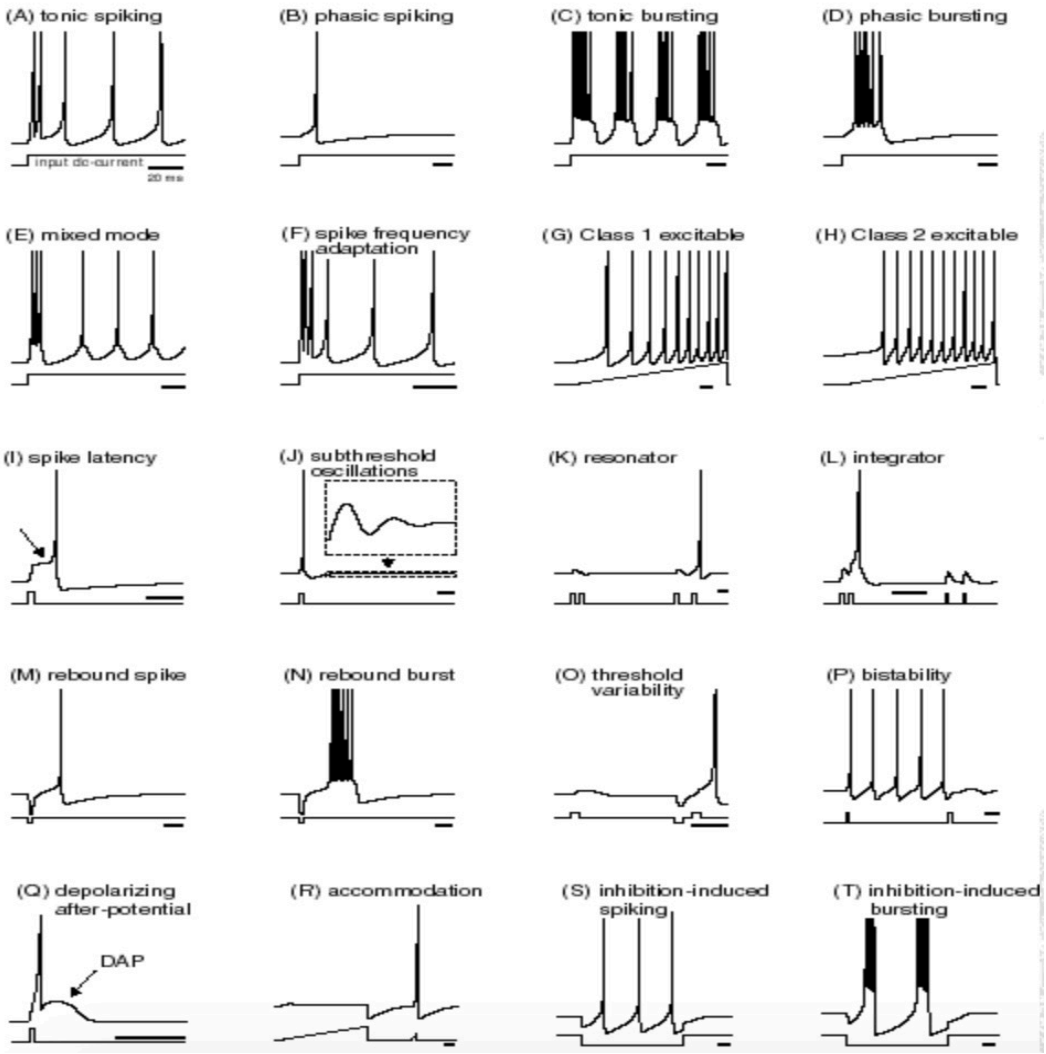

Figure 2.1: Different spiking patterns and parameters of the Izhikevich model. For more details, see[9].

2.2 The population density approach

Now we study the population density approach for a single neuron model from Omurtag and his colleagues [2]. The derivation below is taken entirely from that paper.

In the general case we regard the state of a neuron $\mathbf{v}$ to be governed by the dynamical system:

$$\frac{d\mathbf{v}}{dt} = \mathbf{F}(\mathbf{v}) + \mathbf{S}(\mathbf{v}, g(t)). \tag{2.3}$$

For example, the direction field $\mathbf{F}$ could be that of the H-H-like system[3]. $\mathbf{S}$(v,g(t)) refers to the incoming synaptic currents to the neuron and as indicated generally depends on $\mathbf{v}$ as well as conductance $g(t)$.

We are looking for the evolution of a probability density $\rho = \rho(\mathbf{v}, t)$ in the phase space determined by $\mathbf{v} \in \mathbb{R}^d$, where d means dimension here. We define $\rho(\mathbf{v}, t)$ as the probability density that a neuron of the population is in a state $\mathbf{v}$ at a time t. To determine ρ, we imagine a large number of replicas of the population, say N. If $\Delta\mathbf{v}$ is a small volume in the phase space, so that $n_k(\mathbf{v}, t)\Delta\mathbf{v}$ is the number of neurons in $\Delta\mathbf{v}$ at time t of the kth replica, then the number density at $\mathbf{v}$ is defined as:

$$n(\mathbf{v}, t) = \langle n_k \rangle = \lim_{N\to\infty} \frac{1}{N} \sum_{k=1}^{N} n_k(\mathbf{v}, t) \tag{2.4}$$

and probability density as:

$$\rho(\mathbf{v}, t) = \frac{n(\mathbf{v}, t)}{\int n(\mathbf{v}, t) d\mathbf{v}} = \frac{n(\mathbf{v}, t)}{P}, \tag{2.5}$$

where P is the fixed number of neurons in each replicate population. Next, we want

to calculate the average firing rate $r(t)$ per neuron, where $\{t_{i_k}^m\}$ are the firing times of the m^{th} neuron. Using angle brackets for an average over population replicates, the firing rate is defined by:

$$\begin{aligned} r(t) &= \frac{1}{P} \lim_{\Delta t \to 0} \left\langle \frac{1}{\Delta t} \int_t^{t+\Delta t} \sum_{m=1}^{P} \sum_{i_k} \delta(t - t_{i_k}^m) dt \right\rangle \\ &= \frac{1}{P} \lim_{\Delta t \to 0} \left(\lim_{N \to \infty} \frac{1}{N} \sum_k \frac{1}{\Delta t} \int_t^{t+\Delta t} \sum_{m=1}^{P} \sum_{i_k} \delta(t - t_{i_k}^m) dt \right). \end{aligned} \tag{2.6}$$

External sources (indexed by $m = 0$) are given by:

$$\sigma^0(t) = \lim_{\Delta t \to 0} \left\langle \frac{1}{\Delta t} \int_t^{t+\Delta t} \sum_{i_k} \delta(t - t_{i_k}^0) dt \right\rangle. \tag{2.7}$$

Thus, the average impulse (input) rate per neuron is:

$$\sigma(t) = \sigma^0(t) + Gr(t), \tag{2.8}$$

where G is the average number of afferents to a neuron. Now, let D be a small enough fixed volume in $\mathbf{v}$ space, and consider the time rate of change of the number of elements in D. This is:

$$\frac{\partial}{\partial t} \int_D \rho d\mathbf{v} = - \int_{\partial D} \mathbf{F}(\mathbf{v}) \cdot n\rho ds - \int_D \left(\frac{\delta \rho}{\delta t} \right)_{imp}^{-} d\mathbf{v} + \int_D \left(\frac{\delta \rho}{\delta t} \right)_{imp}^{+} d\mathbf{v}. \tag{2.9}$$

The first term on the right $-\int_{\partial D} \mathbf{F}(\mathbf{v}) \cdot n\rho ds$ is the flux across the boundary of D (i.e., the rate of loss of probability within D), n is the outward normal to the surface ∂D for which ds is a surface element. Next assume D small enough so that any neuron within D leaves D on receiving an impulse, then the loss rate is given by:

$$\left(\frac{\delta \rho}{\delta t} \right)_{imp}^{-} = \sigma(t) \rho(\mathbf{v}, t). \tag{2.10}$$

If V is the potential in D, and after an impulse it becomes V', then we write (see figure 2.2):

$$(V, v_2, v_3, v_4 \ldots) = \mathbf{v} \to \mathbf{v}' = (V', v_2, v_3, v_4 \ldots), \tag{2.11}$$

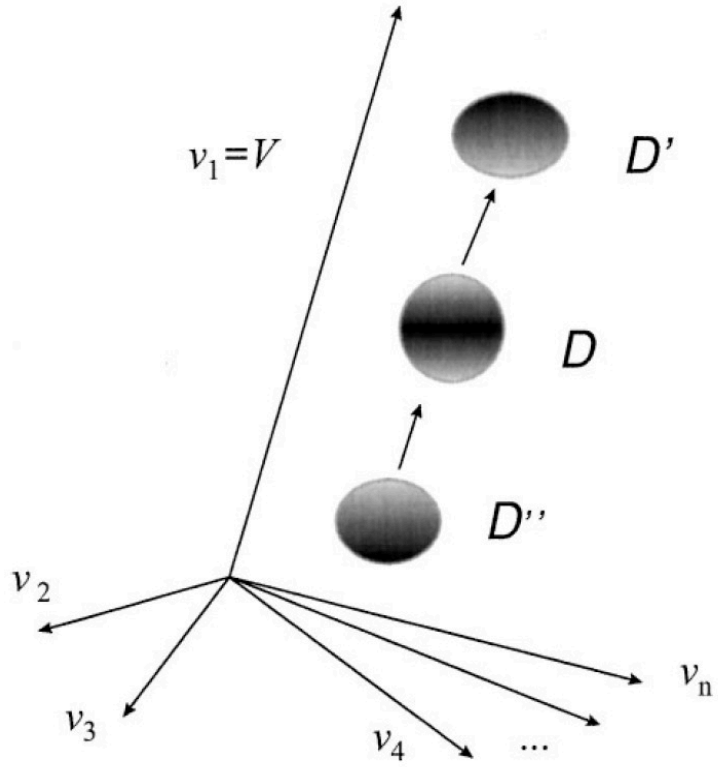

Figure 2.2: Phase space defined by the state vector $\mathbf{v} = (v_1 \ldots v_n)$ of an individual neuron. D'', D, and D' show displacement of volumes under an impulse.

where $V' = V + h$ for every $V' \in D'$, $V'' = V - h$ for every $V'' \in D''$ and the jump size h is fixed in this case. We know that loss rate in D'' equals gain rate in D. Thus,

the last term on the right is:

$$\begin{aligned}\int_D \left(\frac{\delta\rho}{\delta t}\right)^+_{imp} d\mathbf{v} &= \sigma(t)\int_{D''}\rho(\mathbf{v}'')d\mathbf{v}'' \\ &= \sigma(t)\int_D \rho(\mathbf{v}''(\mathbf{v}))\cdot\tilde{J}d\mathbf{v} \\ &= \sigma(t)\int_D \rho(\mathbf{v}''(\mathbf{v}))\frac{\partial\mathbf{v}''}{\partial\mathbf{v}}d\mathbf{v},\end{aligned} \tag{2.12}$$

where to obtain the last expression we have transformed from D'' to D and thus we have the Jacobian of the transformation $\tilde{J} = \frac{\partial\mathbf{v}''}{\partial\mathbf{v}}$. Then $\left(\frac{\delta\rho}{\delta t}\right)^+_{imp} = \sigma(t)\rho(\mathbf{v}''(\mathbf{v}),t)\frac{\partial\mathbf{v}''}{\partial\mathbf{v}}$. Therefore, applying the divergence theorem we find:

$$\frac{\partial\rho}{\partial t} = -\frac{\partial}{\partial\mathbf{v}}\cdot(\mathbf{F}(\mathbf{v})\rho) - \sigma(t)\left(\rho(\mathbf{v},t) - \rho(\mathbf{v}''(\mathbf{v}),t)\frac{\partial\mathbf{v}''}{\partial\mathbf{v}}\right), \tag{2.13}$$

where $\frac{\partial\mathbf{v}''}{\partial\mathbf{v}} = 1$ because $V'' = V - h$ here, i.e.,

$$\frac{\partial\rho}{\partial t} = -\frac{\partial}{\partial\mathbf{v}}\cdot(\mathbf{F}(\mathbf{v})\rho) - \sigma(t)(\rho(\mathbf{v},t) - \rho(\mathbf{v}''(\mathbf{v}),t)), \tag{2.14}$$

where $\mathbf{v}''(\mathbf{v}) = (V'' - h, v_2, v_3, ...)$. Finally, we define J to be the flux and

$$\begin{aligned}J &= J_{str} + J_{imp}, \\ J_{str} &= \rho\mathbf{F}(\mathbf{v}), \\ J_{imp} &= -\sigma(t)\int_V^{V''(V)} e_v\rho(W, v_2..)dW,\end{aligned} \tag{2.15}$$

where e_v is the unit vector in the V-direction. Thus, equation (2.14) can be written as:

$$\frac{\partial\rho}{\partial t} = -\frac{\partial}{\partial\mathbf{v}}\cdot J \tag{2.16}$$

which is a conservation law. The flux J has the form of a linear operator acting on the density, $J = C(\sigma)\rho$, where the linear operator $C(\sigma)$ depends on the incoming firing

rate. Note: the firing of a single neuron can be based on the action potential reaching its maximum, so the firing rate, r, per neuron of the population can be determined by the flux of neurons of the population passing a threshold. It therefore is a functional of $J, r(t) = R[J]$. If we integrate the continuity equation $\frac{\partial \rho}{\partial t} = -\frac{\partial}{\partial \mathbf{v}} \cdot J$, we have:

$$\frac{\partial}{\partial t} \int \rho(\mathbf{v}) d\mathbf{v}' = -\int_{\partial D} n \cdot J dS, \tag{2.17}$$

where we require that the total probability be conserved so that $\int_{\partial D} n \cdot J dS = 0$.

2.3 The derivation of the population density equation for the Izhikevich model

Now we apply the population density approach to the Izhikevich model [10].

Population equation: Let $w = (v, u)$ be a vector in $\mathbb{R}^2$, where v is the membrane potential and u is the recovery variable. Let $P(w,t) = \lim_{|A|\to 0} \frac{n(w,t,A)}{\int\int dw}$, expressed in terms of $[neurons] \times [mV]^{-2}$, be the population density, where $A = \Delta v \cdot \Delta u$ in the phase space and $n(w,t,A)$ is the number of neurons in A at time t. Let

$$N = \int\int_{\Omega} P(w,t) dw, \tag{2.18}$$

where $P(w,t)dw$ is density $\times$ area = number of neurons in an area element, and N is the total number of neurons. The phase space $\Omega = ([v_{min}, c) \cup (c, v_{max}]) \times (u_{min}, u_{max})$. By the results of section 2.2, we know that the conservation law is:

$$\frac{\partial}{\partial t} P(w,t) = -\nabla \cdot J(w,t), \tag{2.19}$$

$$J(w,t) = J_s(w,t) + J_i(w,t), \tag{2.20}$$

$$J_s(w,t) = F(w)P(w,t), \tag{2.21}$$

$$F(w) = \begin{bmatrix} 0.04v^2 + 5v + 140 - u + I(t) \\ a(bv - u) \end{bmatrix}, \tag{2.22}$$

$$J_i(w,t) = e_v \sigma(t) \int_{v-\epsilon}^{v} P(\tilde{v}, u, t) d\tilde{v}, \tag{2.23}$$

where $J(w,t)$ is the neural flux expressed in $[neurons] \times [mV]^{-1} \times [ms]^{-1}$, e_v is a unit vector in the direction v in the phase space, $\sigma(t)$ expressed in terms of $[spikes] \times [ms]^{-1}$ is the average individual spike reception rate of a single neuron in the population and as in section 2.2 we hypothesize that a synaptic input causes a "jump" of amplitude ϵ of the membrane potential v. The boundary condition here is $J(c^+, u+d, t) = J(c^-, u+d, t) + |J(s,u,t)|\text{sgn}(J(c^-, u+d, t))$ and $\tilde{v} \in [v-\epsilon, v]$. Thus

$$J(w,t) = F(w)P(w,t) + e_v \sigma(t) \int_{v-\epsilon}^{v} P(\tilde{v}, u, t) d\tilde{v}. \tag{2.24}$$

As in section 2.2, the average individual spike reception rate $\sigma(t) = G \times \tilde{r}(t)$, where G is the mean number of synaptic afferents per neuron and $\tilde{r}(t)$ is the average individual firing rate such that $\tilde{r}(t) \approx \frac{r(t)}{N}$, where $r(t)$ is the total firing rate of the population. However, Omurtag and his colleagues do not take into account spike conduction delays from one neuron to another in the network. Since every connection has different length l_0 and causes different conduction delay time τ, we should use a spike conduction delay kernel $\alpha(t)$ leading to an improved expression of the individual spike reception rate:

$$\sigma(t) = \frac{G}{N} \int_{\tau_-}^{\tau_+} r(t-\tau)\alpha(\tau) d\tau, \tag{2.25}$$

where $\tau_{+/-}$ are the extremum values of spike conduction delays with $\tau_{+/-} > 0$. Then

the interaction flux becomes:

$$J_i(w,t) = \frac{G}{N}\left(\int_{\tau_-}^{\tau_+} r(t-\tau)\alpha(\tau)d\tau\right) \times e_v \left(\int_{v-\epsilon}^{v} P(\tilde{v},u,t)d\tilde{v}\right). \tag{2.26}$$

The total firing rate $r(t)$ at each time t is computed as: $r(t) = \int_{u_{min}}^{u_{max}} J_v(s,u,t)du$. To sum up, the evolution of a population of Izhikevich neurons is:

$$\begin{cases} \dfrac{\partial}{\partial t}P(w,t) = -\nabla \cdot J(w,t), \\ J(w,t) = J_s(w,t) + J_i(w,t), \\ J_s(w,t) = F(w)P(w,t), \\ J_i(w,t) = e_v\sigma(t)\displaystyle\int_{v-\epsilon}^{v} P(\tilde{v},u,t)d\tilde{v}, \\ \sigma(t) = \dfrac{G}{N}\left(\displaystyle\int_{\tau_-}^{\tau_+} r(t-\tau)\alpha(\tau)d\tau\right), \\ J(c^+,u+d,t) = J(c^-,u+d,t) + |J(s,u,t)|\mathrm{sgn}(J(c^-,u+d,t)). \end{cases} \tag{2.27}$$

Therefore,

$$\frac{\partial}{\partial t}P(w,t) = -\nabla \cdot \left(F(w)P(w,t) + e_v\sigma(t)\int_{v-\epsilon}^{v} P(\tilde{v},u,t)d\tilde{v}\right). \tag{2.28}$$

Clearly, this is an integro-differential equation, which is hard to solve theoretically. We will solve it numerically in the next chapter.

Chapter 3

Numerical Simulation of the Population Density Equation for the Izhikevich Model

3.1 First-order numerical method

3.1.1 Finite-volume method

We use the finite-volume method [16] to solve the integro-differential equation because it is a conservation equation. The finite-volume method is widely used because many physical laws are conservation laws and the method respects the conservation. Here, the total density (i.e., number of neurons) remains constant. Change in density in a given cell is given by flux entering the cell minus flux leaving the cell. No neurons are created or destroyed. They only move between cells. Following this idea, we end up with a formulation that consists of flux conservation equations defined in an averaged sense over the cells. Historically, this method has been very successful in solving, for example, electromagnetism and fluid flow problems.

The specific finite volume method we use is Godunov's method (as suggested by Modolo and his colleagues). First we explain this method in the scalar case, then in $\mathbb{R}^2$.

(i) Godunov's method in $\mathbb{R}$

We are looking for the numerical solution of the scalar conservation law in $\mathbb{R}$:

$$u_t + f(u)_x = 0, \tag{3.1}$$

where $u(x,t) \in \mathbb{R}$ and $f(u) : \mathbb{R} \to \mathbb{R}$. By applying the chain rule we have:

$$u_t + f'(u)u_x = 0, \tag{3.2}$$

where $f'(u)$ is a scalar. Next, we use the numerical solution U^n to define a piecewise constant function $\tilde{u}^n(x,t_n)$ with the value U_j^n on the grid cell $x_{j-\frac{1}{2}} < x < x_{j+\frac{1}{2}}$. We use $\tilde{u}^n(x,t_n)$ as initial data for the conservation law, which we now solve exactly to obtain $\tilde{u}^n(x,t)$ for $t_n \leq t \leq t_{n+1}$. The equation can be solved exactly over a short time interval because the initial data $\tilde{u}^n(x,t_n)$ is piecewise constant, and hence defines a sequence of Riemann problems. After obtaining this solution over the interval $t_n \leq t \leq t_{n+1}$, we define the approximate solution U^{n+1} at time t_{n+1} by averaging this exact solution at time t_{n+1}:

$$U_j^{n+1} = \frac{1}{h}\int_{x_{j-\frac{1}{2}}}^{x_{j+\frac{1}{2}}} \tilde{u}^n(x,t_{n+1})dx. \tag{3.3}$$

Now, Godunov's scheme in $\mathbb{R}$ is:

$$U_j^{n+1} = U_j^n - \frac{k}{h}[F(U_j^n, U_{j+1}^n) - F(U_{j-1}^n, U_j^n)], \tag{3.4}$$

where k is the time step, h is the space step in x and the numerical flux function F

is given by:

$$F(U_j^n, U_{j+1}^n) = \frac{1}{k}\int_{t_n}^{t_{n+1}} f(\tilde{u}^n(x_{j+\frac{1}{2}}, t))dt. \tag{3.5}$$

Since the constant value of $\tilde{u}^n$ along the line $x = x_{j+\frac{1}{2}}$ depends only on the data U_j^n and U_{j+1}^n for the Riemann problem, if we define this value by $u^*(U_j^n, U_{j+1}^n)$, then the flux (3.5) reduces to:

$$F(U_j^n, U_{j+1}^n) = f(u^*(U_j^n, U_{j+1}^n)). \tag{3.6}$$

Thus, Godunov's method in $\mathbb{R}$ becomes:

$$U_j^{n+1} = U_j^n - \frac{k}{h}[f(u^*(U_j^n, U_{j+1}^n) - f(u^*(U_{j-1}^n, U_j^n))]. \tag{3.7}$$

For a physical solution, we use the entropy-satisfying weak solution in implementing Godunov's method. If $f(u)$ is convex, there are four cases that must be considered, which are:

1. $f'(u_l), f'(u_r) \geq 0 \rightarrow u^* = u_l$,
2. $f'(u_l), f'(u_r) \leq 0 \rightarrow u^* = u_r$,
3. $f'(u_l) \geq 0 \geq f'(u_r) \rightarrow u^* = u_l$ if $[f]/[u] > 0$ or $u^* = u_r$ if $[f]/[u] < 0$,
4. $f'(u_l) < 0 < f'(u_r) \rightarrow u^* = u_s$(transonic rarefaction),

where u_l and u_r are initial data of the Riemann problem, the intermediate value u_s with the property $f'(u_s) = 0$ is the value of u for which the characteristic speed is zero, and is called the sonic point. Since there are no case 3 and case 4 in our PDE equation, we consider case 1 and case 2 only. We also have a more general form:

$$F(u_l, u_r) = \begin{cases} \min_{u_l \leq u \leq u_r} f(u) & \text{if} \quad u_l \leq u_r \\ \max_{u_r \leq u \leq u_l} f(u) & \text{if} \quad u_l > u_r \end{cases} \tag{3.8}$$

Finally, the CFL (Courant-Friedrichs-Lewy) condition in $\mathbb{R}$ is : $|\frac{k}{h}\lambda_p(U_j^n)| \leq 1$, for all

eigenvalues λ_p of the scalar $f'(u)$ in the scalar conservation law:

$$u_t + f'(u)u_x = 0. \tag{3.9}$$

We will state how the CFL condition applies to the numerical scheme in $\mathbb{R}^2$.

(ii) Godunov's method in $\mathbb{R}^2$

Now we are looking for the numerical solution of the scalar conservation law in $\mathbb{R}^2$. Let $w = (x, y)$, then we have:

$$u_t + f(u)_x + g(u)_y = 0, \tag{3.10}$$

where $u(w,t) : \mathbb{R}^2 \to \mathbb{R}$, $f(u) : \mathbb{R} \to \mathbb{R}$ and $g(u) : \mathbb{R} \to \mathbb{R}$. By applying the chain rule we have:

$$u_t + f'(u)u_x + g'(u)u_y = 0, \tag{3.11}$$

where $f'(u)$ and $g'(u)$ are scalar. By the same argument as in $\mathbb{R}$, we define

$$U_{ij}^{n+1} = \frac{1}{\Delta x \Delta y} \int_{x_{i-\frac{1}{2}}}^{x_{i+\frac{1}{2}}} \int_{y_{j-\frac{1}{2}}}^{y_{j+\frac{1}{2}}} \tilde{u}^n(x, y, t_{n+1}) dx dy. \tag{3.12}$$

Thus, Godunov's scheme in $\mathbb{R}^2$ is:

$$\begin{aligned} U_{ij}^{n+1} = U_{ij}^n &- \frac{\Delta t}{\Delta x}[F(U_{ij}^n, U_{i+1,j}^n) - F(U_{i-1,j}^n, U_{ij}^n)] \\ &- \frac{\Delta t}{\Delta y}[G(U_{ij}^n, U_{i,j+1}^n) - G(U_{i,j-1}^n, U_{ij}^n)], \end{aligned} \tag{3.13}$$

where Δt is the time step, Δx is the space step in x, Δy is the space step in y and

the numerical flux functions F and G are given by:

$$\begin{aligned} F(U_{ij}^n, U_{i+1,j}^n) &= \frac{1}{\Delta t \Delta x} \int_{t_n}^{t_{n+1}} \int_{x_{i-\frac{1}{2}}}^{x_{i+\frac{1}{2}}} f(\tilde{u}^n(x, y_{i+\frac{1}{2}}, t)) dx dt, \\ G(U_{ij}^n, U_{i,j+1}^n) &= \frac{1}{\Delta t \Delta y} \int_{t_n}^{t_{n+1}} \int_{y_{j-\frac{1}{2}}}^{y_{j+\frac{1}{2}}} g(\tilde{u}^n(x_{j+\frac{1}{2}}, y, t)) dy dt. \end{aligned} \tag{3.14}$$

By the same argument as in $\mathbb{R}$, $F(U_{ij}^n, U_{i+1,j}^n) = f(u^*(U_{ij}^n, U_{i+1,j}^n))$ and $G(U_{ij}^n, U_{i,j+1}^n) = g(u^*(U_{ij}^n, U_{i,j+1}^n))$. Thus Godunov's method in $\mathbb{R}^2$ becomes:

$$\begin{aligned} U_{ij}^{n+1} = U_{ij}^n &- \frac{\Delta t}{\Delta x}[f(u^*(U_{ij}^n, U_{i+1,j}^n)) - f(u^*(U_{i-1,j}^n, U_{ij}^n))] \\ &- \frac{\Delta t}{\Delta y}[g(u^*(U_{ij}^n, U_{i,j+1}^n)) - g(u^*(U_{i,j-1}^n, U_{ij}^n))]. \end{aligned} \tag{3.15}$$

For a physical solution, we use the entropy-satisfying weak solution in implementing Godunov's method. If $f(u)$ and $g(u)$ are convex, there are four cases that must be considered, which are:

1. $f'(u_l), f'(u_r) \geq 0 \rightarrow u^* = u_l$,
2. $f'(u_l), f'(u_r) \leq 0 \rightarrow u^* = u_r$,
3. $f'(u_l) \geq 0 \geq f'(u_r) \rightarrow u^* = u_l$ if $[f]/[u] > 0$ or $u^* = u_r$ if $[f]/[u] < 0$,
4. $f'(u_l) < 0 < f'(u_r) \rightarrow u^* = u_s$(transonic rarefaction),

and

1. $g'(u_l), g'(u_r) \geq 0 \rightarrow u^* = u_l$,
2. $g'(u_l), g'(u_r) \leq 0 \rightarrow u^* = u_r$,
3. $g'(u_l) \geq 0 \geq g'(u_r) \rightarrow u^* = u_l$ if $[g]/[u] > 0$ or $u^* = u_r$ if $[g]/[u] < 0$,
4. $g'(u_l) < 0 < g'(u_r) \rightarrow u^* = u_s$(transonic rarefaction),

where u_l and u_r are initial data of the Riemann problem, the intermediate value u_s with the property $f'(u_s) = 0$ is the value of u for which the characteristic speed is zero, and is called the sonic point. Since there are no case 3 and case 4 in our PDE

equation, we consider case 1 and case 2 only. We also have a more general form:

$$F(u_l, u_r) = \begin{cases} \min_{u_l \le u \le u_r} f(u) & \text{if} \quad u_l \le u_r \\ \max_{u_r \le u \le u_l} f(u) & \text{if} \quad u_l > u_r \end{cases} \tag{3.16}$$

and

$$G(u_l, u_r) = \begin{cases} \min_{u_l \le u \le u_r} g(u) & \text{if} \quad u_l \le u_r \\ \max_{u_r \le u \le u_l} g(u) & \text{if} \quad u_l > u_r \end{cases} \tag{3.17}$$

Finally, the CFL (Courant-Friedrichs-Lewy) condition in $\mathbb{R}^2$ is: $\frac{k}{h} \max\{\max_u\{|f'(u)|\}, \max_u\{|g'(u)|\}\} \le \frac{1}{2}$. We need to find the maximum eigenvalues of two scalar $f'(u)$ and $g'(u)$ in the scalar conservation law:

$$u_t + f'(u)u_x + g'(u)u_y = 0. \tag{3.18}$$

In our numerical scheme, the Courant-Friedrichs-Lewy (CFL) condition is to ensure that a cell content in state space does not "move" by more than one cell during one time step, an essential criterion for numerical stability [10]. It constrains the time step to a small number depending on the applied current and the spatial discretization.

3.1.2 Applying Godunov's method in $\mathbb{R}^2$ to the population density equation for the Izhikevich model

According to (2.28), we have:

$$\begin{aligned} \frac{\partial P(w,t)}{\partial t} &= -\nabla \cdot \left(F(w)P(w,t) + e_v \sigma(t) \int_{v-\epsilon}^{v} P(\tilde{v}, u, t) d\tilde{v} \right) \\ &= -\nabla \cdot \left(\begin{bmatrix} F_v(w)P(w,t) + \sigma(t) \int_{v-\epsilon}^{v} P(\tilde{v}, u, t) d\tilde{v} \\ F_u(w)P(w,t) \end{bmatrix} \right). \end{aligned}$$

Then,

$$\frac{\partial P(w,t)}{\partial t} = -\frac{\partial \left(F_v(w)P(w,t) + \sigma(t)\int_{v-\epsilon}^{v} P(\tilde{v},u,t)d\tilde{v}\right)}{\partial v} - \frac{\partial \left(F_u(w)P(w,t)\right)}{\partial u}. \quad (3.19)$$

If we consider indexes i, j accounting for the variables, u, v, respectively, this leads to the first order Godunov's scheme in $\mathbb{R}^2$ [10]:

$$\begin{aligned} \frac{P_{ij}^{n+1} - P_{ij}^{n}}{\Delta t} &= -\frac{j_v^+ - j_v^-}{\Delta v} - \frac{j_u^+ - j_u^-}{\Delta u} \\ &= -\frac{\left((j_{v,s}^+ - j_{v,s}^-) + (j_{v,i}^+ - j_{v,i}^-)\right)}{\Delta v} - \frac{j_{u,s}^+ - j_{u,s}^-}{\Delta u}, \end{aligned} \quad (3.20)$$

where $j_{v,s}$ and $j_{u,s}$ are streaming flux, $j_{v,i}$ is interaction flux. Therefore,

$$\begin{aligned} P_{ij}^{n+1} - P_{ij}^{n} &= -\frac{\Delta t}{\Delta v}[(j_{v,s}^+ - j_{v,s}^-) + (j_{v,i}^+ - j_{v,i}^-)] - \frac{\Delta t}{\Delta u}(j_{u,s}^+ - j_{u,s}^-), \\ P_{ij}^{n+1} &= P_{ij}^{n} - \frac{\Delta t}{\Delta v}[(j_{v,s}^+ - j_{v,s}^-) + (j_{v,i}^+ - j_{v,i}^-)] - \frac{\Delta t}{\Delta u}(j_{u,s}^+ - j_{u,s}^-). \end{aligned} \quad (3.21)$$

Since the streaming flux terms depend on the direction of flow in phase space, we have:

If $v' > 0$, then

$$\begin{aligned} j_{v,s}^+(t^n) &= P_{ij}^n F_v(v_j^+, u_i) = P(i,j)F_v(v(j+1), u(i)), \\ j_{v,s}^-(t^n) &= P_{i,j-1}^n F_v(v_j^-, u_i) = P(i,j-1)F_v(v(j), u(i)). \end{aligned} \quad (3.22)$$

If $v' \leq 0$, then

$$\begin{aligned} j_{v,s}^+(t^n) &= P_{i,j+1}^n F_v(v_j^+, u_i) = P(i,j+1)F_v(v(j+1), u(i)), \\ j_{v,s}^-(t^n) &= P_{i,j}^n F_v(v_j^-, u_i) = P(i,j)F_v(v(j), u(i)). \end{aligned} \quad (3.23)$$

If $u' > 0$, then

$$\begin{aligned} j^+_{u,s}(t^n) &= P^n_{ij} F_u(v_j, u^+_i) = P(i,j) F_u(v(j), u(i+1)), \\ j^-_{u,s}(t^n) &= P^n_{i-1,j} F_u(v_j, u^-_i) = P(i-1,j) F_u(v(j), u(i)). \end{aligned} \tag{3.24}$$

If $u' \leq 0$, then

$$\begin{aligned} j^+_{u,s}(t^n) &= P^n_{i+1,j} F_u(v_j, u^+_i) = P(i+1,j) F_u(v(j), u(i+1)), \\ j^-_{u,s}(t^n) &= P^n_{i,j} F_u(v_j, u^-_i) = P(i,j) F_u(v(j), u(i)). \end{aligned} \tag{3.25}$$

Now we consider the interaction flux terms. If $v > v_{min} + \epsilon$, then

$$j^+_{v,i} - j^-_{v,i} = \sigma(t) \cdot \Delta v \cdot \left(P^n_{i,j} - P^n_{i,j-n_\epsilon} \right), \tag{3.26}$$

where $n_\epsilon \cdot \Delta v = \epsilon$. n_ϵ is number of cells in length ϵ in v. Otherwise

$$j^+_{v,i} - j^-_{v,i} = \sigma(t) \cdot \Delta v \cdot P^n_{i,j}, \tag{3.27}$$

where $\sigma(t) = \frac{G}{N} \times r(t - \tau_0)$. Since $r(t) = \int_{u_{min}}^{u_{max}} J_v(s, u_i, t) du \approx \sum_{i=1}^{n_u} J_v(s, u_i, t) \Delta u = \sum_{i=1}^{n_u} j^+_v(v_{n_v+1}, u_i, t^n) \Delta u = \sum_{i=1}^{n_u} P(i, n_v) F_v(v = s, u(i)) \Delta u$, where n_u is the number of grid cells between u_{min} and u_{max} and n_v is the number of grid cells between v_{min} and v_{max}, then $r(t - \tau_0) = \int_{u_{min}}^{u_{max}} J_v(s, u_i, t - \tau_0) du \approx \sum_{i=1}^{n_u} J_v(s, u_i, t - \tau_0) \Delta u$.

Boundary Conditions: The main condition is that the incoming flux is zero on the boundaries, i.e. $\overrightarrow{J} \cdot \overrightarrow{n} = 0$ where $\overrightarrow{n}$ is a vector normal to each boundary of the phase space, except on the domain $v = s \times u \in [u_{min}, u_{max} - \epsilon]$ where the population density can pass through the spike apex value s, before being re-injected at $v = c$.

3.2 Simulations of the population density model

We are interested in the situation where single neurons fire tonically, and bursting only occurs as a result of interactions. Therefore, we consider tonic spiking parameters ($a = 0.02$, $b = 0.2$, $v_0 = c = -65$, $d = 6$) from the Izhikevich model. We choose $v_s = 30$, $\epsilon = 3$, $G = 15$ and the delay time τ=1ms in the following numerical simulations [10]. Following Modolo we will consider first the case of a population of neurons with no coupling between them, after which we will introduce the coupling.

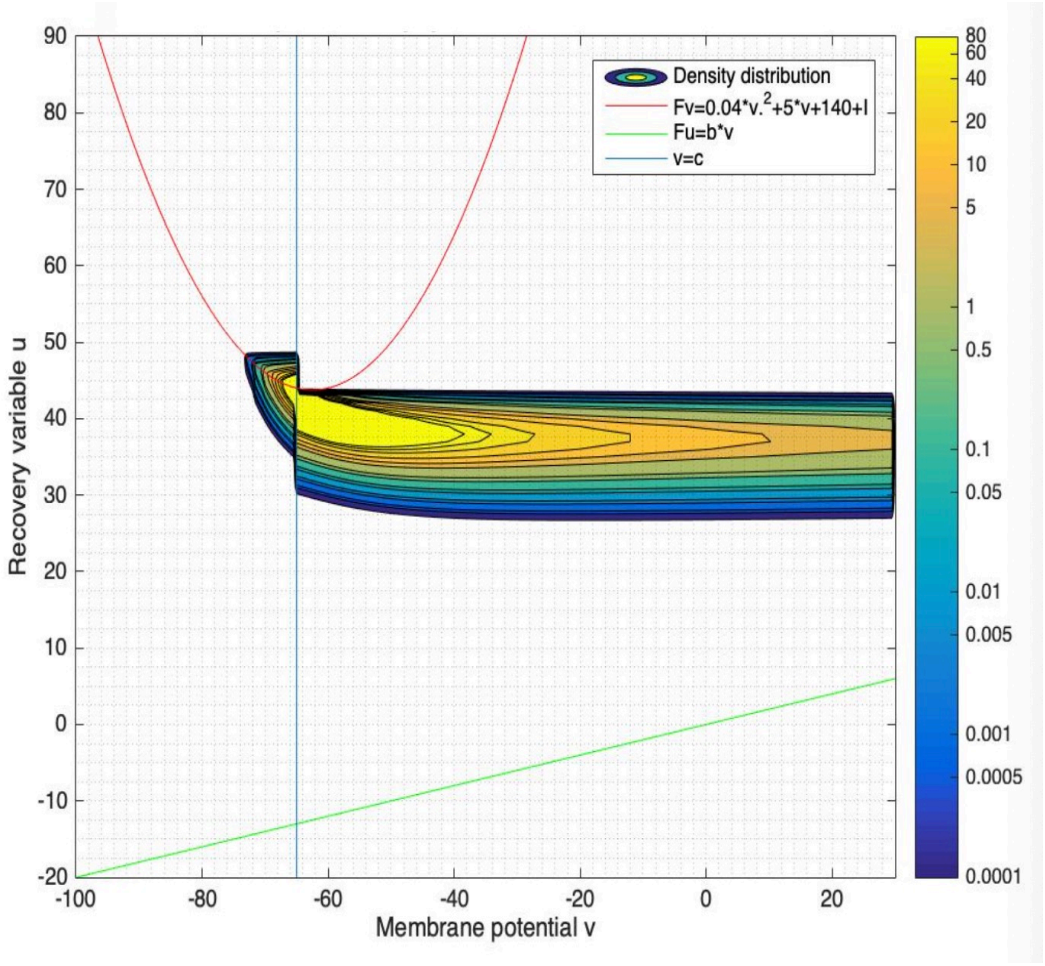

Figure 3.1: Density distribution at $t = 50ms$ of an uncoupled population with an initial Dirac distribution at $u = -14$, $v = -70$.

Uncoupled case: A constant current $I = 60$pA was applied to the numerical simulations. The v-nullcline is $u = 0.04v^2 + 5v + 140 + I$ and the u-nullcline is $u = bv$. $v_0 = -65$ is the reset line. The initial condition is chosen to be a Dirac distribution at $u = -14$ and $v = -70$. The total number of neurons is 50000. Both total firing rate $r(t)$ and mean membrane potential ($MMP = \frac{1}{N} \int \left[\int p(v,u,t)du \right] vdv$) become constant after an initial brief oscillation. The density distribution has a stationary state at $t = 50ms$ (see Figures 3.1, 3.2 and 3.3). The behavior of the density distribution is the result of the numerical diffusion. If the neurons are concentrated in a true Delta function they should leave and arrive together from one grid cell to another grid cell. Thus, the trajectory will have a fixed point with tonic firing behavior.

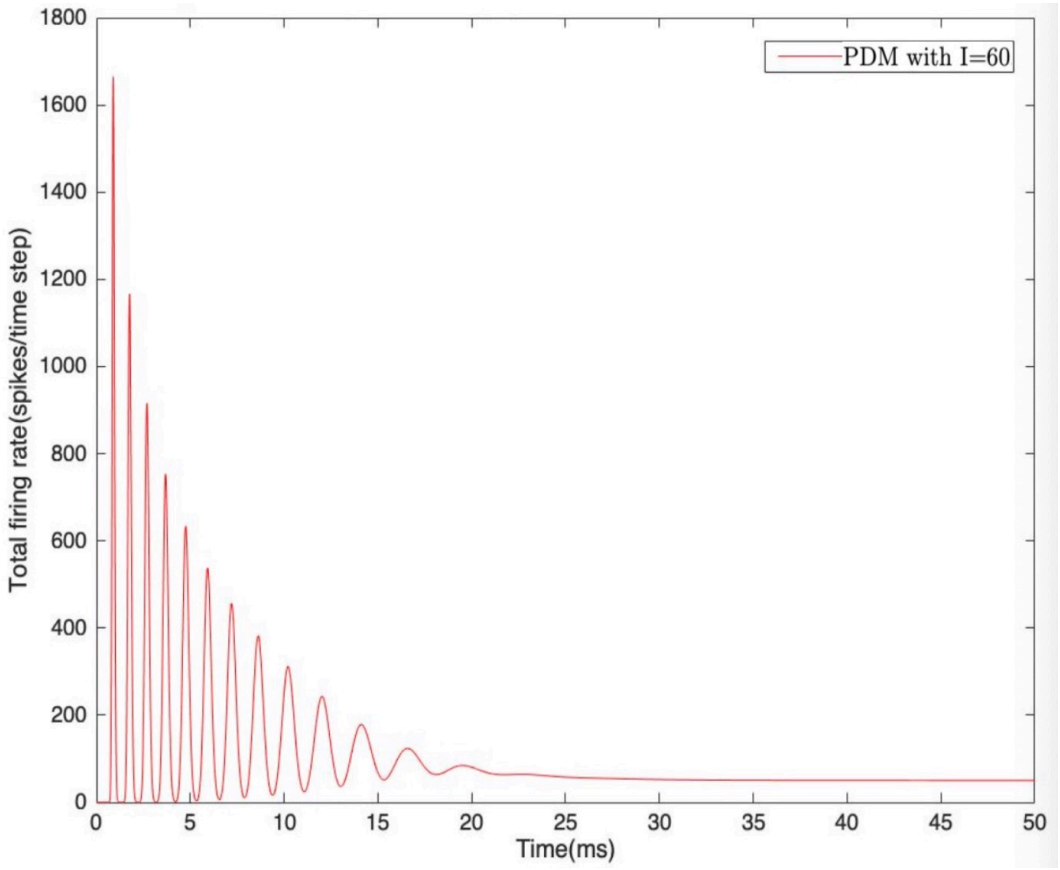

Figure 3.2: Total firing rate of an uncoupled population with an initial Dirac distribution at $u = -14$, $v = -70$.

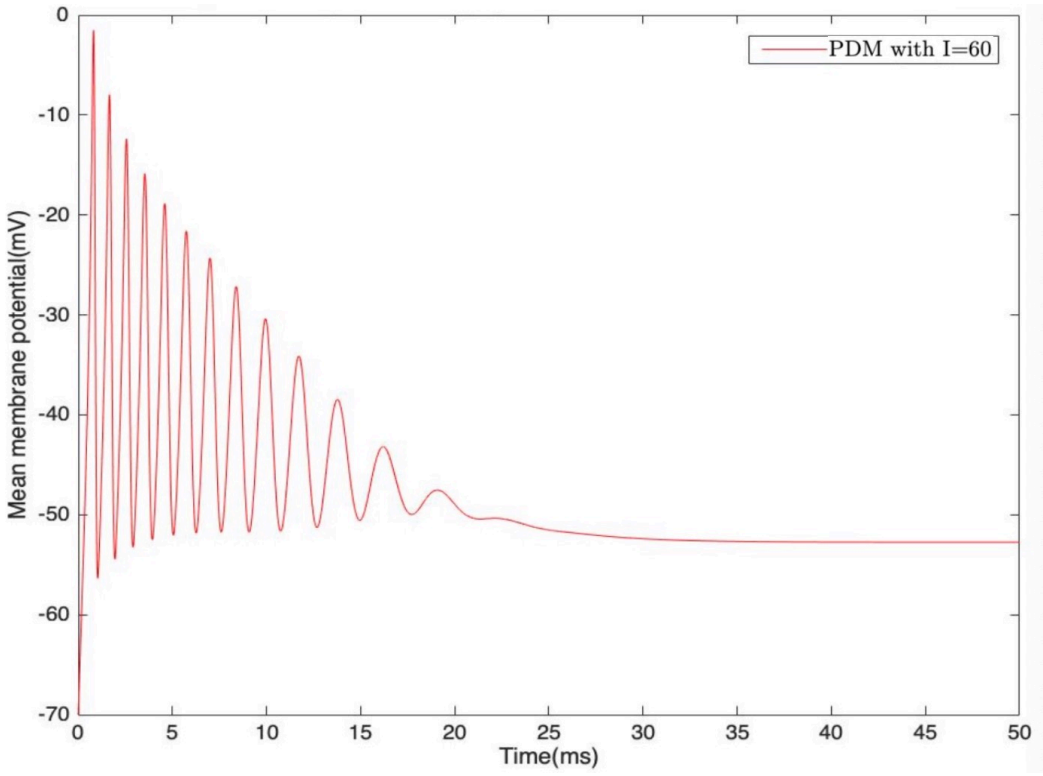

Figure 3.3: Mean membrane potential of an uncoupled population with an initial Dirac distribution at $u = -14$, $v = -70$.

Coupled case with an initial Dirac distribution: A constant current $I = 40$pA was applied to the numerical simulations. The spike conduction delay is 1ms and the "jump" in membrane potential is 3mV. The v-nullcline is $u = 0.04v^2 + 5v + 140 + I$ and the u-nullcline is $u = bv$. $v_0 = -65$ is the reset line. The initial condition is chosen to be a Dirac distribution. The total number of neurons is 10000. Both total firing rate $r(t)$ and mean membrane potential MMP have a periodic pattern after an initial brief oscillation (see Figures 3.4 and 3.5). We can see that the entire density distribution moves up first, then gathers in the recovery phase to move down along the left branch of the v-nullcline. The density distribution always repeats this process in time, so it shows that the evolution of the population density model is a bursting pattern for the whole population of neurons (see Figures 3.6 to 3.18).

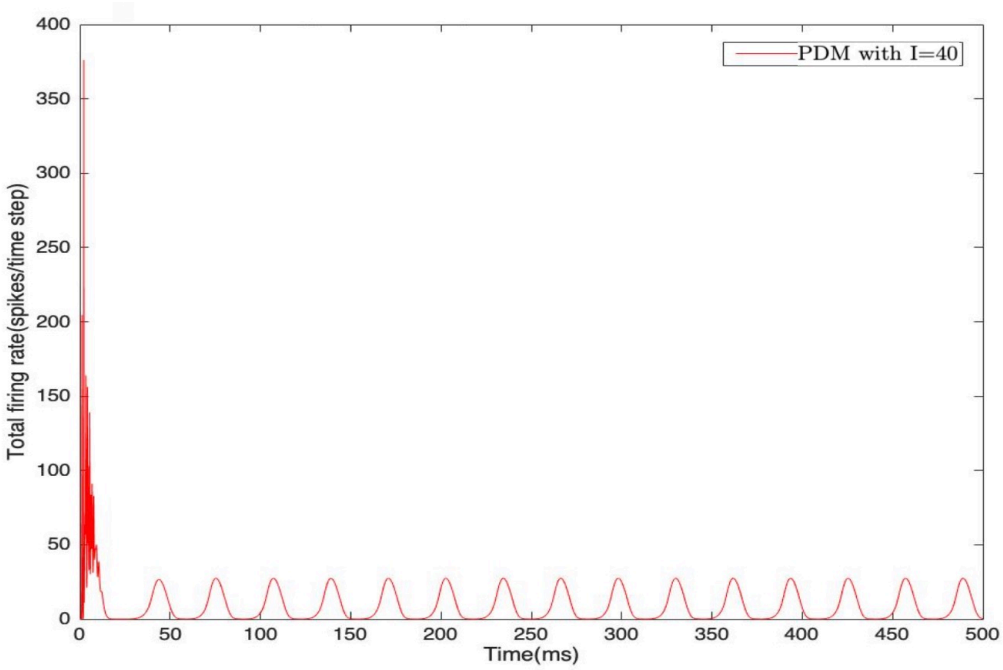

Figure 3.4: Total firing rate of a coupled population with an initial Dirac distribution at $u = -14$, $v = -70$.

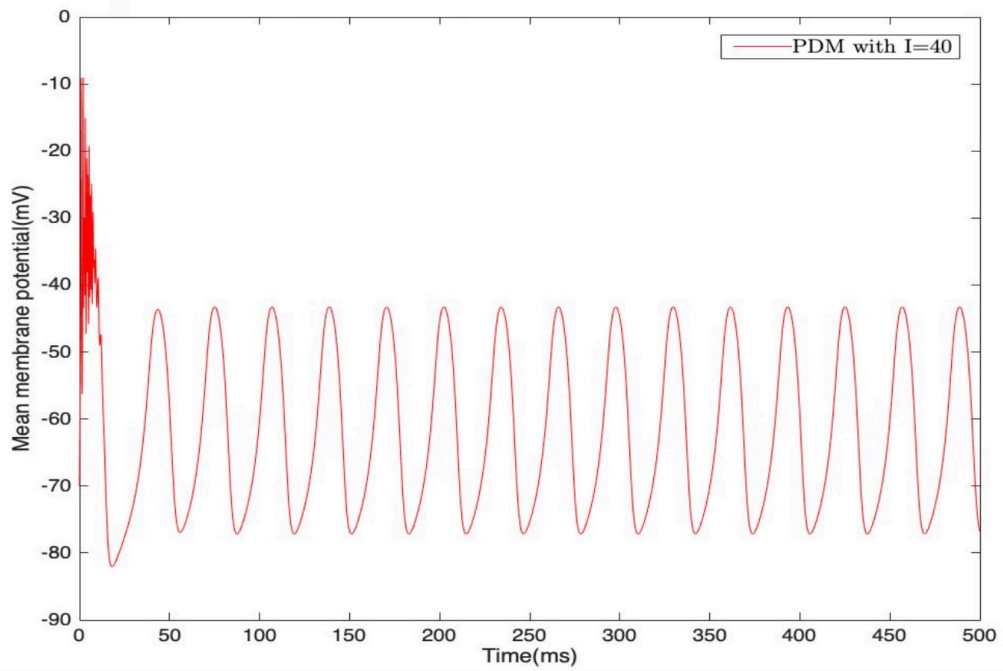

Figure 3.5: Mean membrane potential of a coupled population with an initial Dirac distribution at $u = -14$, $v = -70$.

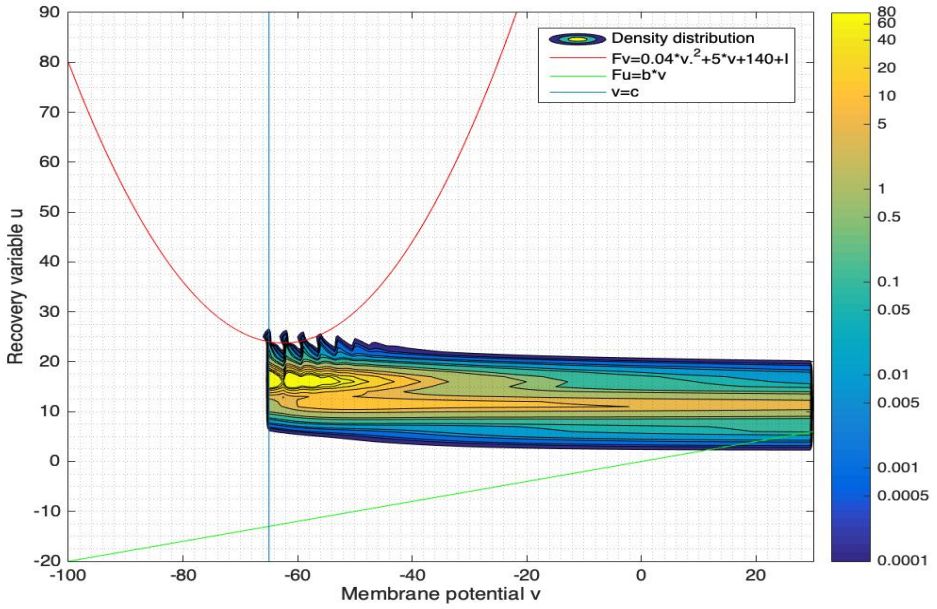

Figure 3.6: Density distribution at $t = 5ms$ of a coupled population with an initial Dirac distribution at $u = -14$, $v = -70$.

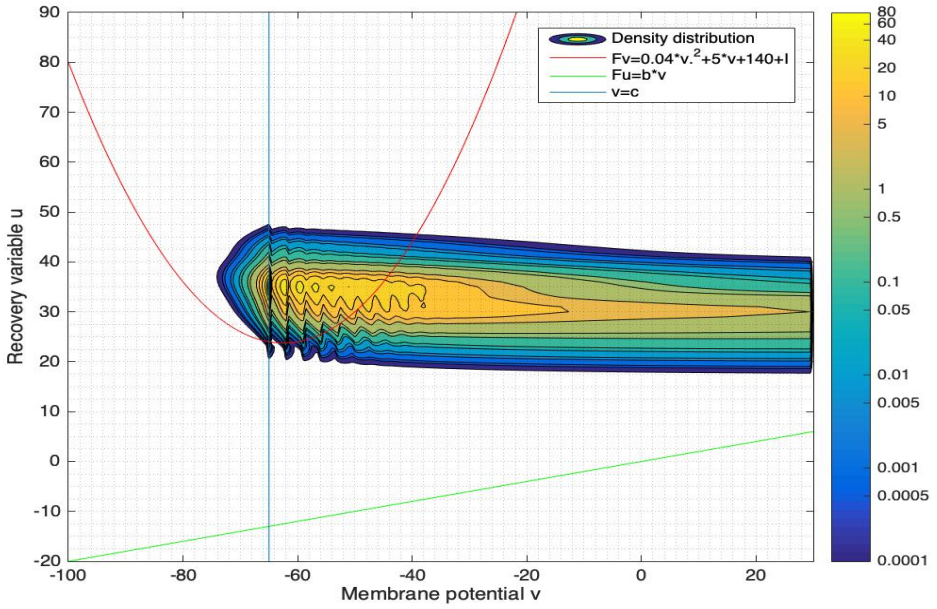

Figure 3.7: Density distribution at $t = 8ms$ of a coupled population with an initial Dirac distribution at $u = -14$, $v = -70$.

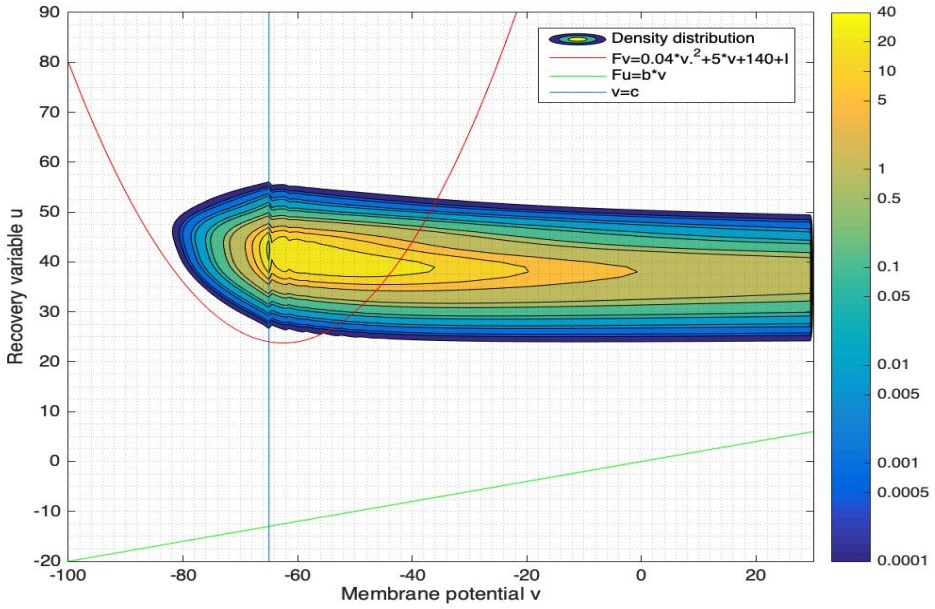

Figure 3.8: Density distribution at $t = 10ms$ of a coupled population with an initial Dirac distribution at $u = -14$, $v = -70$.

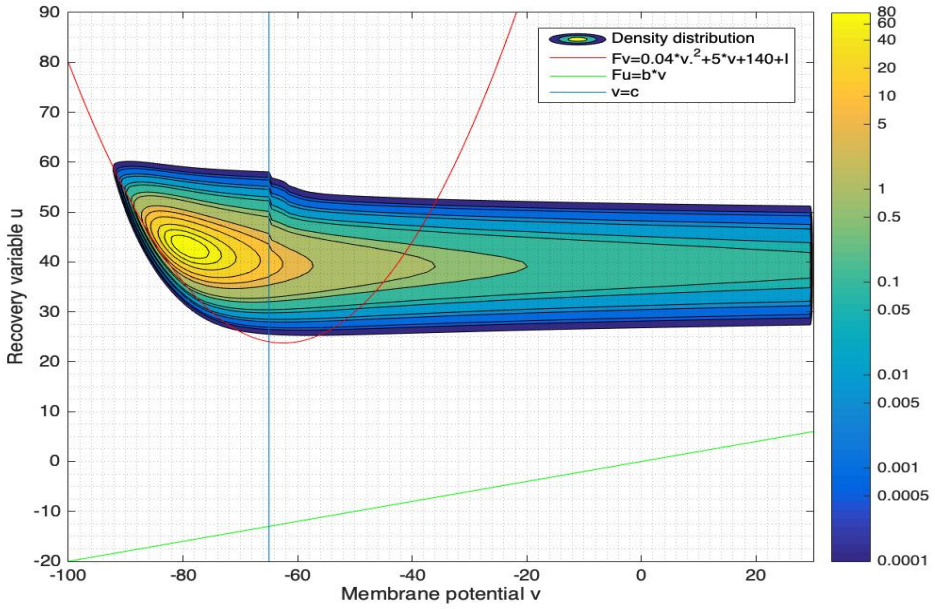

Figure 3.9: Density distribution at $t = 15ms$ of a coupled population with an initial Dirac distribution at $u = -14$, $v = -70$.

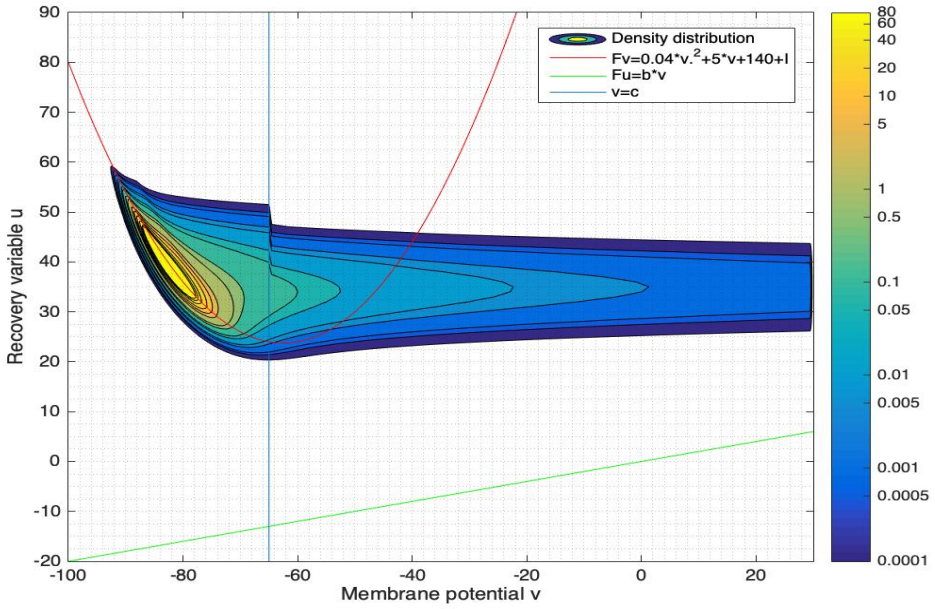

Figure 3.10: Density distribution at $t = 18ms$ of a coupled population with an initial Dirac distribution at $u = -14$, $v = -70$.

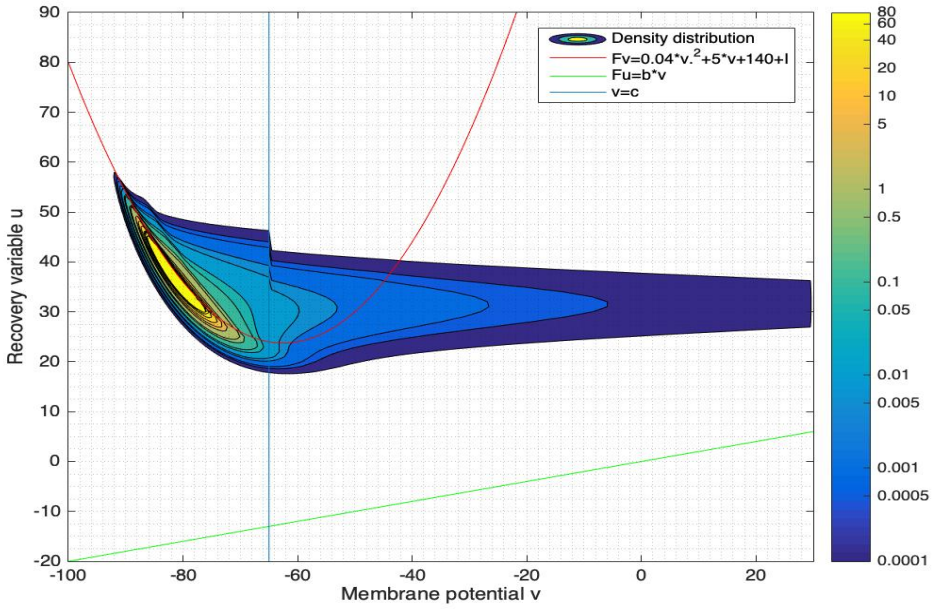

Figure 3.11: Density distribution at $t = 20ms$ of a coupled population with an initial Dirac distribution at $u = -14$, $v = -70$.

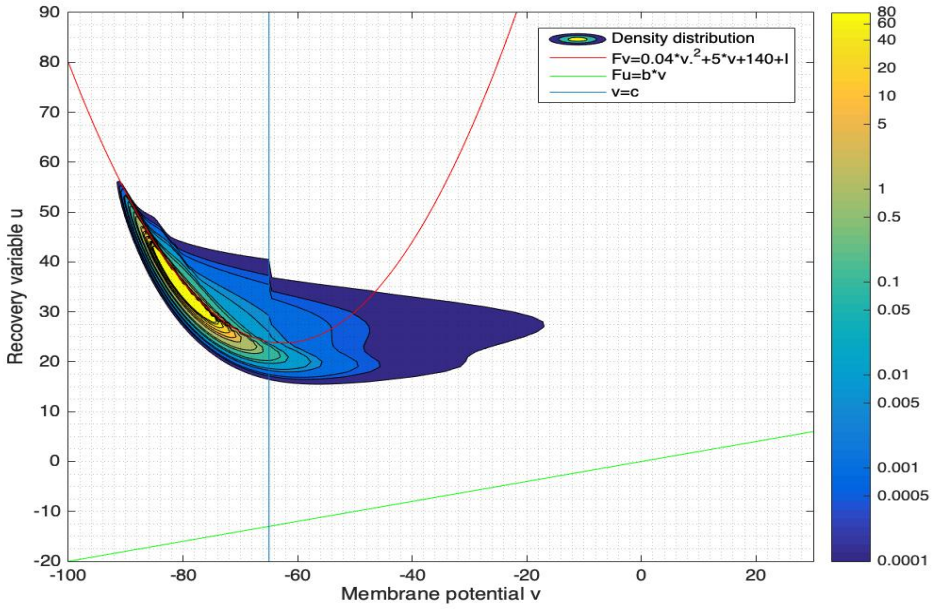

Figure 3.12: Density distribution at $t = 22ms$ of a coupled population with an initial Dirac distribution at $u = -14$, $v = -70$.

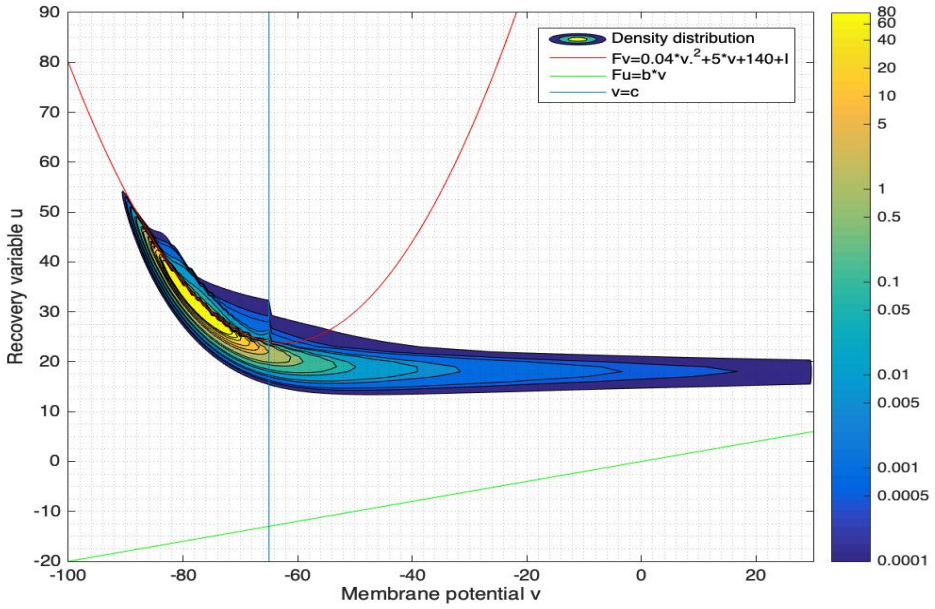

Figure 3.13: Density distribution at $t = 25ms$ of a coupled population with an initial Dirac distribution at $u = -14$, $v = -70$.

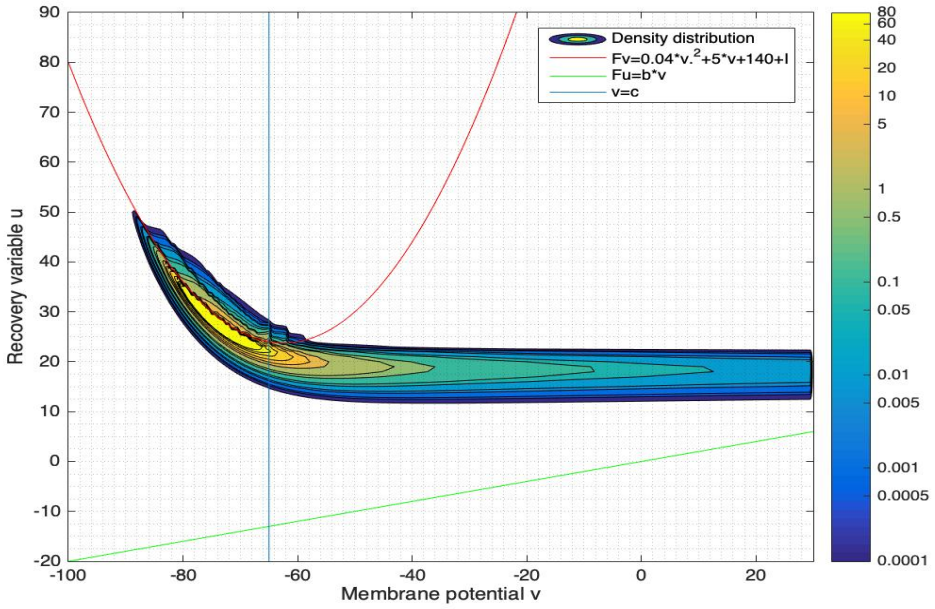

Figure 3.14: Density distribution at $t = 30ms$ of a coupled population with an initial Dirac distribution at $u = -14$, $v = -70$.

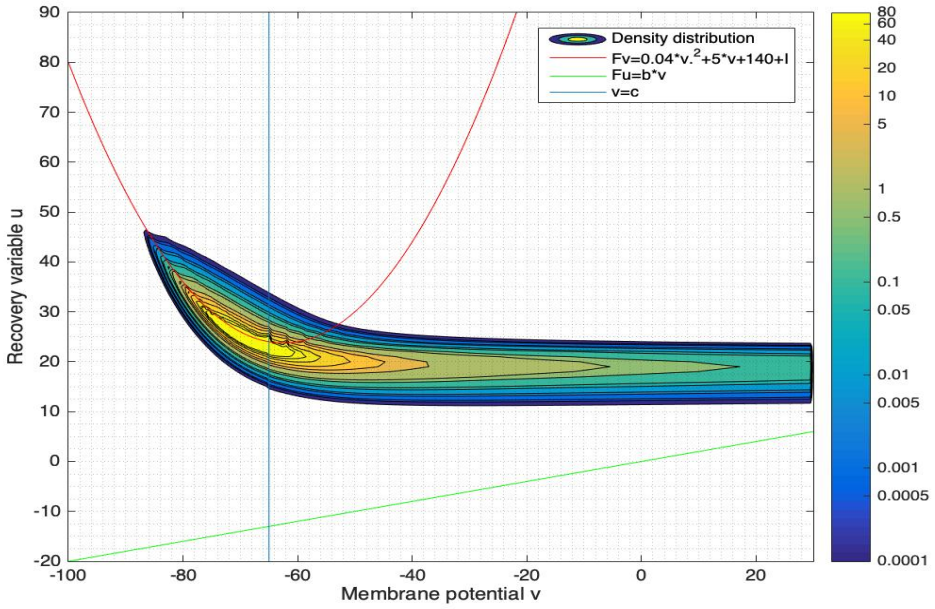

Figure 3.15: Density distribution at $t = 35ms$ of a coupled population with an initial Dirac distribution at $u = -14$, $v = -70$.

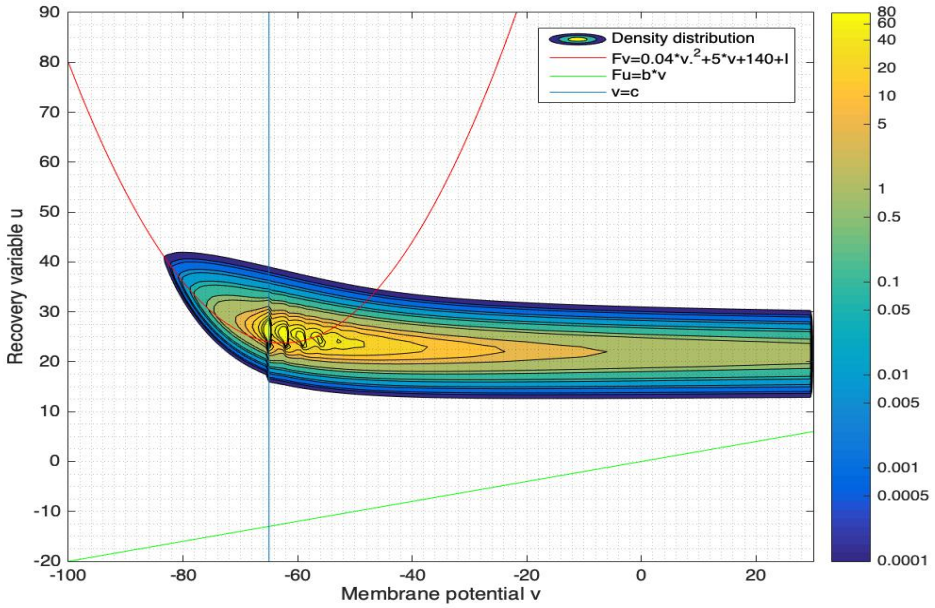

Figure 3.16: Density distribution at $t = 40ms$ of a coupled population with an initial Dirac distribution at $u = -14$, $v = -70$.

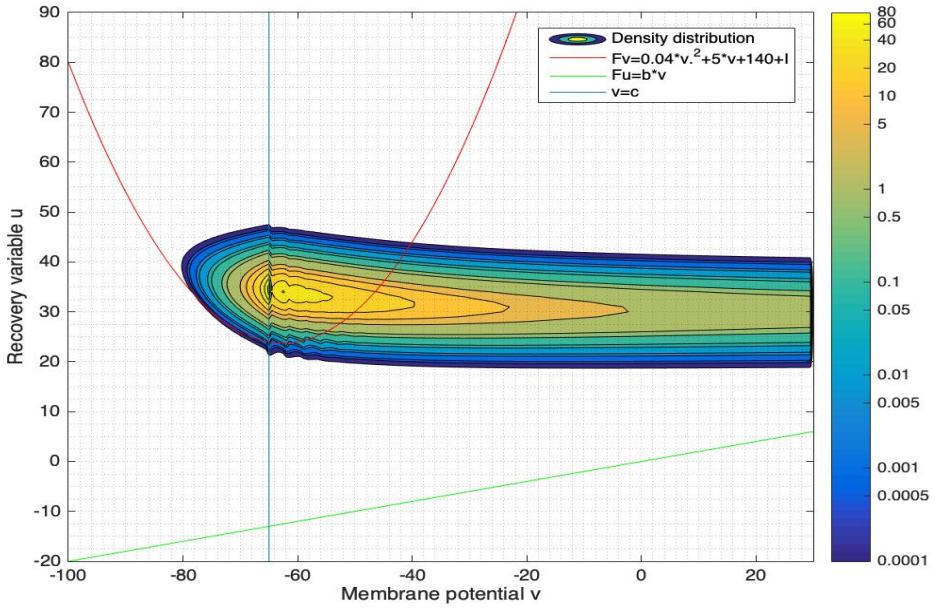

Figure 3.17: Density distribution at $t = 45ms$ of a coupled population with an initial Dirac distribution at $u = -14$, $v = -70$.

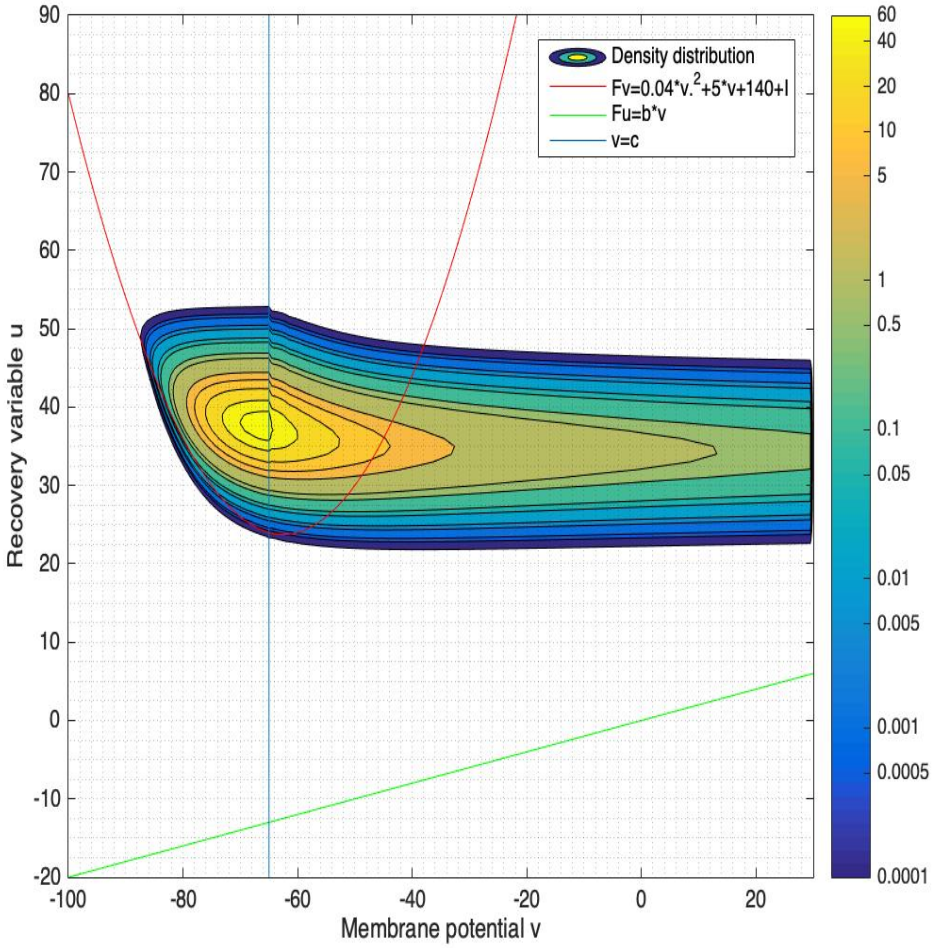

Figure 3.18: Density distribution at $t = 50ms$ of a coupled population with an initial Dirac distribution at $u = -14$, $v = -70$.

Coupling with a uniform initial condition: By replacing the Dirac distribution by a smoother distribution (i.e. uniform on the state space), we found that the transient oscillations of both total firing rate $r(t)$ and mean membrane potential MMP at the beginning have almost disappeared but the long-term behaviour is very similar (see Figures 3.19 and 3.20).

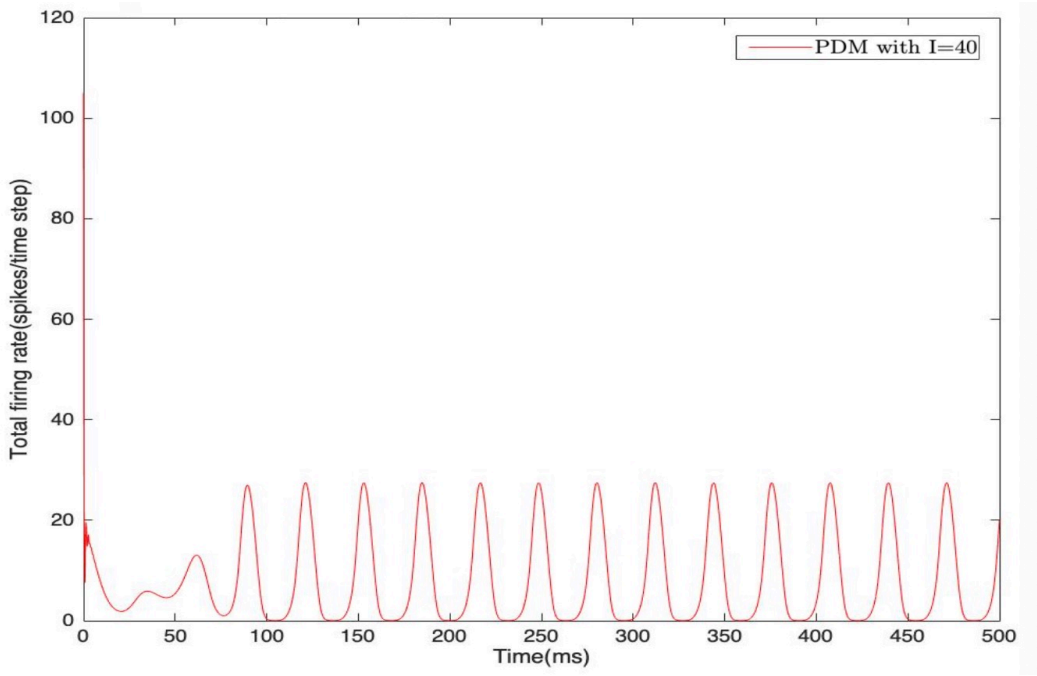

Figure 3.19: Total firing rate of a coupled population with a uniform initial condition.

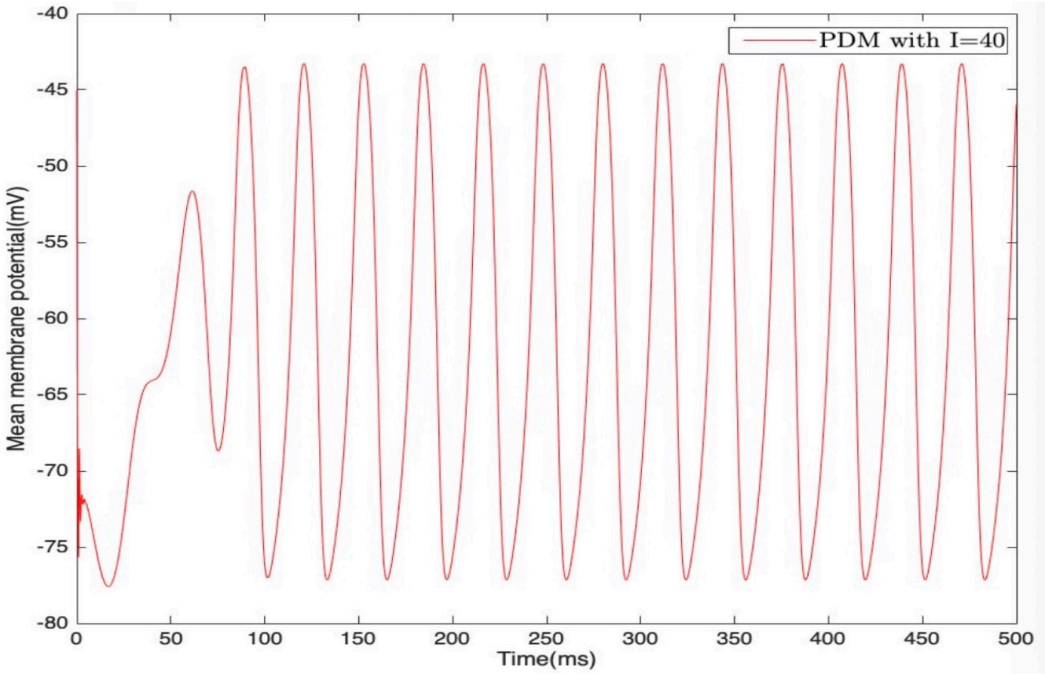

Figure 3.20: Mean membrane potential of a coupled population with a uniform initial condition.

Narrower v-nullcline: We use a narrower v-nullcline to try to see interaction-induced bursting more clearly. The narrower v-nullcline is $u = 0.4v^2 + 50v + 1546.25 + I$. Although the movement of density along the narrower v-nullcline is slower than that of the original v-nullcline, the number of spikes per burst is increased. Again, the whole density distribution moves up at the beginning, then gathers in the recovery phase. The density distribution also repeats this process in time. It is more clear that the evolution of the population density model is a bursting pattern (see Figures 3.23 to 3.39).

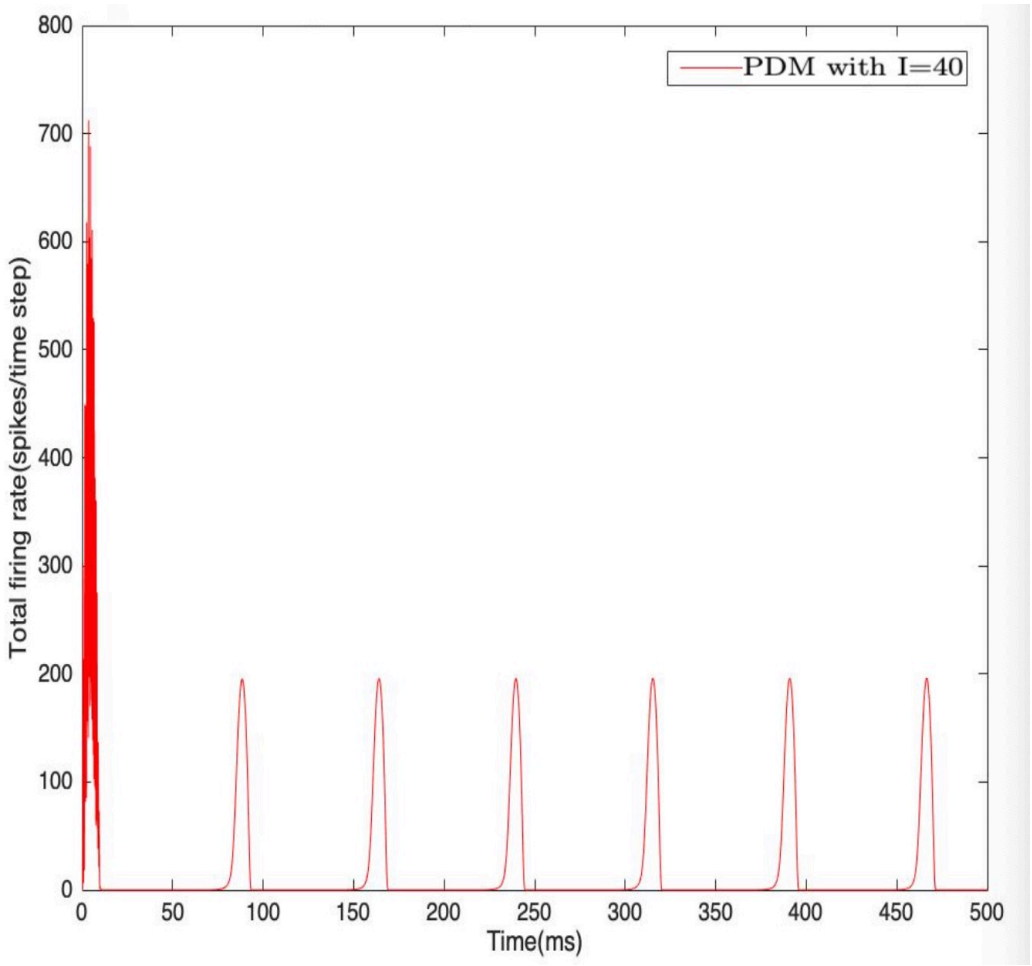

Figure 3.21: Total firing rate of a coupled population with a narrower v-nullcline and an initial Dirac distribution at $u = -14$, $v = -70$.

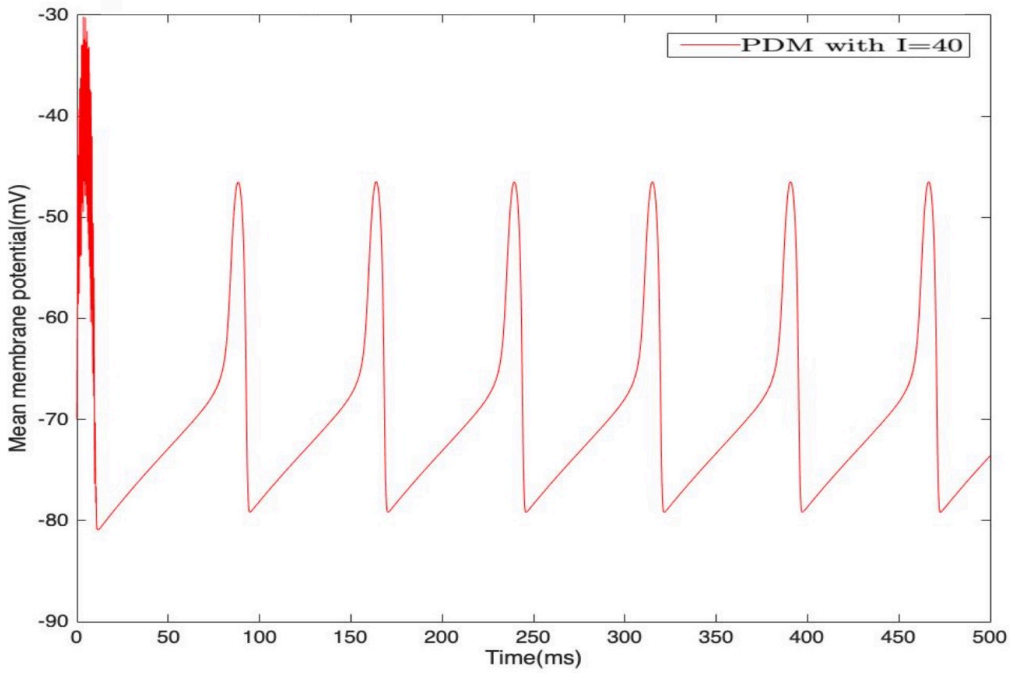

Figure 3.22: Mean membrane potential of a coupled population with a narrower v-nullcline and an initial Dirac distribution at $u = -14$, $v = -70$.

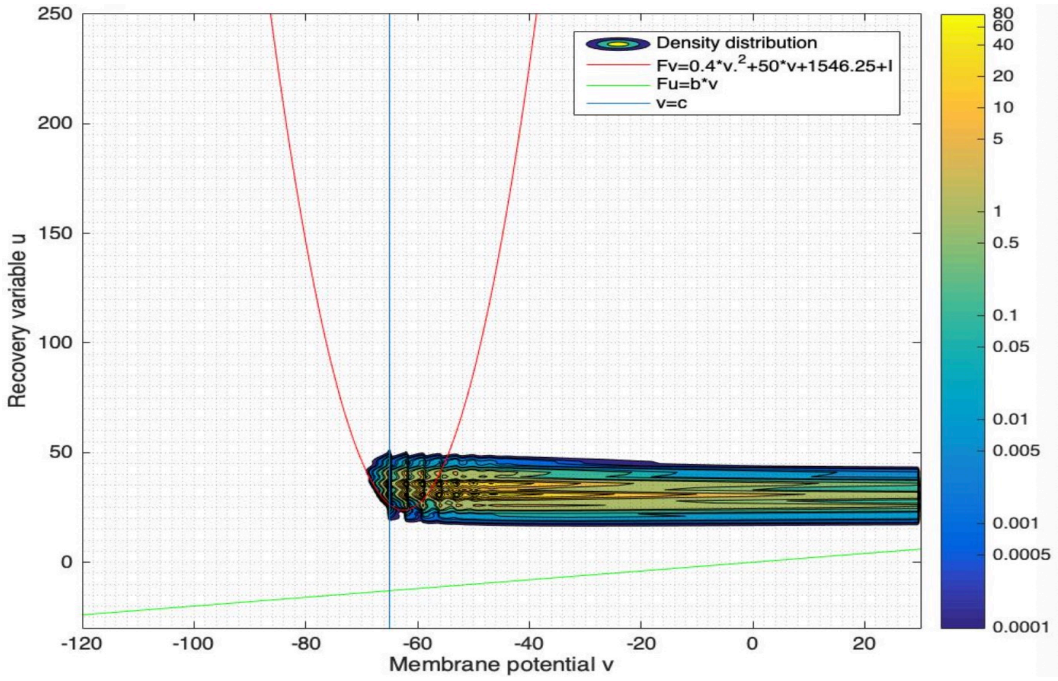

Figure 3.23: Density distribution at $t = 3ms$ of a coupled population with a narrower v-nullcline and an initial Dirac distribution at $u = -14$, $v = -70$.

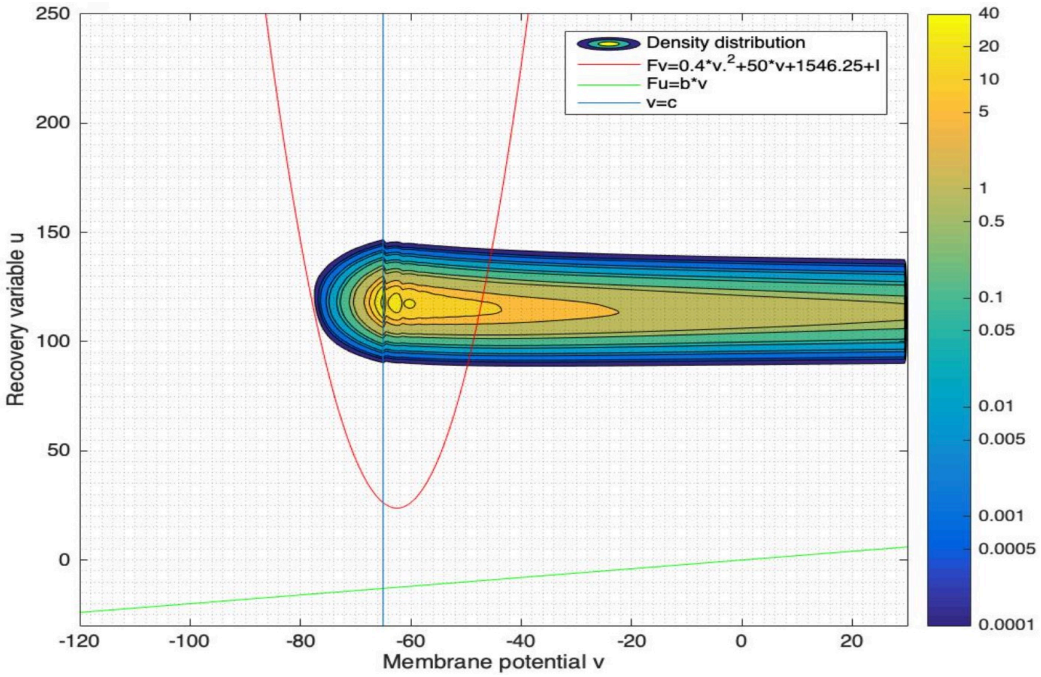

Figure 3.24: Density distribution at $t = 6ms$ of a coupled population with a narrower v-nullcline and an initial Dirac distribution at $u = -14$, $v = -70$.

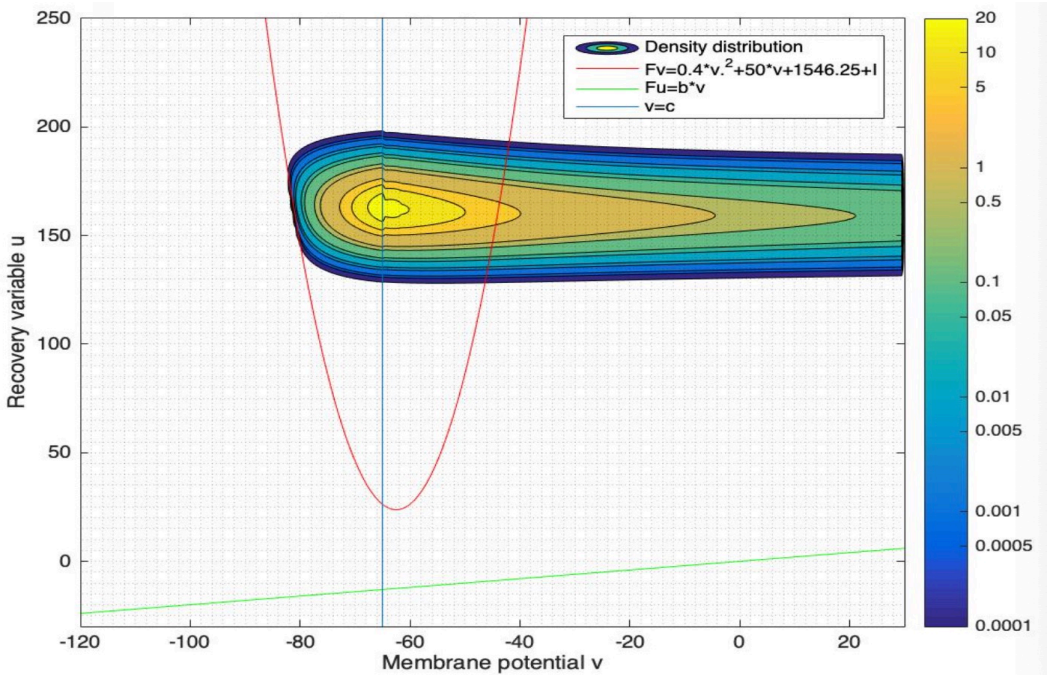

Figure 3.25: Density distribution at $t = 9ms$ of a coupled population with a narrower v-nullcline and an initial Dirac distribution at $u = -14$, $v = -70$.

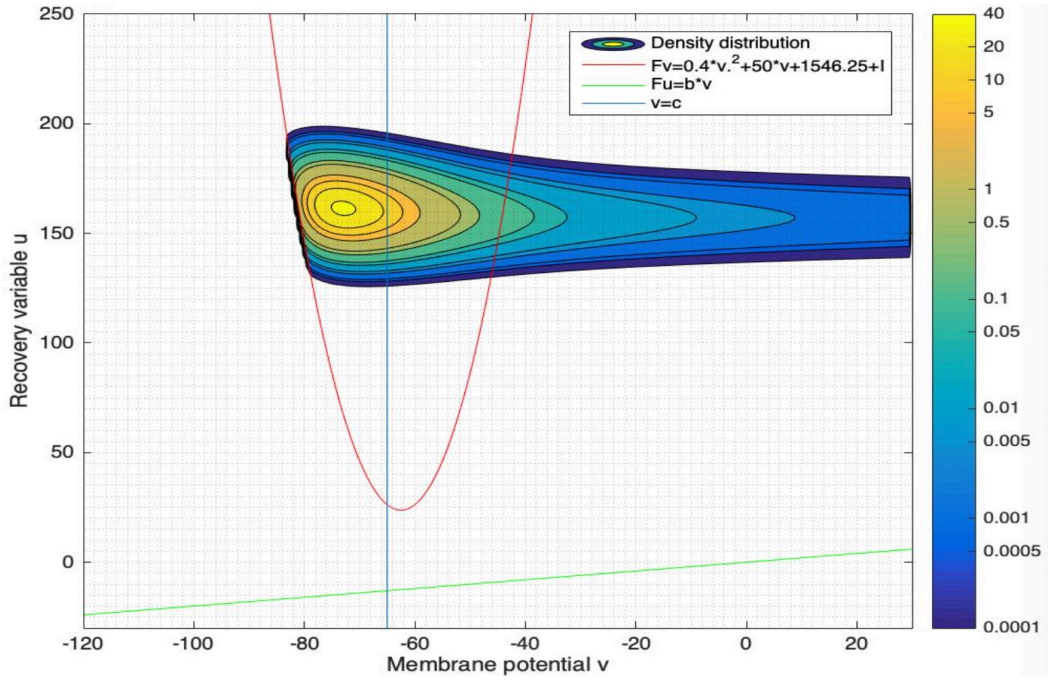

Figure 3.26: Density distribution at $t = 10ms$ of a coupled population with a narrower v-nullcline and an initial Dirac distribution at $u = -14$, $v = -70$.

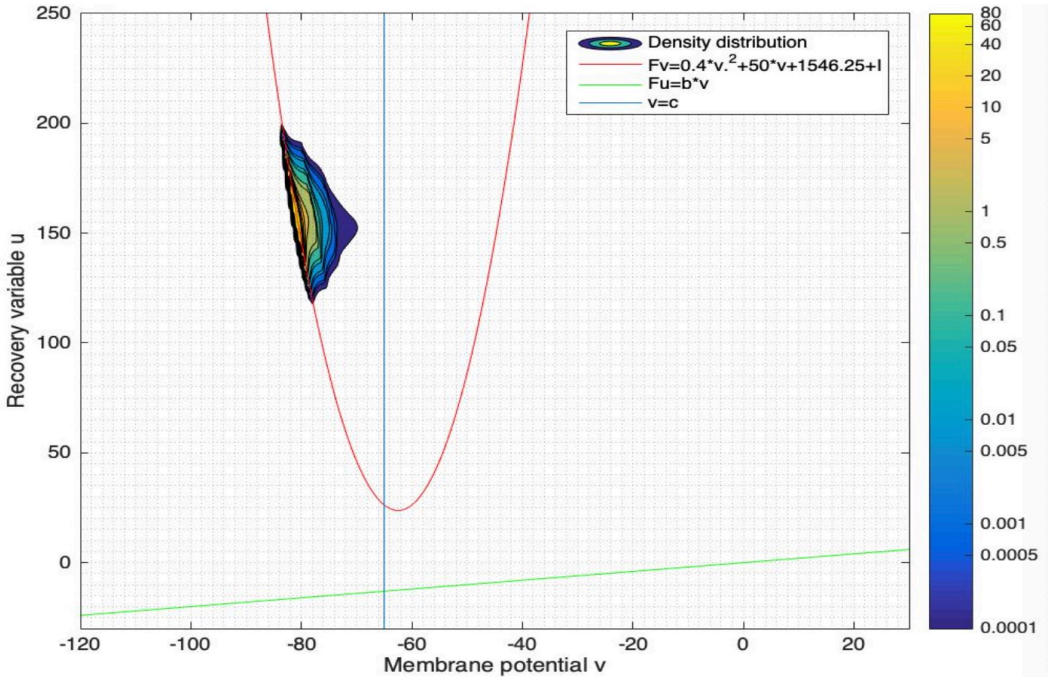

Figure 3.27: Density distribution at $t = 11ms$ of a coupled population with a narrower v-nullcline and an initial Dirac distribution at $u = -14$, $v = -70$.

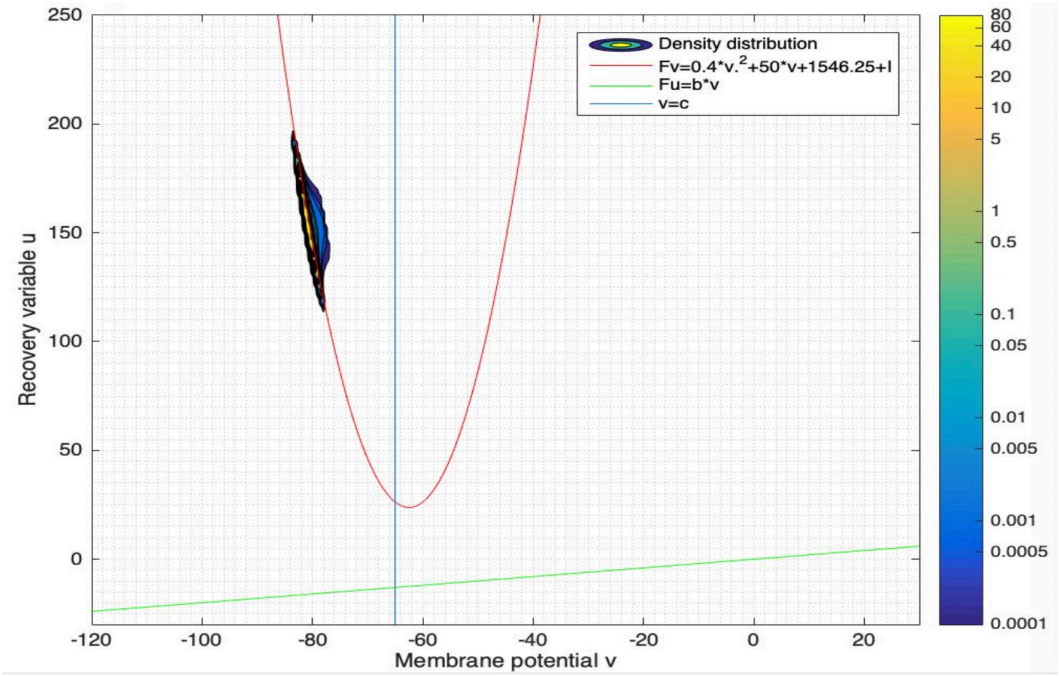

Figure 3.28: Density distribution at $t = 12ms$ of a coupled population with a narrower v-nullcline and an initial Dirac distribution at $u = -14$, $v = -70$.

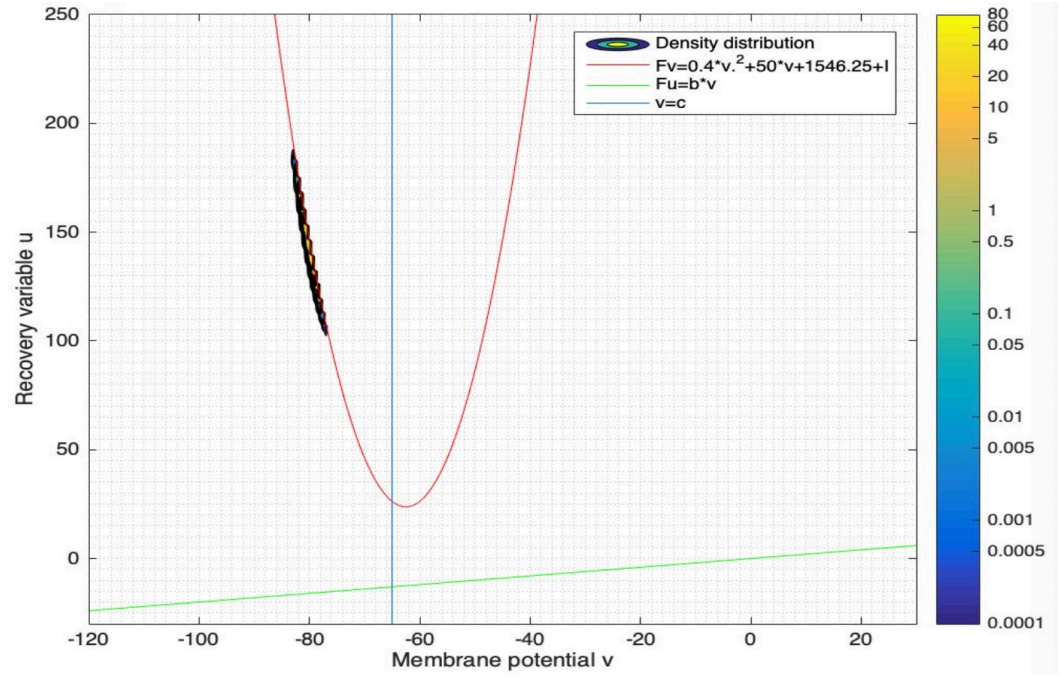

Figure 3.29: Density distribution at $t = 15ms$ of a coupled population with a narrower v-nullcline and an initial Dirac distribution at $u = -14$, $v = -70$.

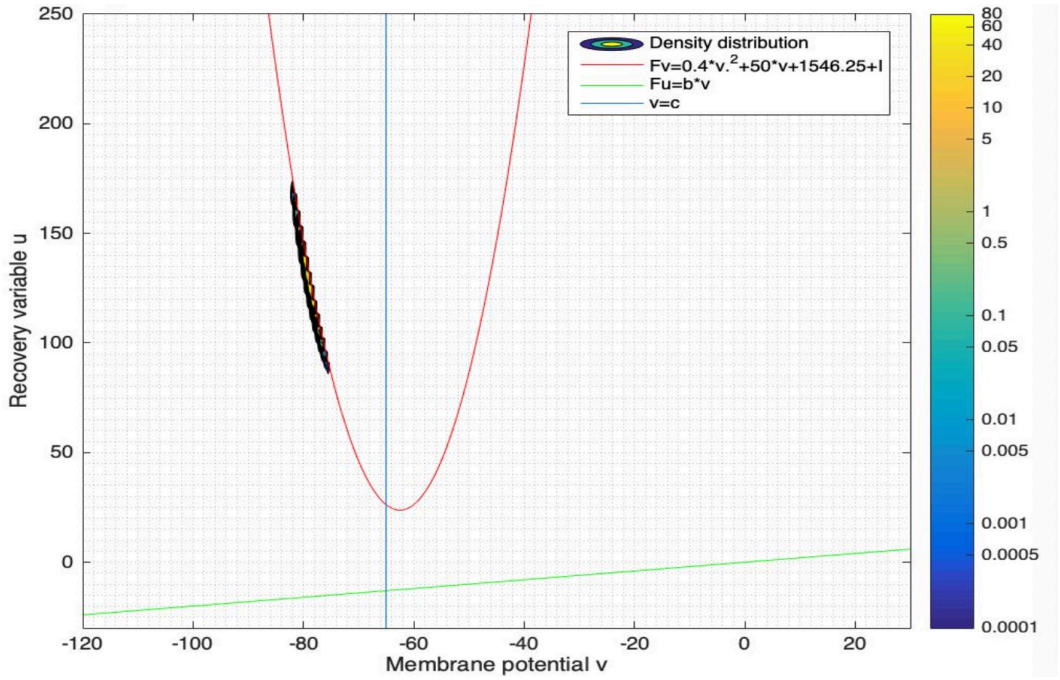

Figure 3.30: Density distribution at $t = 20ms$ of a coupled population with a narrower v-nullcline and an initial Dirac distribution at $u = -14$, $v = -70$.

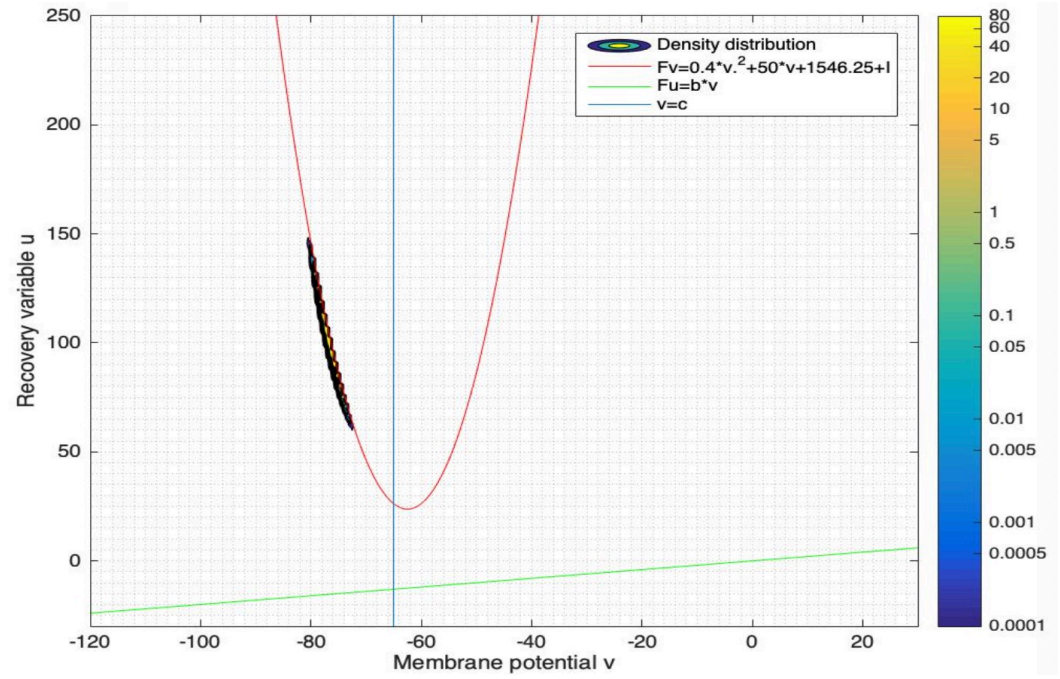

Figure 3.31: Density distribution at $t = 30ms$ of a coupled population with a narrower v-nullcline and an initial Dirac distribution at $u = -14$, $v = -70$.

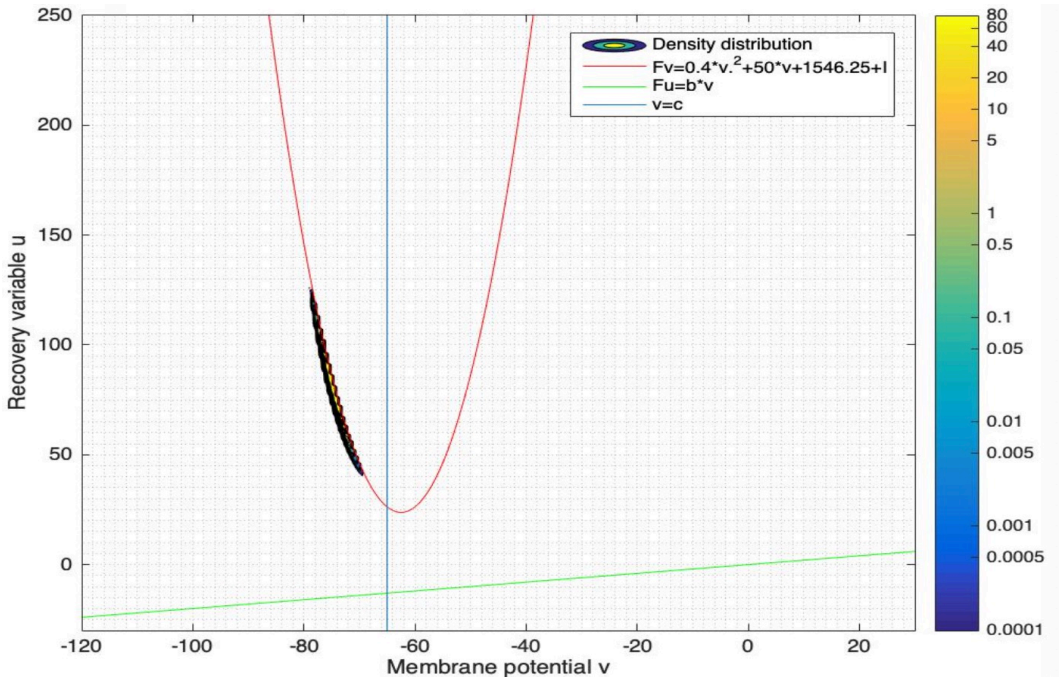

Figure 3.32: Density distribution at $t = 40ms$ of a coupled population with a narrower v-nullcline and an initial Dirac distribution at $u = -14$, $v = -70$.

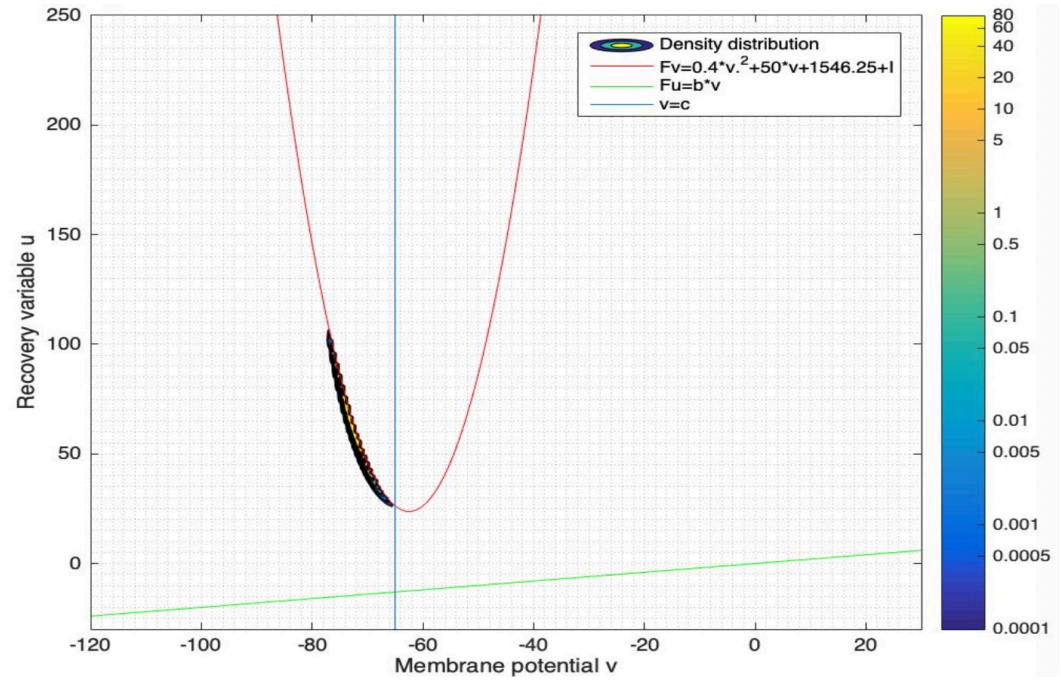

Figure 3.33: Density distribution at $t = 50ms$ of a coupled population with a narrower v-nullcline and an initial Dirac distribution at $u = -14$, $v = -70$.

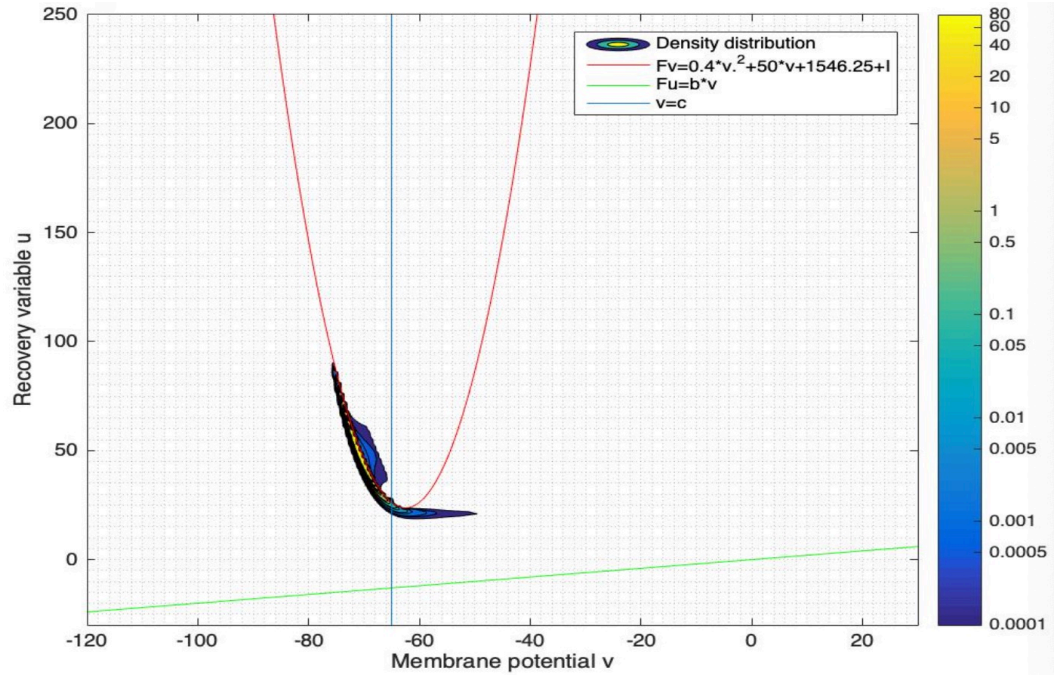

Figure 3.34: Density distribution at $t = 60ms$ of a coupled population with a narrower v-nullcline and an initial Dirac distribution at $u = -14$, $v = -70$.

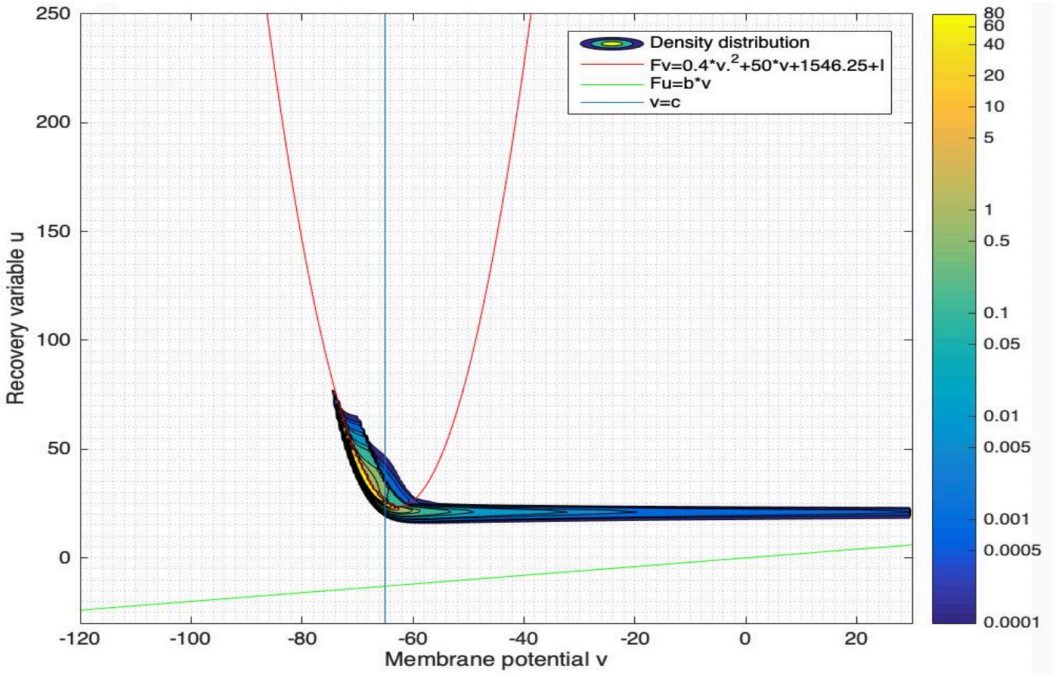

Figure 3.35: Density distribution at $t = 70ms$ of a coupled population with a narrower v-nullcline and an initial Dirac distribution at $u = -14$, $v = -70$.

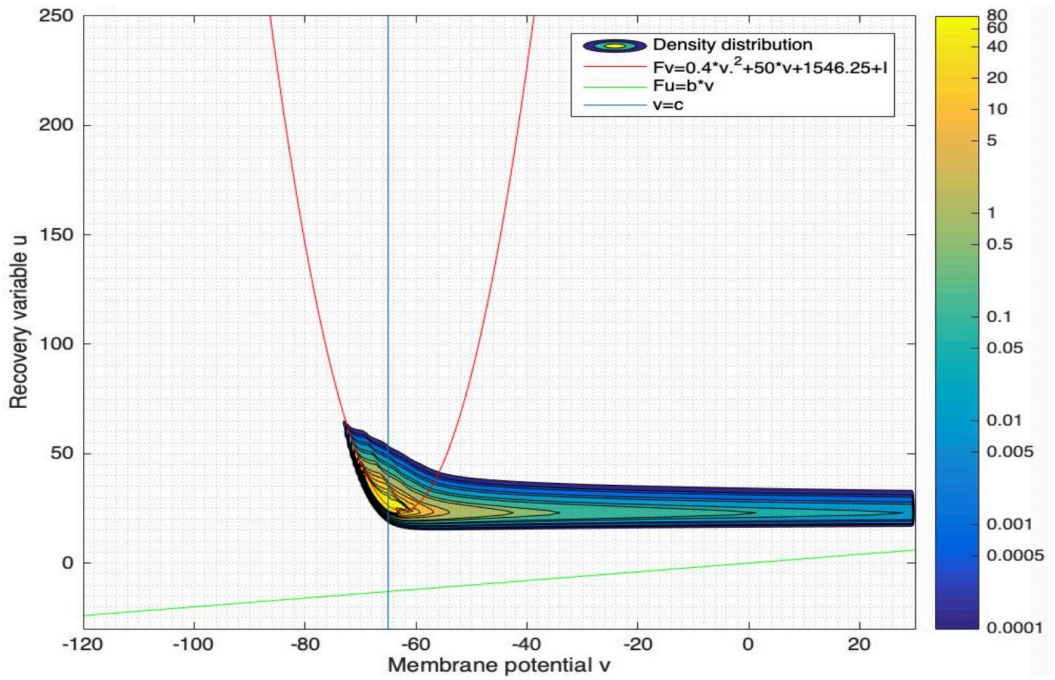

Figure 3.36: Density distribution at $t = 80ms$ of a coupled population with a narrower v-nullcline and an initial Dirac distribution at $u = -14$, $v = -70$.

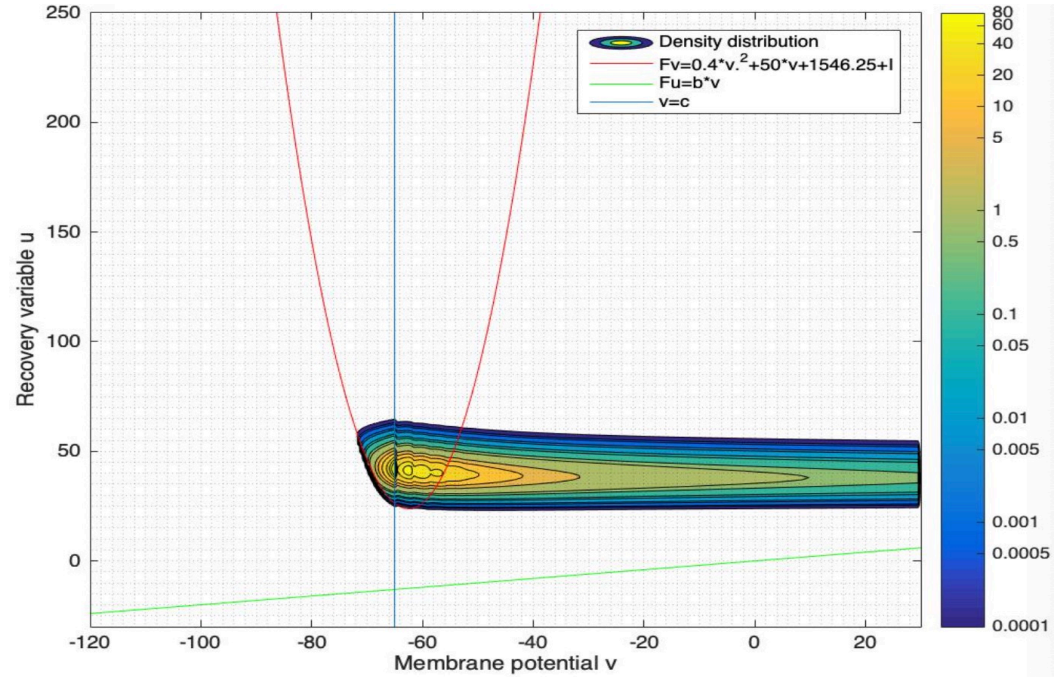

Figure 3.37: Density distribution at $t = 85ms$ of a coupled population with a narrower v-nullcline and an initial Dirac distribution at $u = -14$, $v = -70$.

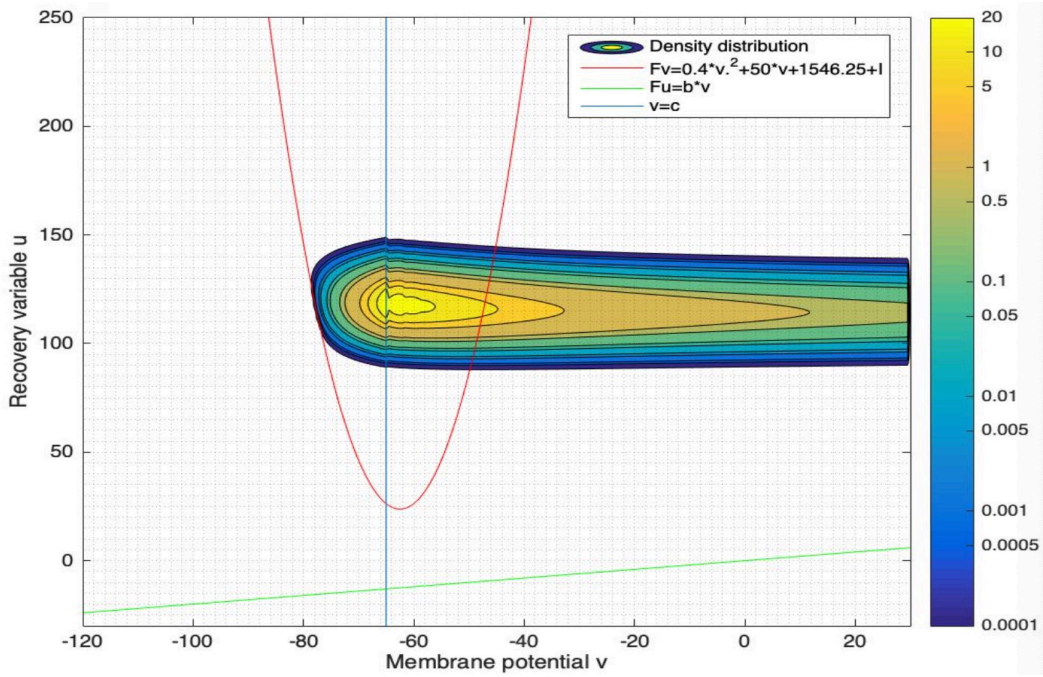

Figure 3.38: Density distribution at $t = 90ms$ of a coupled population with a narrower v-nullcline and an initial Dirac distribution at $u = -14$, $v = -70$.

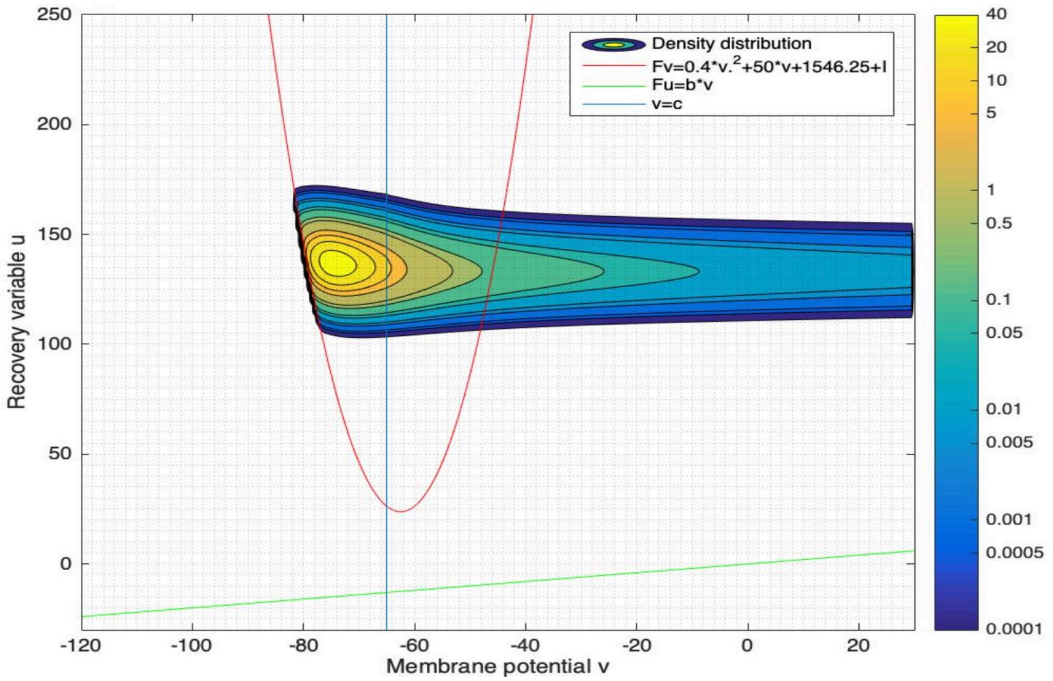

Figure 3.39: Density distribution at $t = 93ms$ of a coupled population with a narrower v-nullcline and an initial Dirac distribution at $u = -14$, $v = -70$.

Chapter 4

Interaction-Induced Bursting

4.1 From PDE to ODE

The density pictures from 3.2 show us the distribution of the population of neurons at a sequence of specific times. Although the density is somewhat spread out, there is a fairly localized pool of neurons (in phase space) that spikes several times, moving upwards in u and then falling into a recovery phase on the left branch of the v nullcline. In order to understand the behavior of a localized (in phase space) pool of neurons, we consider a Dirac distribution as initial condition. In the numerical scheme, this implies that all neurons are initially in a single grid cell, and analytically they must leave together under the flow of the vector field when they receive an impulse. However, in the numerical simulations, the nonzero spatial resolution leads to numerical diffusion, only a proportion of the neurons leave the initial grid cell in a small time step. That is why we can see many different colors (densities) in different grid cells. Actually, if the neurons are concentrated in a true Delta function they should leave and arrive together from one grid cell to another grid cell.

Without numerical approximation, however, and assuming identical neurons with identical numbers of afferents (inputs), we can analytically treat the population of

neurons as a single neuron. This leads to a new ODE system to describe the population dynamics. This ODE behavior is different from the Izhikevich model because the single cell that represents the whole population receives an impulse following a spike and reset after a small delay time. The impulse causes a "jump" in the v direction after a delay time 1ms [10]. Here we have a question: since the impulse size is fixed and the v-nullcline becomes arbitrarily wide as u increases, the single neuron (i.e. Dirac distribution of the population of neurons) cannot cross the right branch of the v-nullcline by neuron interaction for large u, so can neuron interaction cause bursting behavior?

To investigate this mechanism, we need to define a Poincaré map on the reset line (call it Φ), that describes the Izhikevich model with impulse ϵG in the v direction following a spike after a delay time τ=1ms, where $G > 0$ is the mean number of synaptic afferents per neuron, $\epsilon > 0$ is the distance of the "jump" for a single spike. We treat the Dirac distribution of the population of neurons as a single neuron, thus all neurons spike instantaneously and the total distance of the "jump" of the Dirac distribution is ϵG. Now we give the Izhikevich model with the "jumps":

$$\begin{aligned} \frac{dv}{dt} &= F_v + \epsilon G \sum_k \delta(t_k + \tau) + \sum_k (v_0 - v_s)\delta(t_k), \\ \frac{du}{dt} &= F_u + d \sum_k \delta(t_k), \end{aligned} \tag{4.1}$$

where $F_v = f(v) - u$, where $f(v) = 0.04v^2 + 5v + 140 + I$, $F_u = a(bv - u)$, $\{a, b, d\}$ are positive nonphysical parameters, I is fixed, ϵG is the total distance of the "jump" of the Dirac distribution in v, $v = v_0 = c$ is the reset line, $v = v_s$ is the spiking line, $\tau = 1$ms is the delay time and t_k are the times of spikes for $k = 1, 2, 3...$

We want to know if the Φ map has fixed points u_{fp} and the stability of the fixed points because Φ has a tonic firing behavior if the fixed point is stable ($-1 < \Phi'(u_{fp}) < 1$)

and Φ perhaps has a bursting behavior if the fixed point is unstable ($\Phi'(u_{fp}) < -1$). We consider the typical parameter values $a = 0.02$, $b = 0.2$, $v_0 = c = -65$, $v_s = 30$, $I = 40$, $\epsilon = 3$, $G = 15$ and the delay time τ=1ms [8][10] in this chapter. Next, we will give the description of Φ and study the mechanism of Φ.

4.2 The Φ map

4.2.1 The description of Φ

In Figure 4.1, $v = v_0 < 0$ is the reset line, $v = v_s > 0$ is the spiking line, $F_u = a(bv - u) = 0$ is the u-nullcline, the parabola $F_v = 0.04v^2 + 5v + 140 + I - u = 0$ is the v-nullcline, where I is fixed. Let (v_0, u_0) be the initial condition and let (v_a, u_a) be the vertex of the parabola $F_v = 0$.

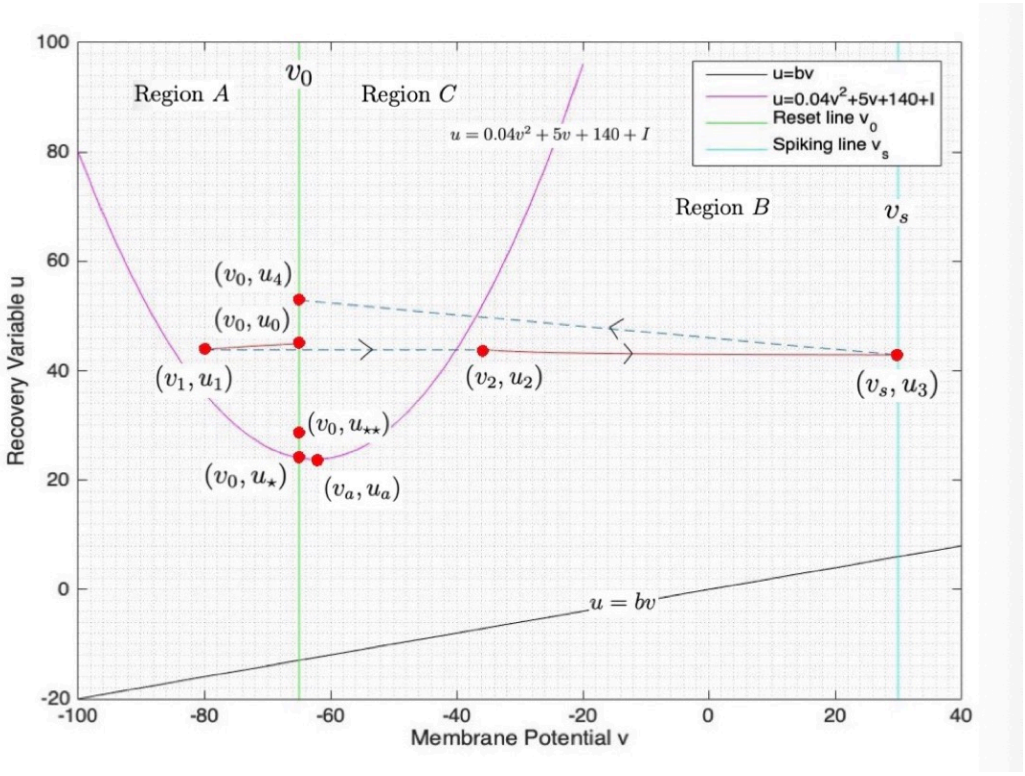

Figure 4.1: The Φ map is defined through four steps: Φ_1: $u_0 \mapsto (v_1, u_1)$, Φ_2: $(v_1, u_1) \mapsto (v_2, u_2)$, Φ_3: $(v_2, u_2) \mapsto u_3$ and Φ_4: $u_3 \mapsto u_4$.

Definition 1. *Define $u_\star$ so that the point $(v_0, u_\star)$ is the intersection between the reset line $v = v_0$ and the v-nullcline $F_v = 0$.*

Definition 2. *Define region $A = \{(v, u) : u > f(v), v \leq v_0\}$.*

Definition 3. *Define region $C = \{(v, u) : u > f(v), v > v_0\}$.*

The Φ map is defined through four steps:

Step I: Φ_1: $u_0 \mapsto (v_1, u_1)$, following the Izhikevich flow from (v_0, u_0) for $t = \tau = 1$ms.

Step II: Φ_2: $(v_1, u_1) \mapsto (v_2, u_2)$, instantaneous with $u_2 = u_1$, $v_2 = v_1 + \epsilon G$, where ϵG is sufficiently small such that $v_2 < v_s$ for any (v_0, u_0) with $u_0 > bv_0$.

Step III: Φ_3: $(v_2, u_2) \mapsto u_3$, following the Izhikevich flow from (v_2, u_2) to (v_s, u_3).

Step IV: Φ_4: $u_3 \mapsto u_4$ where $u_4 = u_3 + d$, instantaneously reset from (v_s, u_3) to (v_0, u_4).

The Φ map can be defined on $(bv_0, +\infty)$. Note: Actually, Φ is defined for some $u_0 < bv_0$, but $\exists u_{0,min} < bv_0$ such that $\Phi_1(u_{0,min}) = (v_s, u_1)$ and then Φ_1 can not be defined as above for $u_0 < u_{0,min}$ because v reaches v_s before $t = 1$ms. However, we will consider $u_0 > bv_0$ only.

Assumption 1. *Assume the v-nullcline is always above the u-nullcline such that $u_a > bv_s$. Also we assume $u_a > u_{3,min} > bv_s$, where $u_{3,min}$ will be defined in section 4.2.4.5, and which will imply that the trajectories beginning above the v-nullcline must stay above the u-nullcline.*

Definition 4. *Define region $B = \{(v, u) : u_{3,min} < u < f(v), -\infty < v \leq v_s\}$.*

Definition 5. *Let $u_{\star\star}$ be the smallest $u_0 > u_\star$ such that the trajectory reaches the left branch of the parabola $F_v = 0$ at $t = 1ms$.*

In the region A (see Figure 4.1), we have $\frac{dv}{dt} < 0$ and $\frac{du}{dt} < 0$. There exists an interval of initial conditions u_0 above $u_\star$, say $u_0 \in (u_\star, u_{\star\star})$ in Figure 4.2, such that

the trajectory reaches the left branch of the parabola $F_v = 0$ before $t = 1$ms. This case involves v going in both directions, so it is difficult to make a precise estimation of (v_1, u_1) later. When $u_0 \to +\infty$, although the width of parabola $F_v = 0$ is getting larger, it is still possible for the trajectory to cross the left branch of the parabola $F_v = 0$ before $t = 1$ms because $\frac{dv}{dt}$ is also getting larger as u increases. If there exists a $u_0 = u_{\star\star\star} > u_{\star\star}$ such that the trajectory reaches the left branch of the parabola $F_v = 0$ at $t = 1$ms, then we have an upper bound of the initial condition u_0. For the standard choices of parabola and v_0 chosen here and for typical values of parameters a, b, which are small, it is easy to verify that $u_{\star\star\star}$ is very large ($u_{\star\star\star} \gg u_a$).

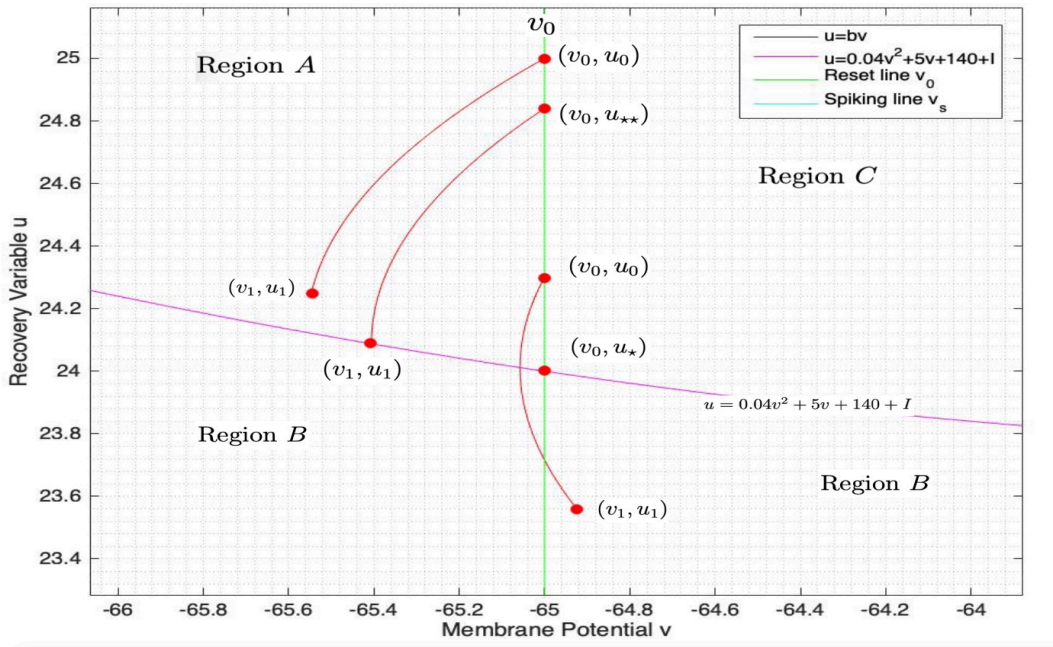

Figure 4.2: The trajectory with initial condition $u_0 \in (u_\star, u_{\star\star})$ reaches the parabola $F_v = 0$ before $t = 1$ms and it involves v going in both directions.

Definition 6. *Let $u_{\star\star\star}$ be the biggest $u_0 > u_{\star\star}$ if it exists such that the trajectory reaches the left branch of the parabola $F_v = 0$ at $t = 1ms$, otherwise we take $u_{\star\star\star} = +\infty$.*

Let $\mathcal{D} = (u_{\star\star}, u_{\star\star\star})$. If $u_0 \in \mathcal{D}$ in Figure 4.2, then the trajectory that starts from

(v_0, u_0), stays in the region A up to $t = 1$ms. Moreover, if $u_0 \in (bv_0, u_\star]$, then the Φ map has a different dynamic that we are not interested in. Therefore, for our convenience, we define the Φ map on $\mathcal{D}$.

4.2.2 Φ_1: $u_0 \mapsto (v_1, u_1)$

4.2.2.1 The estimation of u_1 and v_1

Recall that $\frac{du}{dt} = a(bv - u) < 0$ is always true from Assumption 1 (given our initial condition above the v-nullcline) and $\frac{dv}{dt} = 0.04v^2 + 5v + 140 - u + I < 0$ in the region A, where $0 < a < b$ and $I = 40$ [10]. Both $v_0 < 0$ and $u_0 > 0$ are the maximum value in v and u respectively and $\tau = 1$ms. If we use the given initial condition (v_0, u_0) to evaluate (v_1, u_1), then for u_1 we have

$$\begin{aligned} \int_0^\tau dt &= \int_{u_0}^{u_1} \frac{du}{a(bv(u) - u)} \\ \Rightarrow \tau &= \int_{u_0}^{u_1} \frac{du}{abv(u) - au} \\ &= \int_{u_1}^{u_0} \frac{du}{au - abv(u)}, \end{aligned} \tag{4.2}$$

where $abv(u) - au < 0$.

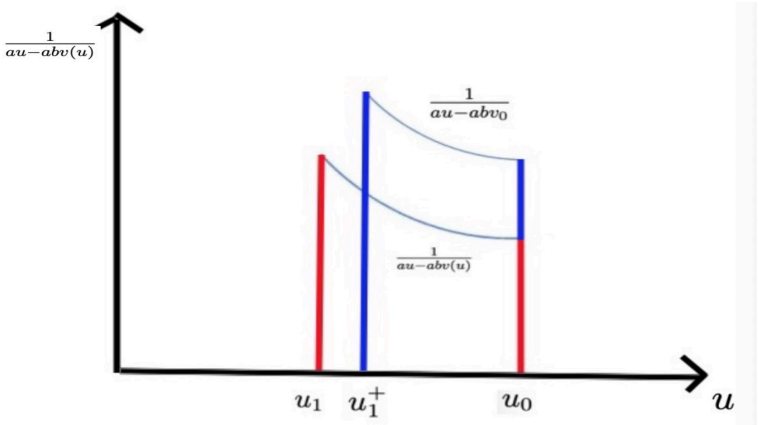

Figure 4.3: An upper bound for u_1. $\frac{1}{au-abv(u)} < \frac{1}{au-abv_0}$, the area is fixed and u_0 is fixed, so $u_1^+ > u_1$.

Since $v(u) < v_0 < 0$ for $0 < u < u_0$, we let $u_1^+ > u_1$ be defined such that

$$\tau = \int_{u_1}^{u_0} \frac{du}{au - abv(u)} = \int_{u_1^+}^{u_0} \frac{du}{au - abv_0}. \tag{4.3}$$

Then, $\frac{1}{au-abv(u)} < \frac{1}{au-abv_0}$ and u_0 is fixed, so $u_1^+ > u_1$ (see Figure 4.3). Thus, we are looking for u_1^+, which is an upper bound for u_1. Let $w = au - abv_0 \Rightarrow dw = adu \Rightarrow du = \frac{dw}{a}$. Then

$$\begin{aligned}
\tau &< \int_{u_1}^{u_0} \frac{du}{au - abv_0} \\
&= \int_{w(u_1)}^{w(u_0)} \frac{1}{w} \cdot \frac{dw}{a} \\
&= \frac{1}{a} \int_{w(u_1)}^{w(u_0)} \frac{1}{w} dw \\
&= \frac{1}{a} \ln |w|_{w(u_1)}^{w(u_0)} \\
&= \frac{1}{a} \ln |au - abv_0|_{u_1}^{u_0} \\
&= \frac{1}{a} \left(\ln |au_0 - abv_0| - \ln |au_1 - abv_0| \right).
\end{aligned} \tag{4.4}$$

Since $au_0 - abv_0 > 0$, $au_1 - abv_0 > 0$ and $a > 0$, we have

$$\begin{aligned}
a\tau &< \ln(au_0 - abv_0) - \ln(au_1 - abv_0) \\
\Leftrightarrow \ln(au_1 - abv_0) &< \ln(au_0 - abv_0) - a\tau \\
\Leftrightarrow au_1 - abv_0 &< \exp(\ln(au_0 - abv_0) - a\tau) \\
&= (au_0 - abv_0) \exp(-a\tau) \\
\Leftrightarrow au_1 &< (au_0 - abv_0) \exp(-a\tau) + abv_0 \\
&= a \left(\frac{u_0 - bv_0}{e^{a\tau}} + bv_0 \right)
\end{aligned} \tag{4.5}$$

$$\Leftrightarrow u_1 < \frac{u_0 - bv_0}{e^{a\tau}} + bv_0. \tag{4.6}$$

So here we have found the upper bound of u_1. Therefore $u_1^+ = \frac{u_0 - bv_0}{e^{a\tau}} + bv_0$, where

$\tau = 1$ms.

Next for v_1 we have

$$\begin{aligned} \int_0^{\tau} dt &= \int_{v_0}^{v_1} \frac{1}{0.04v^2 + 5v + 140 + I - u(v)} dv \\ \Rightarrow \tau &= \int_{v_0}^{v_1} \frac{1}{0.04v^2 + 5v + 140 + I - u(v)} dv \\ &= \int_{v_1}^{v_0} \frac{1}{u(v) - (0.04v^2 + 5v + 140 + I)} dv, \end{aligned} \tag{4.7}$$

where $0.04v^2 + 5v + 140 + I - u(v) < 0$ in the region A. Recall that $f(v) = 0.04v^2 + 5v + 140 + I$, then $u(v) - f(v) > 0$. Since $u_0 > u(v) > 0$ for $v < v_0 < 0$, where $u_0 \in \mathcal{D}$, we let $v_1^- < v_1$ be defined such that

$$\tau = \int_{v_1}^{v_0} \frac{dv}{u(v) - f(v)} = \int_{v_1^-}^{v_0} \frac{dv}{u_0 - f(v)}. \tag{4.8}$$

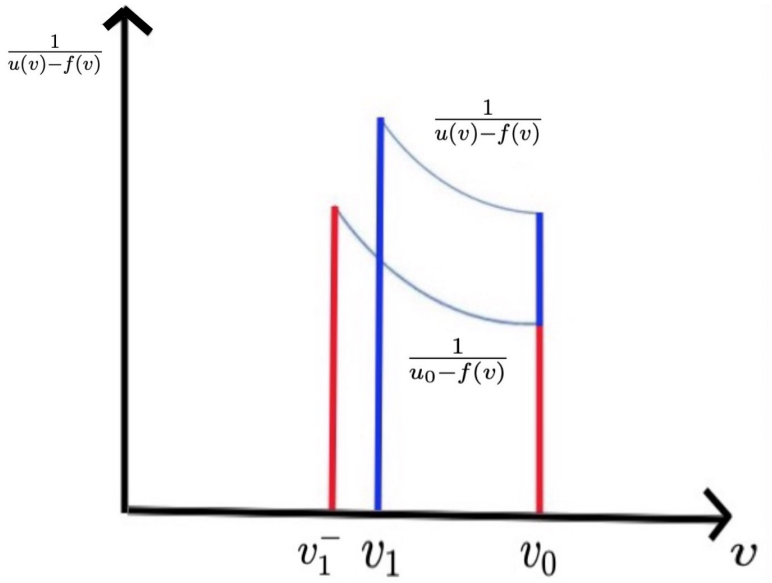

Figure 4.4: A lower bound for v_1. $\frac{1}{u(v)-f(v)} > \frac{1}{u_0-f(v)}$, the area is fixed and v_0 is fixed, so $v_1 > v_1^-$.

Then, $\frac{1}{u(v)-f(v)} > \frac{1}{u_0-f(v)}$ and v_0 is fixed, so $v_1 > v_1^-$ (see Figure 4.4). Thus, we are

looking for v_1^-, which is a lower bound of v_1. Now

$$\begin{aligned}\tau &> \int_{v_1}^{v_0} \frac{1}{u_0 - (0.04v^2 + 5v + 140 + I)} dv \\ &= \int_{v_1}^{v_0} \frac{1}{u_0 - [0.04(v + 62.5)^2 - 156.25 + 140 + I]} dv \\ &= \int_{v_1}^{v_0} \frac{1}{u_0 - 0.04(v + 62.5)^2 + 16.25 - I} dv.\end{aligned} \tag{4.9}$$

Let $\mu = u_0 + 16.25 - I > 0$ be a constant, where $u_0 \in \mathcal{D}$ and $I = 40$. Thus,

$$\tau > \int_{v_1}^{v_0} \frac{1}{\mu - 0.04(v + 62.5)^2} dv. \tag{4.10}$$

It is easy to find that $\frac{dv}{dt} = f(v) - u = 0$ at $v = -62.5$ and $u = 23.75$, so the vertex of parabola $F_v = 0$ is

$$v_a = -62.5, u_a = 23.75 \tag{4.11}$$

Let $s = v + 62.5 \Rightarrow ds = dv$, then

$$\begin{aligned}\Rightarrow \tau &> \int_{s(v_1)}^{s(v_0)} \frac{1}{\mu - 0.04s^2} ds \\ &= \int_{s(v_1)}^{s(v_0)} \frac{1}{0.04(\frac{\mu}{0.04} - s^2)} ds \\ &= \int_{s(v_1)}^{s(v_0)} \frac{1}{0.04(25\mu - s^2)} ds \\ &= 25 \int_{s(v_1)}^{s(v_0)} \frac{1}{25\mu - s^2} ds\end{aligned} \tag{4.12}$$

Since $25\mu > 0$, we let $\alpha^2 = 25\mu \Rightarrow \alpha = 5\sqrt{\mu} = 5\sqrt{u_0 - u_a} > 0$, thus

$$\begin{aligned}\Rightarrow \tau &> 25 \int_{s(v_1)}^{s(v_0)} \frac{1}{\alpha^2 - s^2} ds \\ &= 25 \int_{s(v_1)}^{s(v_0)} \frac{1}{(\alpha - s)(\alpha + s)} ds \\ &= \frac{25}{2\alpha} \ln \left| \frac{s + \alpha}{s - \alpha} \right|_{s(v_1)}^{s(v_0)}.\end{aligned} \tag{4.13}$$

Obviously, $s = \alpha$ and $s = -\alpha$ are the singular points of the integration. Clearly $\alpha = 5\sqrt{u_0 - u_a} > v_0 + 62.5 = s(v_0)$ as $u_0 \in \mathcal{D}$, where $I = 40$ and $v_0 = -65$, so $s(v_1) < s(v_0) < \alpha$. Moreover, if $s(v_1) < -\alpha$, then the integration blows up. However, it is bounded by the fixed $\tau = 1$ms. Thus, this is a contradiction. Hence, we have $-\alpha < s(v_1) < s(v_0) < \alpha$. $s(v_1) = v_1 + 62.5 > -5\sqrt{u_0 - u_a} = -\alpha \Rightarrow v_1 > -5\sqrt{u_0 - u_a} - 62.5$. Therefore,

$$v_1^- = -5\sqrt{u_0 - u_a} + v_a. \tag{4.14}$$

Please note that this is not a good bound; however it is a simple bound.

Now, if we want a better lower bound of v_1, then we can continue to solve for v_1

$$\tau > \frac{25}{2\alpha} \ln \left| \frac{s+\alpha}{s-\alpha} \right|_{s(v_1)}^{s(v_0)}$$

$$\Leftrightarrow \frac{2\tau\alpha}{25} > \ln \left| \frac{s(v_0)+\alpha}{s(v_0)-\alpha} \right| - \ln \left| \frac{s(v_1)+\alpha}{s(v_1)-\alpha} \right|$$

$$\Leftrightarrow \ln \left| \frac{s(v_1)+\alpha}{s(v_1)-\alpha} \right| > \ln \left| \frac{s(v_0)+\alpha}{s(v_0)-\alpha} \right| - \frac{2\tau\alpha}{25}$$

$$\Leftrightarrow \left| \frac{s(v_1)+\alpha}{s(v_1)-\alpha} \right| > \exp\left(\ln \left| \frac{s(v_0)+\alpha}{s(v_0)-\alpha} \right| - \frac{2\tau\alpha}{25} \right)$$

$$= \left| \frac{s(v_0)+\alpha}{s(v_0)-\alpha} \right| \exp\left(-\frac{2\tau\alpha}{25} \right) > 0.$$

Since $s(v_1) > -\alpha \Rightarrow s(v_1) + \alpha > 0$ and $s(v_1) < \alpha \Rightarrow s(v_1) - \alpha < 0$, we have

$$-\left(\frac{s(v_1)+\alpha}{s(v_1)-\alpha} \right) > \left| \frac{s(v_0)+\alpha}{s(v_0)-\alpha} \right| \exp\left(-\frac{2\tau\alpha}{25} \right) > 0.$$

Replacing $s(v_1)$ and $s(v_0)$ by $v_1 + 62.5$ and $v_0 + 62.5$, we get

$$-\left(\frac{v_1+62.5+\alpha}{v_1+62.5-\alpha} \right) > \left| \frac{v_0+62.5+\alpha}{v_0+62.5-\alpha} \right| e^{\frac{-2\tau\alpha}{25}}$$

$$\Leftrightarrow -(v_1+62.5+\alpha) < \left|\frac{v_0+62.5+\alpha}{v_0+62.5-\alpha}\right| e^{\frac{-2\tau\alpha}{25}}(v_1+62.5-\alpha)$$

$$\Leftrightarrow -v_1-62.5-\alpha < \left|\frac{v_0+62.5+\alpha}{v_0+62.5-\alpha}\right| e^{\frac{-2\tau\alpha}{25}} v_1 + \left|\frac{v_0+62.5+\alpha}{v_0+62.5-\alpha}\right| e^{\frac{-2\tau\alpha}{25}}(62.5-\alpha)$$

$$\Leftrightarrow -\left(1+\left|\frac{v_0+62.5+\alpha}{v_0+62.5-\alpha}\right| e^{\frac{-2\tau\alpha}{25}}\right) v_1 < \left|\frac{v_0+62.5+\alpha}{v_0+62.5-\alpha}\right| e^{\frac{-2\tau\alpha}{25}}(62.5-\alpha)+62.5+\alpha$$

$$\Leftrightarrow v_1 > \frac{\left|\frac{v_0+62.5+\alpha}{v_0+62.5-\alpha}\right| e^{\frac{-2\tau\alpha}{25}}(62.5-\alpha)+62.5+\alpha}{-\left(1+\left|\frac{v_0+62.5+\alpha}{v_0+62.5-\alpha}\right| e^{\frac{-2\tau\alpha}{25}}\right)}, \tag{4.15}$$

So here we have a better lower bound of v_1, say $\tilde{v}_1^-$ which is

$$\tilde{v}_1^- = \frac{\left|\frac{v_0+62.5+\alpha}{v_0+62.5-\alpha}\right| e^{\frac{-2\tau\alpha}{25}}(62.5-\alpha)+62.5+\alpha}{-\left(1+\left|\frac{v_0+62.5+\alpha}{v_0+62.5-\alpha}\right| e^{\frac{-2\tau\alpha}{25}}\right)}, \tag{4.16}$$

where $\alpha = 5\sqrt{\mu} = 5\sqrt{u_0-u_a} > 0$. However, the better lower bound of v_1 is too complicated, so we will not use it later unless we want to apply the typical parameter values. Now we have an upper bound for u_1 and a lower bound for v_1. By a similar argument, we can find a lower bound for u_1 using v_1^- in (4.3) instead of v_0, which is $u_1^- = \frac{u_0-bv_1^-}{e^a} + bv_1^-$. Then using u_1^- in (4.8) instead of u_0, we get an upper bound for v_1, which is $v_1^+ = -5\sqrt{u_1^- - u_a} + v_a$. The better upper bound for v_1 is

$$\tilde{v}_1^+ = \frac{\left|\frac{v_0+62.5+\alpha}{v_0+62.5-\alpha}\right| e^{\frac{-2\tau\alpha}{25}}(62.5-\alpha)+62.5+\alpha}{-\left(1+\left|\frac{v_0+62.5+\alpha}{v_0+62.5-\alpha}\right| e^{\frac{-2\tau\alpha}{25}}\right)}, \tag{4.17}$$

where $\alpha = 5\sqrt{\mu} = 5\sqrt{u_1^- - u_a} > 0$. We will not use it later.

Remark 1. *$\frac{du}{dt} < 0$ is always true from Assumption 1, so u_1^+ is valid for all $u_0 \in (u_{\star\star}, +\infty)$. However, $\frac{dv}{dt} < 0$ in the region A and $\frac{dv}{dt} > 0$ in the region B, so v_1^-, u_1^-, v_1^+ are valid for $u_0 \in \mathcal{D}$ only.*

4.2.2.2 The description of Φ_1

For later use, we need some properties of Φ_1, given by the following Lemmas.

Lemma 1. *For $a, b > 0$, we have $\frac{du_1}{du_0} > 0$ for a fixed $\tau = 1$ ms.*

Proof. We have $\frac{du}{dt} = a(bv - u) < 0$ from Assumption 1 (given our initial condition above the v-nullcline) and fix $\tau = 1$ ms, then

$$\begin{aligned} \int_0^1 dt &= \int_{u_0}^{u_1} \frac{1}{a(bv(u) - u)} du \\ \Rightarrow 1 &= \int_{u_0}^{u_1} \frac{1}{a(bv(u) - u)} du. \end{aligned} \tag{4.18}$$

Applying the Fundamental Theorem of Calculus, we have

$$1 = G(u_1) - G(u_0) \tag{4.19}$$

for $G(u)$ such that $G'(u) = \frac{1}{a(bv(u)-u)}$. By taking derivatives with respect to u_0 on both sides,

$$\begin{aligned} 0 &= \frac{d[G(u_1) - G(u_0)]}{du_0} \\ &= \frac{dG(u_1)}{du_1} \cdot \frac{du_1}{du_0} - \frac{dG(u_0)}{du_0} \\ &= \frac{1}{a(bv_1 - u_1)} \cdot \frac{du_1}{du_0} - \frac{1}{a(bv_0 - u_0)}. \\ \Leftrightarrow \frac{du_1}{du_0} &= \frac{a(bv_1 - u_1)}{a(bv_0 - u_0)} \\ &= \frac{bv_1 - u_1}{bv_0 - u_0} > 0, \end{aligned} \tag{4.20}$$

because $a > 0$ and $\frac{du}{dt} < 0$, so $bv - u < 0$ at both (v_0, u_0) and (v_1, u_1), so $\frac{du_1}{du_0} > 0$ for a fixed $\tau = 1$ ms.

□

Remark 2. *$\frac{du}{dt} < 0$ is always true from Assumption 1, so $\frac{du_1}{du_0} > 0$ is valid for all*

$u_0 \in (u_{\star\star}, +\infty)$ *for a fixed* $\tau = 1$ *ms.*

Lemma 1 shows that $u_1(u_0)$ is an increasing function with respect to u_0. Next, we want to show that $\frac{dv_1}{du_0} < 0$ for a fixed $\tau = 1$ ms in the following Lemma.

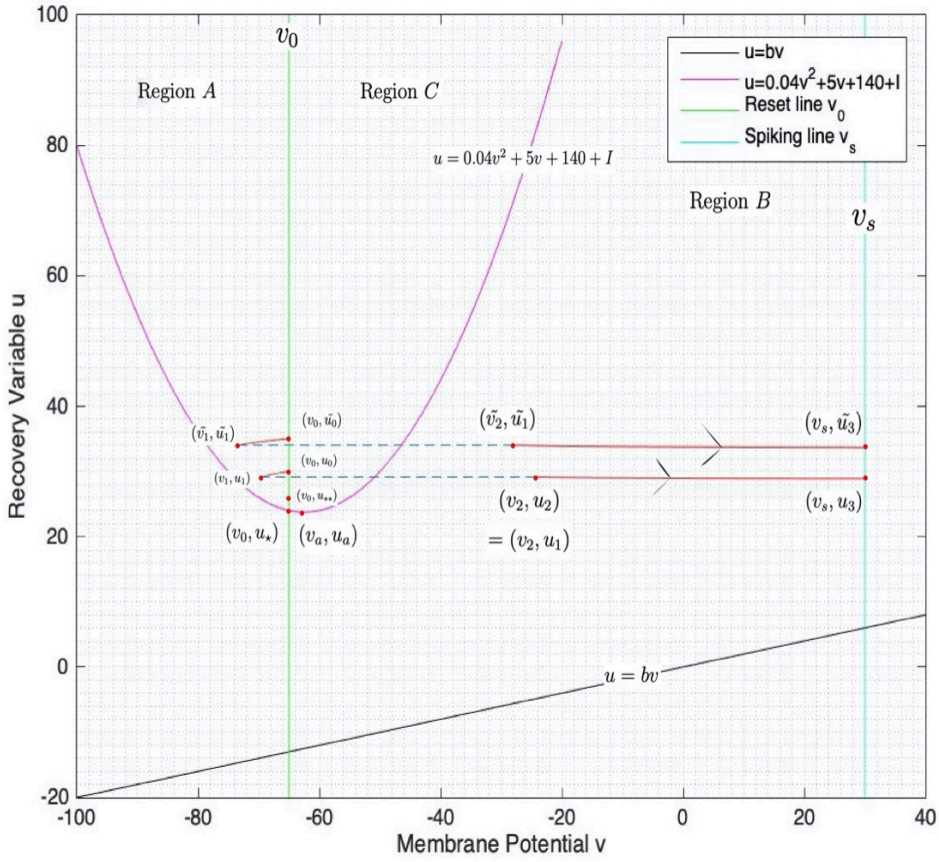

Figure 4.5: Φ with initial conditions u_0 and $\tilde{u}_0$, where $\tilde{u}_0 > u_0$.

Lemma 2. *For* $a, b > 0$*, let* $u_0, \tilde{u}_0 \in \mathcal{D}$*, then* $\tilde{v}_1 < v_1$ *if and only if* $\tilde{u}_0 > u_0$ *for a fixed* $\tau = 1$ *ms.*

Proof. Case 1: $u_{\star\star\star}$ does not exist, then $\mathcal{D} = (u_{\star\star}, +\infty)$.

($\Leftarrow$) Clearly, $u_0, \tilde{u}_0 \in \mathcal{D}$, so (v_1, u_1) and $(\tilde{v}_1, \tilde{u}_1)$ are in the region A (see Figure 4.5). $\frac{dv}{dt} = 0.04v^2 + 5v + 140 - u + I < 0$. Recall that we fix $\tau = 1$ ms and let $u = u_0$ as an

initial condition. Then,

$$\begin{aligned} \int_0^1 dt &= \int_{v_0}^{v_1} \frac{1}{0.04v^2 + 5v + 140 - u(v) + I} dv \\ \Rightarrow 1 &= \int_{v_0}^{v_1} \frac{1}{0.04v^2 + 5v + 140 - u(v) + I} dv, \end{aligned} \tag{4.21}$$

where $u(v) = u(v, u_0)$ is the solution curve. Recall that $f(v) = 0.04v^2 + 5v + 140 + I$, where I is fixed. Then,

$$\begin{aligned} 1 &= \int_{v_0}^{v_1} \frac{1}{f(v) - u(v)} dv \\ &= -\int_{v_1}^{v_0} \frac{1}{f(v) - u(v)} dv \\ &= \int_{v_1}^{v_0} \frac{1}{u(v) - f(v)} dv. \end{aligned} \tag{4.22}$$

Assuming $\tilde{u}_0 > u_0$, by the uniqueness theorem for ODEs, $\tilde{u}(v) > u(v)$, so $\frac{1}{\tilde{u}(v)-f(v)} < \frac{1}{u(v)-f(v)}$. Since the integral is always equal to 1, $\tilde{v}_1 < v_1$ (see Figure 4.6).

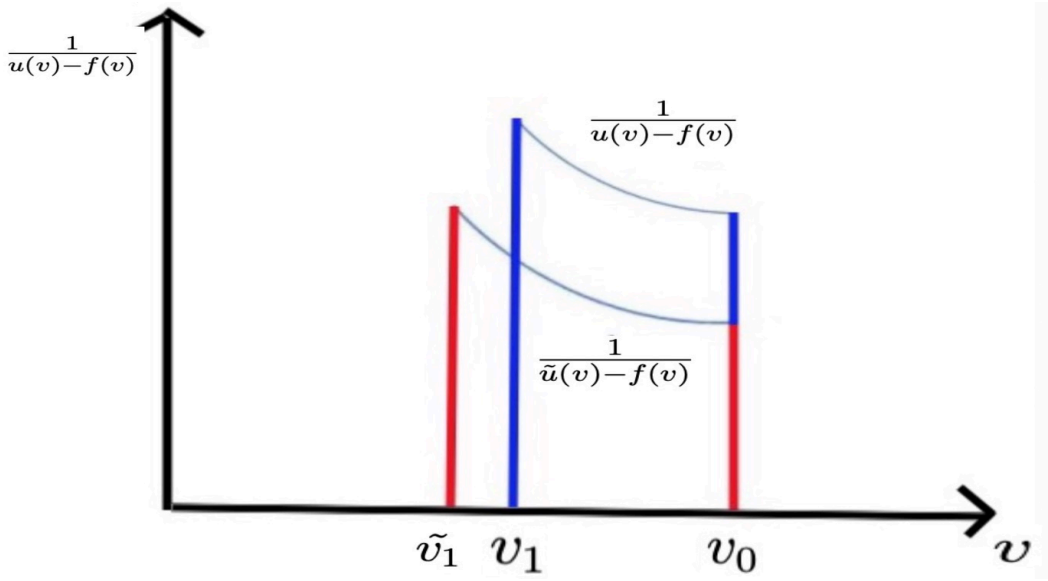

Figure 4.6: The integral is always equal to 1 and v_0 is fixed, so $\tilde{v}_1 < v_1$.

($\Rightarrow$) Next, again we have $\frac{du}{dt} = a(bv - u) < 0$ from Assumption 1 and fix $\tau = 1$ ms. Let $v = v_1$ as an initial condition. Then,

$$\begin{aligned}\int_0^1 dt &= \int_{u_0}^{u_1} \frac{1}{a(bv(u)-u)}du \\ \Rightarrow 1 &= -\int_{u_1}^{u_0} \frac{1}{a(bv(u)-u)}du \\ &= \int_{u_1}^{u_0} \frac{1}{au-abv(u)}du.\end{aligned} \tag{4.23}$$

Assuming $\tilde{v}_1 < v_1$, by the uniqueness theorem for ODEs, $\tilde{v}(u) < v(u)$, so $\frac{1}{au-ab\tilde{v}(u)} < \frac{1}{au-abv(u)}$. Since the integral is always equal to 1, $\tilde{u}_0 > u_0$ (see Figure 4.7).

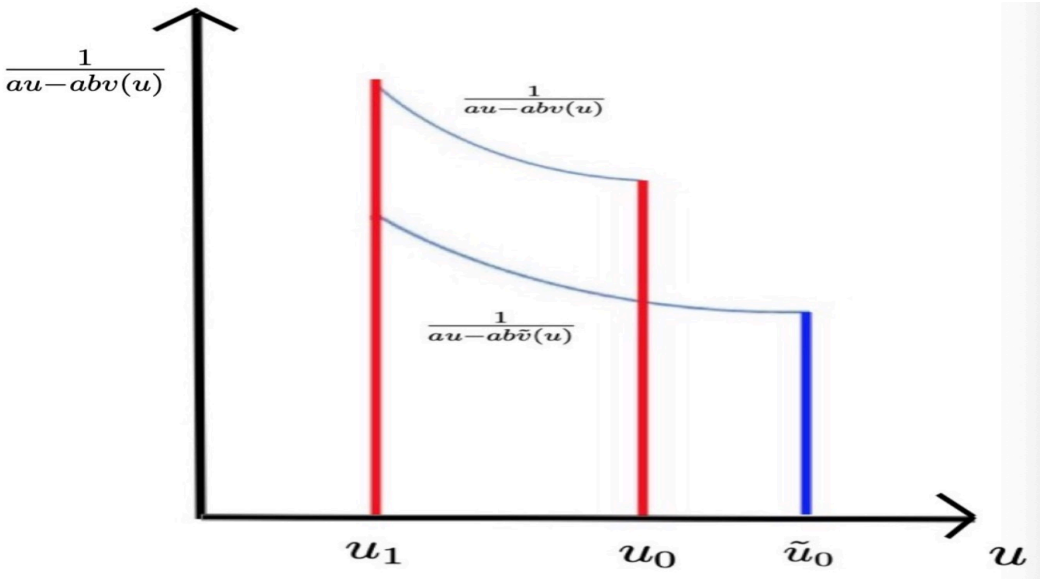

Figure 4.7: The integral is always equal to 1 and u_1 is given, so $\tilde{u}_0 > u_0$.

Case 2: $u_{\star\star\star}$ exists, then the result of case 1 holds for all $u_0 \in \mathcal{D} = (u_{\star\star}, u_{\star\star\star})$. For $u_0 \in [u_{\star\star\star}, +\infty)$, we have

Case 2a: (v_1, u_1) is on the left branch of the v-nullcline and $(\tilde{v}_1, \tilde{u}_1)$ are in the region B (see Figure 4.8).

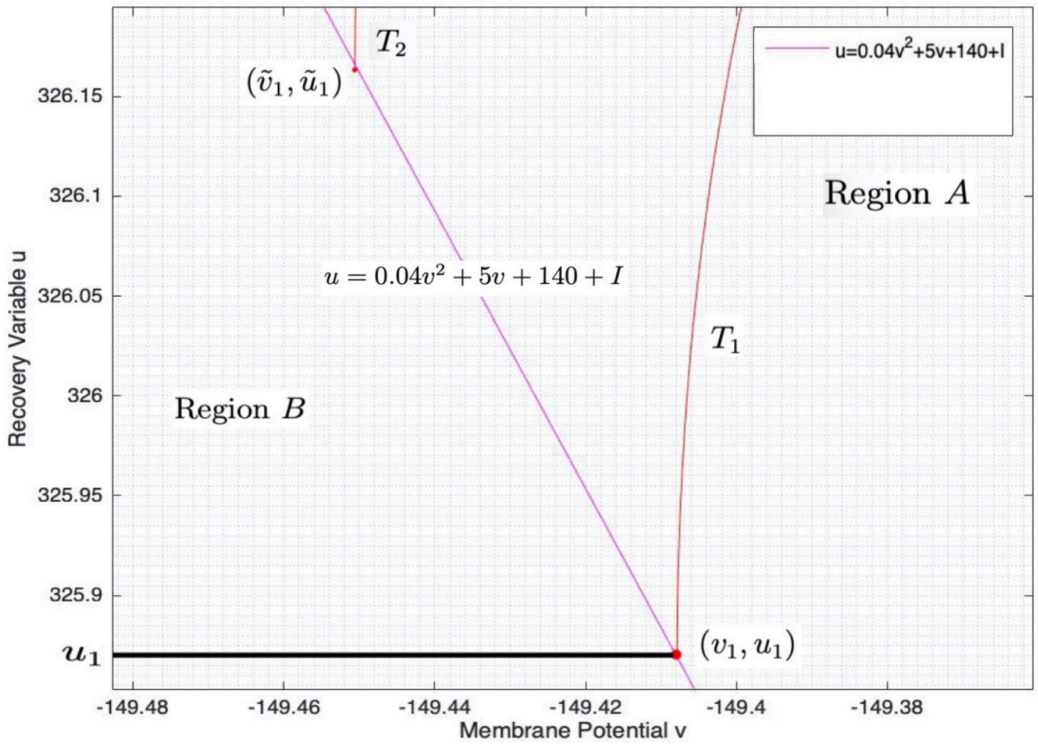

Figure 4.8: (v_1, u_1) is on the left branch of the v-nullcline and $(\tilde{v}_1, \tilde{u}_1)$ is in the region B for a fixed $\tau = 1$ ms.

Clearly, $\Phi_1(u_{\star\star\star}) = (v_1, u_1)$. According to Lemma 1, $\frac{du_1}{du_0} > 0$ is valid for all $u_0 \in (u_{\star\star}, +\infty)$ for a fixed $\tau = 1$ ms, so $\tilde{u}_1 > u_1$ when $\tilde{u}_0 > u_0$. Moreover, $(\tilde{v}_1, \tilde{u}_1)$ are in the region B, so $\tilde{v}_1 < v_1$ because the width of parabola $F_v = 0$ increases with u.

Case 2b: Both (v_1, u_1) and $(\tilde{v}_1, \tilde{u}_1)$ are in the region B for a fixed $\tau = 1$ ms (see Figure 4.9).

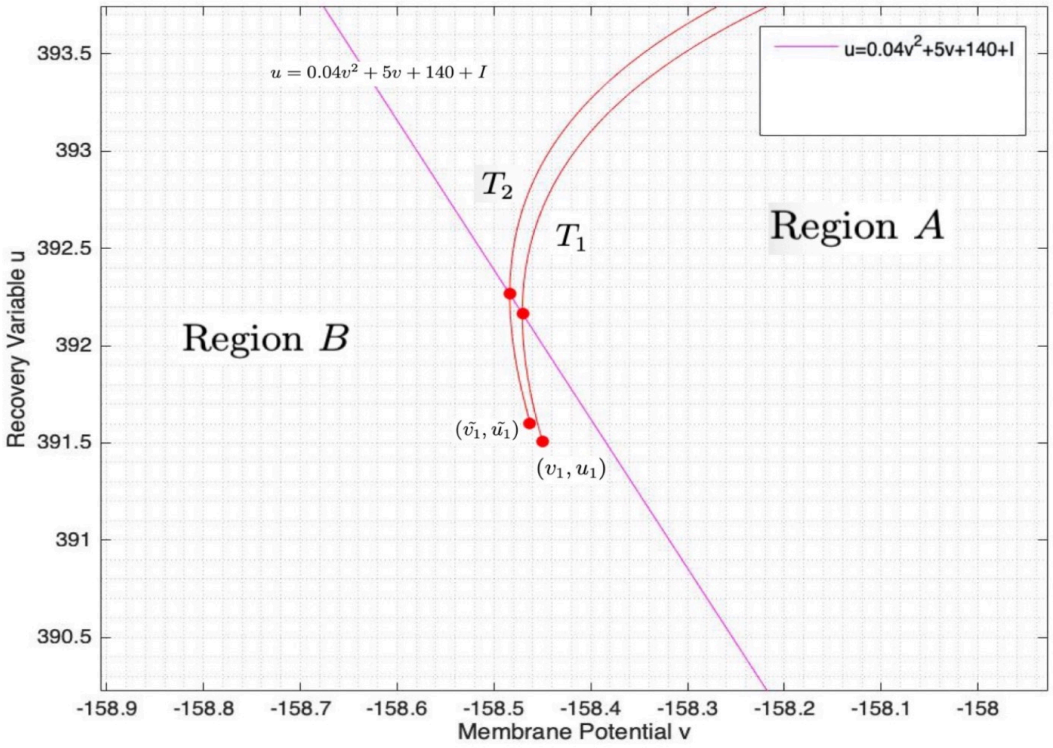

Figure 4.9: Both (v_1, u_1) and $(\tilde{v}_1, \tilde{u}_1)$ are in the region B for a fixed $\tau = 1$ ms.

(By contradiction) Let T_1 be a solution curve from (v_0, u_0) to (v_1, u_1) and T_2 be a solution curve from $(v_0, \tilde{u}_0)$ to $(\tilde{v}_1, \tilde{u}_1)$, where $\tilde{u}_0 > u_0$. We know that $\tilde{v}(t) < v(t)$ at a given t while both T_1 and T_2 are in the region A by the argument of case 1. Now $\tilde{u}_1 > u_1$ in the region B. Assume $\tilde{v}_1 \geq v_1$ in the region B, then T_2 must cross T_1 in the region B because $\tilde{v}(t)$ moves from the left of $v(t)$ to the right of $v(t)$ while $\tilde{u}(t) > u(t)$, so T_1 and T_2 have an intersection in the region B. Clearly, this is a contradiction with the uniqueness theorem for ODEs. Therefore, $\tilde{v}_1 < v_1$ in the region B when $\tilde{u}_0 > u_0$ for a fixed $\tau = 1$ ms.

□

Lemma 2 implies that $\frac{dv_1}{du_0} < 0$ in both region A and B for $u_0 \in (u_{\star\star}, +\infty)$ for a fixed $\tau = 1$ ms.

Lemma 3. *For $a, b > 0$, $u_1(u_0)$ is concave up and if $u_0 \to +\infty$, then $u_1 \to +\infty$.*

Proof. By Lemma 1, we have $\frac{du_1}{du_0} = \frac{u_1 - bv_1}{u_0 - bv_0} > 0$. Now

$$\begin{aligned}
\frac{d}{du_0}\left(\frac{du_1}{du_0}\right) &= \frac{(u_0 - bv_0)\left(\frac{du_1}{du_0} - b\frac{dv_1}{du_0}\right) - (u_1 - bv_1)}{(u_0 - bv_0)^2} \\
&= \frac{(u_0 - bv_0)\frac{du_1}{du_0} - b(u_0 - bv_0)\frac{dv_1}{du_0} - (u_1 - bv_1)}{(u_0 - bv_0)^2} \\
&= \frac{(u_0 - bv_0)\frac{u_1 - bv_1}{u_0 - bv_0} - b(u_0 - bv_0)\frac{dv_1}{du_0} - (u_1 - bv_1)}{(u_0 - bv_0)^2} \\
&= \frac{(u_1 - bv_1) - b(u_0 - bv_0)\frac{dv_1}{du_0} - (u_1 - bv_1)}{(u_0 - bv_0)^2} \\
&= \frac{(-b)(u_0 - bv_0)\frac{dv_1}{du_0}}{(u_0 - bv_0)^2} > 0 \\
&= \frac{(-b)\frac{dv_1}{du_0}}{u_0 - bv_0} > 0,
\end{aligned} \tag{4.24}$$

where $b > 0$, $u_0 - bv_0 > 0$ and $\frac{dv_1}{du_0} < 0$ by Lemma 2, so $u_1(u_0)$ is concave up. Also by Lemma 1, we let

$$\left.\frac{du_1}{du_0}\right|_{u_0 = u_{\star\star}} = \frac{u_1(u_0) - bv_1(u_0)}{u_0 - bv_0} = C > 0, \tag{4.25}$$

where C is a constant. So $\frac{du_1}{du_0} \geq C$ for all $u_0 \geq u_{\star\star}$. Therefore, if $u_0 \to +\infty$, then $u_1 \to +\infty$. □

Lemma 3 implies that the slope of $u_1(u_0)$ is increasing for $u_0 \in (u_{\star\star}, +\infty)$. Finally, we want to show that $\frac{du_1}{du_0} < 1$ for a fixed $\tau = 1$ ms in the following Lemma.

Lemma 4. *For $a, b > 0$, we have $\frac{du_1}{du_0} < 1$ for a fixed $\tau = 1$ ms.*

Proof. (By contradiction) We have $\frac{du}{dt} = a(bv - u) < 0$ from Assumption 1 (given our initial condition above the v-nullcline), so $u_0 > u_1 > 0$. Since $\frac{du_1}{du_0} > 0$ by Lemma 1, we know that $u_1(u_0)$ is an increasing function with respect to u_0. Also $\frac{d}{du_0}\left(\frac{du_1}{du_0}\right) > 0$ by Lemma 3, so $u_1(u_0)$ is concave up, which implies the slope of $u_1(u_0)$ is increasing. Clearly, $0 < u_1(u_0) < u_1^+(u_0)$, where $u_1^+(u_0) = \frac{u_0 - bv_0}{e^a} + bv_0$ from (4.6). Now

$$\frac{du_1^+}{du_0} = \frac{1}{e^a} = e^{-a} < 1, \quad \frac{\partial}{\partial u_0}\left(\frac{du_1^+}{du_0}\right) = 0, \tag{4.26}$$

where $a > 0$. So the slope of $u_1^+(u_0)$ is a constant and it does not change with respect to u_0. So u_1 as a function of u_0 is a straight line.

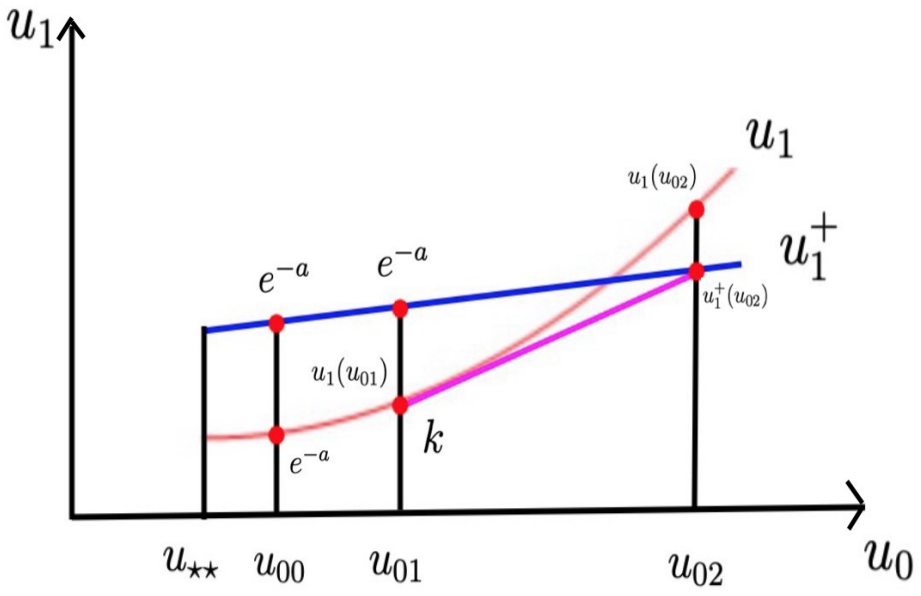

Figure 4.10: If $\frac{du_1}{du_0} > e^{-a}$, then $u_1(u_0)$ grows faster than $u_1^+(u_0)$ as u_0 increases.

Now suppose $\frac{du_1}{du_0} = e^{-a} < 1$ at $u_0 = u_{00} > u_{\star\star}$, then $\frac{du_1}{du_0} = k > e^{-a}$ at $u_0 = u_{01} > u_{00}$ by Lemma 3 (see Figure 4.10). u_1 increases at a slope greater than $k > e^{-a}$ for all $u_0 > u_{01}$. However, u_1^+ increases at a fixed slope $e^{-a} < 1$ as u_0 increases. More precisely, suppose k is fixed, then there must exist a $u_{02} > u_{01}$ such that $u_1(u_{01}) + k(u_{02} - u_{01}) = u_1^+(u_{02})$, but $\frac{du_1}{du_0}$ is increasing as u_0 increases so that $u_1(u_{02}) > u_1(u_{01}) + k(u_{02} - u_{01}) = u_1^+(u_{02})$. Thus, $u_1(u_{02}) > u_1^+(u_{02})$, which is a contradiction. Therefore, $\frac{du_1}{du_0} < e^{-a} < 1$ for $u_0 \in (u_{\star\star}, +\infty)$. □

Corollary 1. $0 < \frac{du_1}{du_0} < 1$ *by Lemma 1 and Lemma 4, which means* Φ_1 *is a contraction in* u. *So* $0 < \Phi_1'(u_0) < 1$ *for* $u_0 \in (u_{\star\star}, +\infty)$.

4.2.3 $\Phi_2 : (v_1, u_1) \mapsto (v_2, u_2)$

4.2.3.1 The estimation of u_2 and v_2

Clearly Φ_2 describes an instantaneous horizontal "jump" by adding $\epsilon G > 0$ in the v direction, and u does not change. Therefore, we have

$$\begin{aligned} v_2^+ &= v_1^+ + \epsilon G, \\ v_2^- &= v_1^- + \epsilon G, \\ u_2^+ &= u_1^+, \\ u_2^- &= u_1^-, \end{aligned} \tag{4.27}$$

where

$$u_2^+ = u_1^+ = \frac{u_0 - bv_0}{e^a} + bv_0, \tag{4.28}$$

$$v_2^- = v_1^- + \epsilon G = -5\sqrt{u_0 - u_a} + v_a + \epsilon G, \tag{4.29}$$

$$u_2^- = u_1^- = \frac{u_0 - bv_1^-}{e^a} + bv_0, \tag{4.30}$$

$$v_2^+ = v_1^+ + \epsilon G = -5\sqrt{u_1^- - u_a} + v_a + \epsilon G. \tag{4.31}$$

4.2.3.2 The description of Φ_2

Φ_2 is neither an expansion nor a contraction in u. As a result, if Φ_1 is a contraction in u, then the composition of Φ_1 and Φ_2 is also a contraction in u, so $0 < (\Phi_2 \circ \Phi_1(u_0))' < 1$. The point (v_1, u_1) is the initial condition of Φ_2, u does not change so $u_2 = u_1$ and if $u_0 \to +\infty$, then $u_2 \to +\infty$ by Lemma 3. v increases by $\epsilon G > 0$, thus $v_2 = v_1 + \epsilon G$. Now we would like to know where the point (v_2, u_2) is. There are five possibilities:

1, (v_2, u_2) is in the region B (below the v-nullcline).

2, (v_2, u_2) is on the right branch of the v-nullcline.

3, (v_2, u_2) is in the region C (above the v-nullcline).

4, (v_2, u_2) is on the reset line $v = v_0$.

5, (v_2, u_2) is also in the region A.

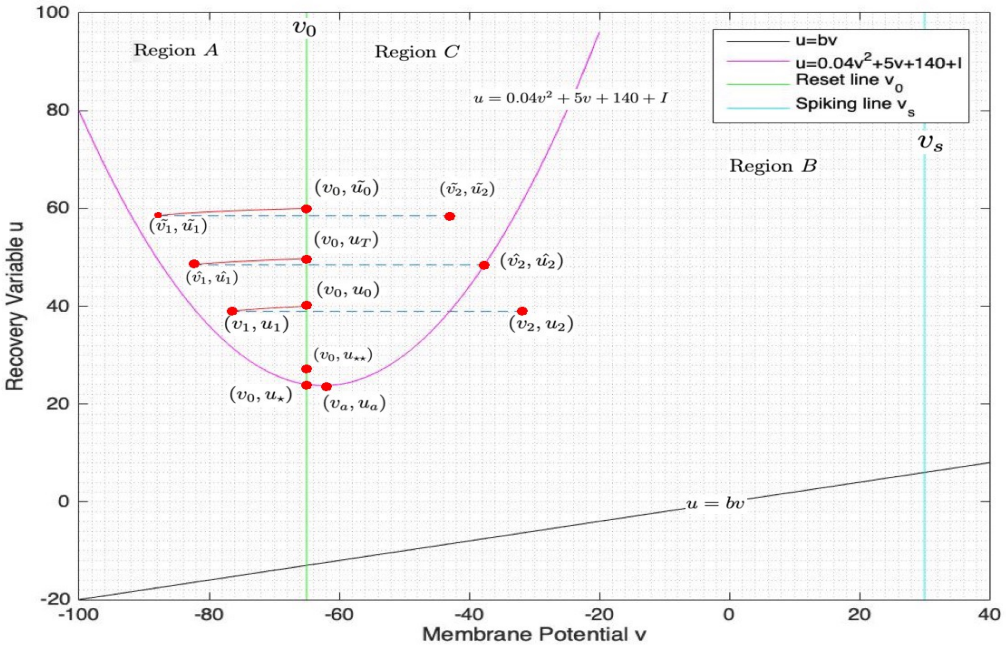

Figure 4.11: Let $u_T \in \mathcal{D}$ be the point such that $(\hat{v}_2, \hat{u}_2)$ is the solution on the v-nullcline.

In both cases 4 and 5, the system goes to the recovery phase. Clearly, the right branch of the v-nullcline is the dividing line between the region B and the region C. No matter what (v_2, u_2) is in the region B or C, although it can reach the spiking line $v = v_s$ eventually, the forms of the trajectories are different. By adding a "jump" in the v direction, if $\tilde{u}_0 > u_0$, then we have $\tilde{v}_2 = \tilde{v}_1 + \epsilon G < v_1 + \epsilon G = v_2$ by Lemma 2. If the v-nullcline and the impulse ϵG are fixed, the width of the parabola $F_v = 0$ increases when u increases, then for a small initial condition u_0, the impulse ϵG is large enough to make (v_2, u_2) cross the right branch of the v-nullcline. However, when the width of the parabola $F_v = 0$ is large enough, (v_2, u_2) does not pass the right branch of the v-nullcline by adding a fixed impulse ϵG. Now if $\tilde{u}_0 > u_0$ then $\tilde{u}_1 > u_1$ by Lemma 1, and there is a possibility that (v_2, u_2) is in the region B and $(\tilde{v}_2, \tilde{u}_2)$ is in the region C (see Figure 4.11). Thus there must exist a $\hat{v}_2 \in (\tilde{v}_2, v_2)$ such that $(\hat{v}_2, \hat{u}_2)$ is a solution on the v-nullcline for some initial conditions by the Intermediate Value Theorem. Thus, we have $\hat{u}_2 = 0.04\hat{v}_2^2 + 5\hat{v}_2 + 140 + I$ with $\hat{u}_2 = \hat{u}_1$, $\hat{v}_2 = \hat{v}_1 + \epsilon G$.

Definition 7. *Let $u_T \in \mathcal{D}$ be the point such that $\Phi_2 \circ \Phi_1(v_0, u_T) = (\hat{v}_2, \hat{u}_2)$ is the solution on the v-nullcline.*

Since $\tilde{v}_2 < \hat{v}_2 < v_2$, we have $\tilde{v}_1 < \hat{v}_1 < v_1$. Applying Lemma 2, we have $u_0 < u_T < \tilde{u}_0$. Here are three cases for the initial condition u_0:

1, $u_{\star\star} < u_0 < u_T$, then (v_2, u_2) is in the region B (below the v-nullcline).

2, $u_0 = u_T$, then (v_2, u_2) is on the right branch of v-nullcline.

3, $u_0 > u_T$, then (v_2, u_2) is in the region A or C (above the v-nullcline).

4.2.4 Φ_3: $(v_2, u_2) \mapsto u_3$

4.2.4.1 Case 1: $u_0 \in (u_{\star\star}, u_T)$

We define ψ be the composition of Φ_3, Φ_2 and Φ_1. Then

$$\psi(u_0) = \Phi_3 \circ \Phi_2 \circ \Phi_1(u_0). \tag{4.32}$$

Lemma 5. *For a, b and I positive constants, if $u_0 \in (u_{\star\star}, u_T)$, then $\psi(u_0)$ is a contraction in u. i.e. $0 < \psi'(u_0) < 1$.*

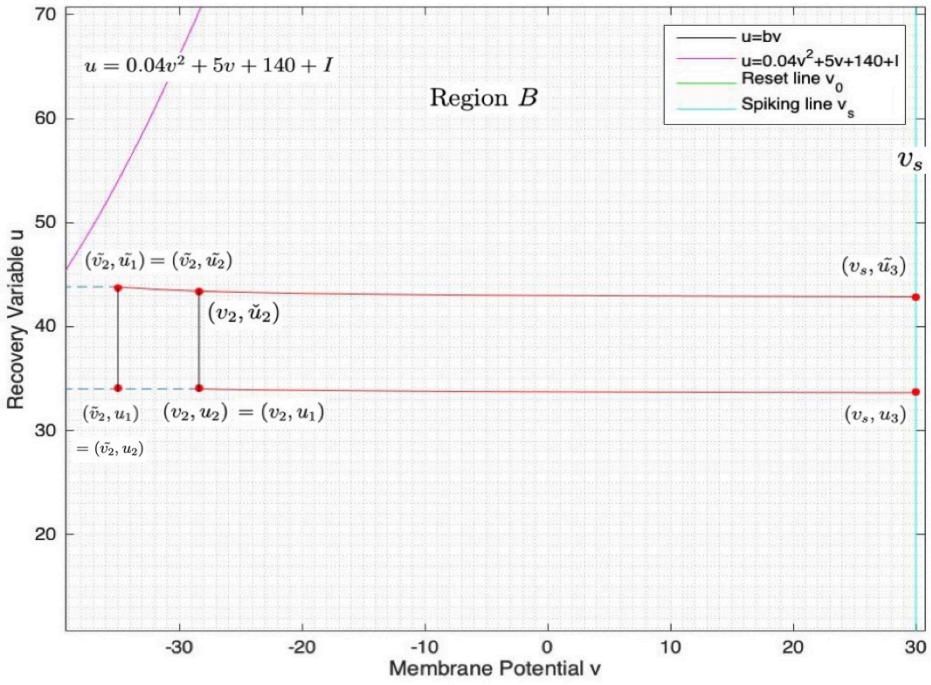

Figure 4.12: $(v_2, \check{u}_2)$ is on the curve of the solution from $(\tilde{v}_2, \tilde{u}_2)$ to $(v_s, \tilde{u}_3)$ vertically aligned with (v_2, u_2), the initial point for another solution.

Proof. For $u_0 \in (u_{\star\star}, u_T)$, (v_2, u_2) is in the region B (see Figure 4.12). Let $u = \gamma(v; \tilde{v}_2, \tilde{u}_2)$ describe the curve of the solution from $(\tilde{v}_2, \tilde{u}_2)$ to $(v_s, \tilde{u}_3)$ for any $\tilde{u}_2$ and

any $v \in [\tilde{v}_2, v_s]$. Then $\tilde{u}_2 = \gamma(\tilde{v}_2; \tilde{v}_2, \tilde{u}_2)$ and $\check{u}_2 = \gamma(v_2; \tilde{v}_2, \tilde{u}_2)$. Since in the region B, we have $\frac{du}{dt} < 0$ and $\frac{dv}{dt} > 0$, then $\frac{du}{dv} < 0$. Thus

$$\frac{\partial \gamma(v; \tilde{v}_2, \tilde{u}_2)}{\partial v} = \frac{du}{dv} < 0. \tag{4.33}$$

Since $\tilde{v}_2 < v_2$, we have $\check{u}_2 < \tilde{u}_2$. Thus $\check{u}_2 - u_2 < \tilde{u}_2 - u_2$.

Next let $u = \gamma(v; v_2, u_2)$ describe the curve of the solution from (v_2, u_2) to (v_s, u_3) for any u_2 and any $v \in [v_2, v_s]$ and let $u = \gamma(v; v_2, \check{u}_2)$ describe the curve of the solution from $(v_2, \check{u}_2)$ to $(v_s, \tilde{u}_3)$ for any $\check{u}_2$ and any $v \in [v_2, v_s]$. Then $u_2 = \gamma(v_2; v_2, u_2)$, $\check{u}_2 = \gamma(v_2; v_2, \check{u}_2)$ and $\frac{\partial \gamma(v; v_2, u_2)}{\partial v} = \frac{du}{dv} = \frac{F_u(\gamma(v; v_2, u_2), v)}{F_v(\gamma(v; v_2, u_2), v)} < 0$. Now we have

$$\frac{\partial}{\partial u_2}\left(\frac{\partial \gamma(v; v_2, u_2)}{\partial v}\right) = \frac{F_v(\gamma(v; v_2, u_2), v)\frac{\partial F_u}{\partial u}\frac{\partial \gamma(v; v_2, u_2)}{\partial u_2} - F_u(\gamma(v; v_2, u_2), v)\frac{\partial F_v}{\partial u}\frac{\partial \gamma(v; v_2, u_2)}{\partial u_2}}{F_v^2(\gamma(v; v_2, u_2), v)}. \tag{4.34}$$

By the uniqueness theorem for ODEs, we have $\frac{\partial \gamma(v; v_2, u_2)}{\partial u_2} > 0$. $\frac{\partial F_u}{\partial u} = -a < 0$ and $\frac{\partial F_v}{\partial u} = -1 < 0$, so $\frac{\partial}{\partial u_2}\left(\frac{\partial \gamma(v; v_2, u_2)}{\partial v}\right) < 0$. Now

$$\begin{aligned}(\tilde{u}_3 - \check{u}_2) - (u_3 - u_2) &= [\gamma(v_s; v_2, \check{u}_2)) - \gamma(v_2; v_2, \check{u}_2)] - [\gamma(v_s; v_2, u_2) - \gamma(v_2; v_2, u_2)] \\ &= \int_{v_2}^{v_s} \frac{\partial \gamma(v; v_2, \check{u}_2)}{\partial v} dv - \int_{v_2}^{v_s} \frac{\partial \gamma(v; v_2, u_2)}{\partial v} dv \\ &= \int_{v_2}^{v_s} \left(\int_{u_2}^{\check{u}_2} \frac{\partial}{\partial u_2}\left(\frac{\partial \gamma(v; v_2, u_2)}{\partial v}\right) du_2 \right) dv.\end{aligned} \tag{4.35}$$

Since $\frac{\partial}{\partial u_2}\left(\frac{\partial \gamma(v; v_2, u_2)}{\partial v}\right) < 0$, we have $\int_{v_2}^{v_s}\left(\int_{u_2}^{\check{u}_2} \frac{\partial}{\partial u_2}\left(\frac{\partial \gamma(v; v_2, u_2)}{\partial v}\right) du_2\right) dv < 0$. Then $(\tilde{u}_3 - \check{u}_2) - (u_3 - u_2) < 0 \Rightarrow \tilde{u}_3 - \check{u}_2 < u_3 - u_2 \Rightarrow \tilde{u}_3 - u_3 < \check{u}_2 - u_2$. So $\tilde{u}_3 - u_3 < \check{u}_2 - u_2 < \tilde{u}_2 - u_2 = \tilde{u}_1 - u_1 < \tilde{u}_0 - u_0$ by Lemma 4, which means $\tilde{u}_3 - u_3 < \tilde{u}_0 - u_0$. Therefore, for $u_0 \in (u_{\star\star}, u_T)$, $\psi(u_0)$ is a contraction in u. □

So, for $u_0 \in (u_{\star\star}, u_T)$, we have $0 < \psi'(u_0) < 1$.

4.2.4.2 Case 2: $u_0 \geq u_T$

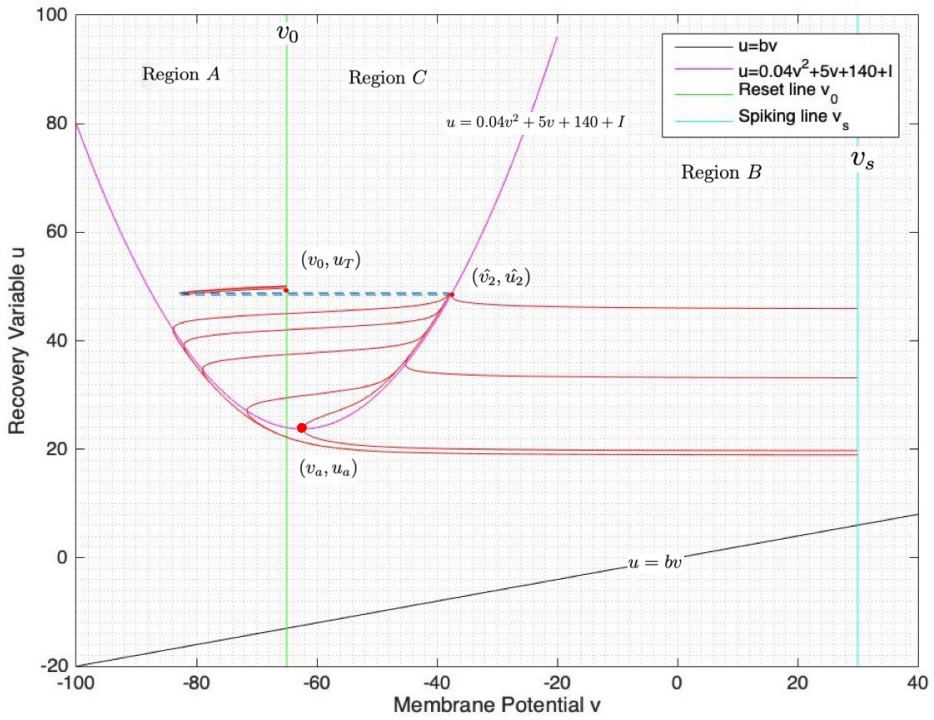

Figure 4.13: Due to the continuity of the flow, when u_0 increases, the intersection between the trajectory and the v-nullcline moves down along the right branch until the vertex (v_a, u_a), then moves up along the left branch.

For $u_0 > u_T$, (v_2, u_2) is in the region C or A. If (v_2, u_2) is close enough to the right branch of the v-nullcline, then the trajectory will cross the right branch of the v-nullcline. However, as long as (v_2, u_2) stays away a little bit from the right branch of the v-nullcline, then the trajectory will cross the left branch of the v-nullcline. Then both trajectories reach v_s. This is because in the Izhikevich neuron model, unless (v_2, u_2) is extremely close to the right branch of the v-nullcline so that $\frac{dv}{dt} \approx 0$ ($\frac{dv}{dt} = 0$ if (v_2, u_2) is on the v-nullcline), we have $\frac{dv}{dt} < 0$ is sufficiently faster than $\frac{du}{dt} < 0$ above the parabola $F_v = 0$, so that the distance moved in the v direction is much greater than that in the u direction in the same time t. Generally, the trajectory with (v_2, u_2)

in the region C will go to the left branch of the v-nullcline (see Figure 4.13).

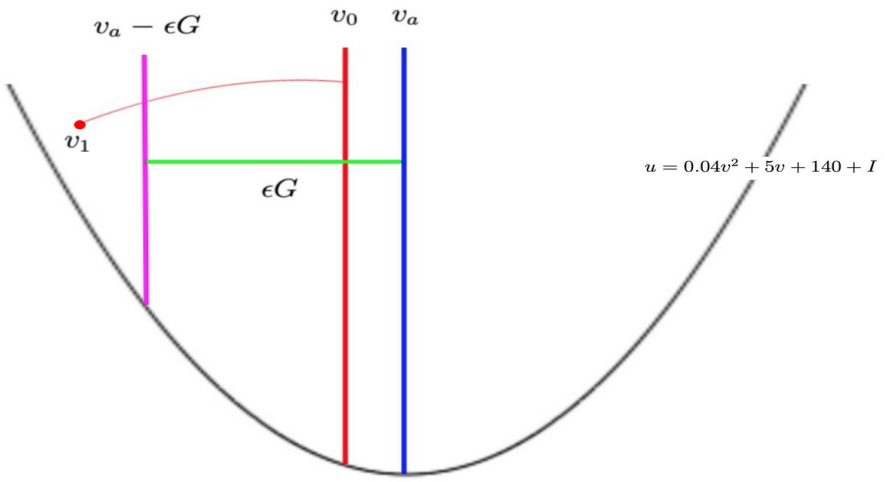

Figure 4.14: $v_1 + \epsilon G = v_2 < v_a$ as $u_0 \to +\infty$.

4.2.4.3 Case 2a: $u_0 \in [u_T, u_T + \delta]$

In this subsection, we deal with a small interval of initial points above u_T. The following Lemma makes this more precise.

Lemma 6. *$\exists\ \delta > 0$, such that the trajectory from $u_0 = u_T + \delta$ along Step III of the trajectory from (v_2, u_2) to (v_s, u_3) crosses the vertex (v_a, u_a) of the parabola $F_v = 0$.*

Proof. Since $u_0 > u_T$, we have that (v_2, u_2) is in the region C or A and we know that $v_2 < \hat{v}_2$ by Lemma 2 and $u_2 > \hat{u}_2$ by Lemma 1. Then the trajectory with the initial condition (v_2, u_2) crosses the right branch or the left branch of the v-nullcline before spiking. If $u_0 = u_T$, then $(v_2, u_2) = (\hat{v}_2, \hat{u}_2)$ is on the right branch of the v-nullcline. Recall that we fix $\tau = 1$ms in Step I and v_a, v_0, I and ϵG are fixed. Let $f(v) = 0.04v^2 + 5v + 140 + I$, we have $\frac{dv}{dt} = 0.04v^2 + 5v + 140 + I - u = f(v) - u < 0$. As $u_0 \to +\infty$ for $v \in [v_a - \epsilon G, v_0]$, $\frac{dv}{dt} = f(v) - u \leq f(v) - u_1$ for all $t \in [0, 1]$ because $u_1 \leq u(t)$. But $u_1 \to +\infty$ as $u_0 \to +\infty$ by Lemma 3 and $f(v)$ is bounded

(see Figure 4.14), so $\frac{dv}{dt} \to -\infty$ for all $t \in [0,1]$ as $u_0 \to +\infty$. Now suppose, by way of contradiction, that $v_1 \geq v_a - \epsilon G$. Then $\frac{dv}{dt} \to -\infty$ for all $t \in [0,1]$ as $u_0 \to +\infty$. So $v_1 = v_0 + \int_0^1 (\frac{dv}{dt})dt \to -\infty$ as $u_0 \to +\infty$. Clearly, this is a contradiction. Therefore, $v_1 < v_a - \epsilon G \Rightarrow v_1 + \epsilon G = v_2 < v_a$ as $u_0 \to +\infty$ when $\tau = 1$ms. Then the trajectory with the initial condition (v_2, u_2) reaches the left branch of the v-nullcline. Due to the continuity of the flow, when u_0 increases, the intersection between the trajectory and the right branch of the v-nullcline moves down along the right branch of the v-nullcline until the vertex (v_a, u_a), then moves up along the left branch of the v-nullcline.

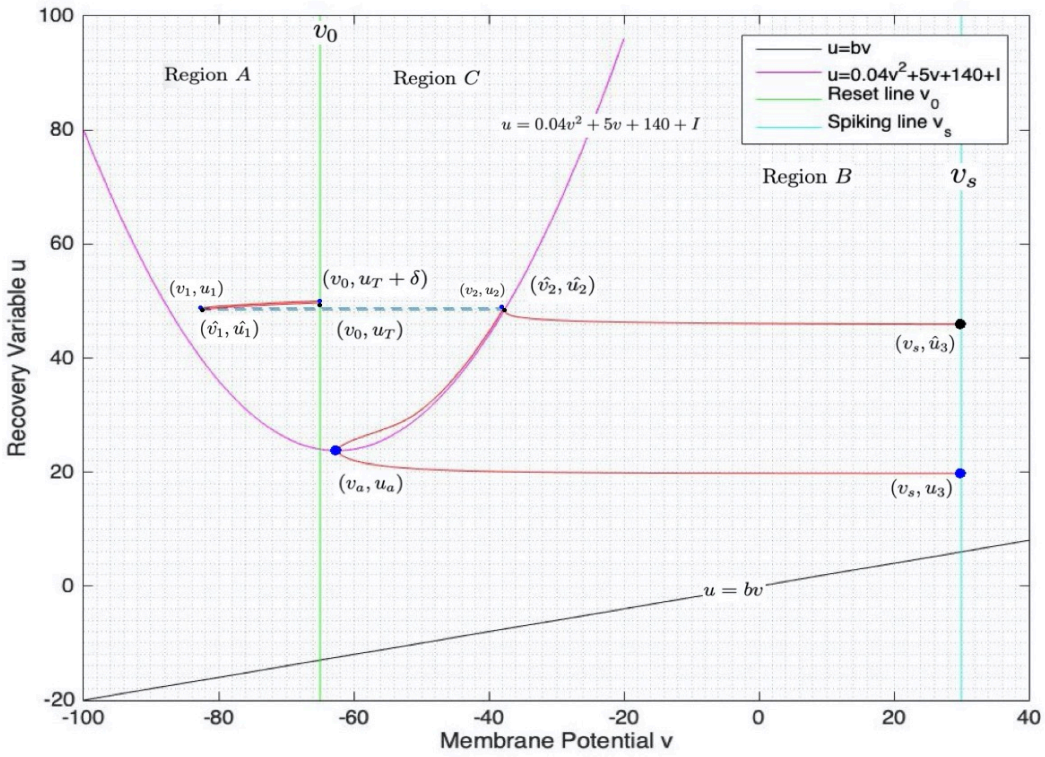

Figure 4.15: For $u_0 \in [u_T, u_T + \delta]$, a small increase in u_0 can lead to a large decrease in the value of u_3.

Therefore, there must exist a $\delta > 0$, such that the trajectory from $u_0 = u_T + \delta$ with the initial condition (v_2, u_2) reaches the vertex (v_a, u_a) of the parabola $F_v = 0$ (see Figure 4.15). □

4.2.4.4 The estimation of δ

In this subsection, we want to show that δ is small so that $\psi'(u_0) < -1$ on a subinterval of $[u_T, u_T + \delta]$, where $\psi(u_0)$ is defined in equation (4.32). In order to say δ is small, we need to find u_T first. We do not know where the exactly u_T is, however we can find the estimation of u_T.

4.2.4.4.1 The estimation of u_T : In principle, u_T has an exact value to lead the trajectory to land on the right branch of the v-nullcline by adding ϵG to v_1. So we need to start from $(v_2, u_2) = (\hat{v}_2, \hat{u}_2)$ and assume it is on the right branch of the v-nullcline. Thus,

$$\begin{cases} u_2 = 0.04v_2^2 + 5v_2 + 140 + I = u_1. \\ v_2 = v_1 + \epsilon G. \end{cases} \tag{4.36}$$

$$\Rightarrow u_1 = 0.04(v_1 + \epsilon G)^2 + 5(v_1 + \epsilon G) + 140 + I. \tag{4.37}$$

Applying the estimates of v_1 and u_1 from Φ_1, we can find a lower bound of u_T, say u_T^- and an upper bound of u_T, say u_T^+. Then,

$$\Rightarrow \begin{cases} u_1^+ = \ 0.04(v_1^- + \epsilon G)^2 + 5(v_1^- + \epsilon G) + 140 + I. \\ u_1^- = \ 0.04(v_1^+ + \epsilon G)^2 + 5(v_1^+ + \epsilon G) + 140 + I, \end{cases} \tag{4.38}$$

where

$$u_2^+ = u_1^+ = \frac{u_T^- - bv_0}{e^a} + bv_0, \tag{4.39}$$

$$v_1^- = -5\sqrt{u_T^- - u_a} + v_a, \tag{4.40}$$

$$v_2^- = v_1^- + \epsilon G = -5\sqrt{u_T^- - u_a} + v_a + \epsilon G, \tag{4.41}$$

$$u_2^- = u_1^- = \frac{u_T^+ - bv_1^-}{e^a} + bv_1^-, \tag{4.42}$$

$$v_1^+ = -5\sqrt{u_1^- - u_a} + v_a, \tag{4.43}$$

$$v_2^+ = v_1^+ + \epsilon G = -5\sqrt{u_1^- - u_a} + v_a + \epsilon G. \tag{4.44}$$

Then $u_T \in [u_T^-, u_T^+]$. So $u_T^- + \delta_{max} = u_T + \delta$, where δ_{max} is an upper bound of δ. Clearly, $\delta_{max} > \delta$. If δ_{max} is small, then δ is small automatically. Firstly, we need to find u_T^-. By 4.39 and 4.40, we have

$$\begin{aligned}
u_1^+ &= 0.04(v_1^- + \epsilon G)^2 + 5(v_1^- + \epsilon G) + 140 + I \\
&= 0.04(v_1^-)^2 + (0.08\epsilon G + 5)v_1^- + 0.04\epsilon^2 G^2 \\
&\quad + 5\epsilon G + 140 + I, \\
\frac{u_T^- - bv_0}{e^a} + bv_0 &= 0.04\left(-5\sqrt{u_T^- - u_a} + v_a\right)^2 \\
&\quad + (0.08\epsilon G + 5)\left(-5\sqrt{u_T^- - u_a} + v_a\right) \\
&\quad + 0.04\epsilon^2 G^2 + 5\epsilon G + 140 + I, \\
e^{-a}u_T^- - bv_0 e^{-a} + bv_0 &= u_T^- + 0.04\epsilon^2 G^2 - 0.4\epsilon G\sqrt{u_T^- - u_a}, \\
-0.4\epsilon G\sqrt{u_T^- - u_a} &= e^{-a}u_T^- - u_T^- - bv_0 e^{-a} + bv_0 - 0.04\epsilon^2 G^2, \\
-0.4\epsilon G\sqrt{u_T^- - u_a} &= (e^{-a} - 1)u_T^- - bv_0 e^{-a} + bv_0 - 0.04\epsilon^2 G^2.
\end{aligned} \tag{4.45}$$

Let $X_1 = e^{-a} - 1$ and $X_2 = bv_0 - bv_0 e^{-a} - 0.04\epsilon^2 G^2$. Now

$$\begin{aligned}
\left(-0.4\epsilon G\sqrt{u_T^- - u_a}\right)^2 &= \left(X_1 u_T^- + X_2\right)^2, \\
0.16\epsilon^2 G^2 u_T^- - 0.16\epsilon^2 G^2 u_a &= X_1^2 (u_T^-)^2 + 2X_1 X_2 u_T^- + X_2^2.
\end{aligned} \tag{4.46}$$

Let $X_3 = 0.16\epsilon^2 G^2$ and $X_4 = -0.16\epsilon^2 G^2 u_a$. We have

$$0 = X_1^2 (u_T^-)^2 + (2X_1 X_2 - X_3)u_T^- + X_2^2 - X_4. \tag{4.47}$$

$$\Leftrightarrow u_T^- = \frac{-(2X_1X_2 - X_3) \pm \sqrt{(2X_1X_2 - X_3)^2 - 4X_1^2(X_2^2 - X_4)}}{2X_1^2}. \tag{4.48}$$

Picking a minimum

$$u_T^- = \frac{-(2X_1X_2 - X_3) - \sqrt{(2X_1X_2 - X_3)^2 - 4X_1^2(X_2^2 - X_4)}}{2X_1^2}. \tag{4.49}$$

Clearly, X_1, X_2, X_3 and X_4 are constants, so u_T^- is a constant.

If δ_{max} is small, then δ is small. So we want to find the estimation of δ_{max}.

4.2.4.4.2 The method and analysis for estimation of δ_{max} :

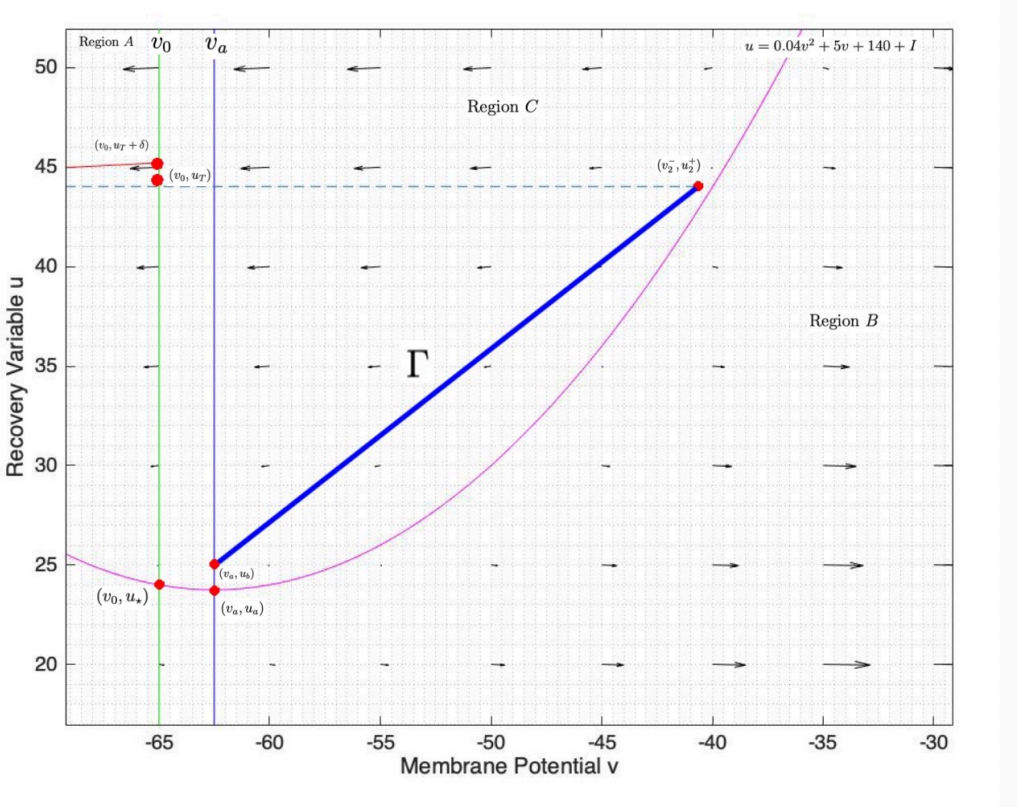

Figure 4.16: Choose δ_{max} to be as small as possible, but still large enough to ensure that the flow crosses Γ from right to left for $v \in (v_a, v_2^-(\delta_{max})]$.

Now, let $u_0(\delta_{max}) = u_T^- + \delta_{max}$, where $\delta_{max} > 0$. Let Γ be the straight line from

$(v_2^-(\delta_{max}), u_2^+(\delta_{max}))$ to (v_a, u_b) above the parabola $F_v = 0$, where

$$u_2^+(\delta_{max}) = \frac{u_T^- + \delta_{max} - bv_0}{e^a} + bv_0, \tag{4.50}$$

$$v_2^-(\delta_{max}) = -5\sqrt{u_T^- + \delta_{max} - u_a} + v_a + \epsilon G \tag{4.51}$$

and $u_b > u_a$ is a constant. We want to know how small δ_{max} can be to ensure that the flow crosses Γ from right to left for $v \in (v_a, v_2^-(\delta_{max})]$ (see Figure 4.16).

Let $K = \frac{u_2^+(\delta_{max}) - u_b}{v_2^-(\delta_{max}) - v_a} > 0$ be the slope of Γ. The equation of Γ is $u = \Gamma(v) = K(v - v_2^-(\delta_{max})) + u_2^+(\delta_{max})$. We want $\frac{du}{dv} < \frac{d\Gamma}{dv}$, $\forall v \in (v_a, v_2^-(\delta_{max})]$ by choosing a small δ_{max} and a minimum real constant u_b. Let $f(v) = 0.04v^2 + 5v + 140 + I$. We want $\forall (v, u) \in \Gamma$

$$\begin{aligned} \frac{du}{dv} &< \frac{d\Gamma}{dv} \\ \Leftrightarrow \frac{abv - au}{f(v) - u} &< K \\ \Leftrightarrow \frac{abv - a[K(v - v_2^-(\delta_{max})) + u_2^+(\delta_{max})]}{f(v) - [K(v - v_2^-(\delta_{max})) + u_2^+(\delta_{max})]} &< K. \end{aligned} \tag{4.52}$$

Recall that $\frac{dv}{dt} = f(v) - u < 0$ in the region A and C,

$$\begin{aligned} &\Leftrightarrow abv - a[K(v - v_2^-(\delta_{max})) + u_2^+(\delta_{max})] > \\ &\quad K[f(v) - [K(v - v_2^-(\delta_{max})) + u_2^+(\delta_{max})]] \\ \Leftrightarrow abv - Kf(v) + (K - a)[K(v - v_2^-(\delta_{max})) + u_2^+(\delta_{max})] &> 0. \end{aligned} \tag{4.53}$$

Let $Q(v) = abv - Kf(v) + (K - a)[K(v - v_2^-(\delta_{max})) + u_2^+(\delta_{max})]$. $Q'(v) = ab + K(K - a) - Kf'(v)$ and $Q''(v) = -0.08K < 0$. So $Q(v)$ is concave down $\forall v \in (v_a, v_2^-(\delta_{max})]$, which means we need $Q(v_a) \geq 0$ and $Q(v_2^-(\delta_{max})) > 0$ to ensure $Q(v) > 0$ $\forall v \in (v_a, v_2^-(\delta_{max})]$.

We first show that $Q(v_a) \geq 0$ by choosing a minimum real constant u_b. Claim 1 confirms that u_b is a real constant and $u_b > u_a$ under a sufficient condition of parameters with $\delta_{max} \geq 2u_a e^a - u_T^- + bv_0(1-e^a)$.

4.2.4.4.3 Choosing a u_b for $Q(v_a)$: Firstly, we need $Q(v_a) \geq 0$ by choosing a minimum real constant u_b.

$$\begin{aligned} Q(v_a) = (K-a)\left(\frac{u_2^+(\delta_{max})-u_b}{v_2^-(\delta_{max})-v_a}(v_a - v_2^-(\delta_{max})) + u_2^+(\delta_{max})\right) \\ +abv_a - Kf(v_a) \geq 0 \\ \Leftrightarrow abv_a - Kf(v_a) + (K-a)u_b \geq 0 \\ \Leftrightarrow abv_a - \frac{u_2^+(\delta_{max})-u_b}{v_2^-(\delta_{max})-v_a}f(v_a) + \frac{u_2^+(\delta_{max})-u_b}{v_2^-(\delta_{max})-v_a}u_b - au_b \geq 0. \end{aligned} \tag{4.54}$$

Since $v_2^-(\delta_{max}) - v_a > 0$, we have

$$\begin{aligned} \Leftrightarrow abv_a(v_2^-(\delta_{max})-v_a) - (u_2^+(\delta_{max})-u_b)f(v_a) \\ +(u_2^+(\delta_{max})-u_b)u_b - au_b(v_2^-(\delta_{max})-v_a) \geq 0 \\ \Leftrightarrow u_b^2 - \left(f(v_a) + u_2^+(\delta_{max}) - a(v_2^-(\delta_{max})-v_a)\right)u_b \\ +u_2^+(\delta_{max})f(v_a) - abv_a(v_2^-(\delta_{max})-v_a) \leq 0 \end{aligned} \tag{4.55}$$

$$\Leftrightarrow u_b \in \left[\frac{-Y_1 - \sqrt{Y_1^2 - 4Y_2}}{2}, \frac{-Y_1 + \sqrt{Y_1^2 - 4Y_2}}{2}\right]. \tag{4.56}$$

Picking a minimum

$$u_b = \frac{-Y_1 - \sqrt{Y_1^2 - 4Y_2}}{2}, \tag{4.57}$$

where $Y_1 = -\left(f(v_a) + u_2^+(\delta_{max}) - a(v_2^-(\delta_{max}) - v_a)\right)$, $Y_2 = u_2^+(\delta_{max})f(v_a) - abv_a(v_2^-(\delta_{max}) - v_a)$, $v_2^-(\delta_{max}) = -5\sqrt{u_T^- + \delta_{max} - u_a} + v_a + \epsilon G$ and $u_2^+(\delta_{max}) = \frac{u_T^- + \delta_{max} - bv_0}{e^a} + bv_0$.

Real constant u_b: Let $\Delta v = v_2^-(\delta_{max}) - v_a > 0$. We want to ensure that u_b is a real constant. We have

$$\begin{aligned} Y_1^2 - 4Y_2 &= \Big(-\Big(f(v_a) + u_2^+(\delta_{max}) - a\Delta v\Big)\Big)^2 - 4\left(u_2^+(\delta_{max})f(v_a) - abv_a\Delta v\right) \\ &= (-f(v_a) - u_2^+(\delta_{max}))^2 + 2a\Delta v(-f(v_a) - u_2^+(\delta_{max})) + a^2(\Delta v)^2 \\ &\quad - 4u_2^+(\delta_{max})f(v_a) + 4abv_a\Delta v \\ &= (f(v_a))^2 + 2u_2^+(\delta_{max})f(v_a) + (u_2^+(\delta_{max}))^2 - 2a\Delta v f(v_a) \\ &\quad - 2a\Delta v u_2^+(\delta_{max}) + a^2(\Delta v)^2 - 4u_2^+(\delta_{max})f(v_a) + 4abv_a\Delta v \\ &= (f(v_a))^2 - 2u_2^+(\delta_{max})f(v_a) + (u_2^+(\delta_{max}))^2 - 2a\Delta v f(v_a) \\ &\quad - 2a\Delta v u_2^+(\delta_{max}) + a^2(\Delta v)^2 + 4abv_a\Delta v. \end{aligned} \tag{4.58}$$

Let $E = (u_2^+(\delta_{max}))^2 - 2u_2^+(\delta_{max})f(v_a)$ and $F = a^2(\Delta v)^2 + (f(v_a))^2 - 2a\Delta v f(v_a) - 2a\Delta v u_2^+(\delta_{max}) + 4abv_a\Delta v$, where $f(v_a) = u_a$. So $Y_1^2 - 4Y_2 = E + F$. We want to choose a δ_{max} as a sufficient condition to ensure that u_b is a real constant and $u_b > u_a$.

Claim 1. *For $0 < a < b < 1$, $v_a < 0$ and $v_0 < 0$, assume $\frac{1}{a} \geq \epsilon G > 0$, $u_a > \max(3 + \sqrt{9 - 4v_a}, \frac{u_T^-}{2}) > 0$, we take $\delta_{max} \geq 2u_a e^a - u_T^- + bv_0(1 - e^a)$, then*
(a) u_b is a real constant, and
(b) $u_b > u_a$.

Proof. (a) Let $\delta_{max1} = 2u_a e^a - u_T^- + bv_0(1 - e^a)$. Clearly, $u_a > \frac{u_T^-}{2} \Rightarrow 2u_a > u_T^-$. Thus $\delta_{max1} = 2u_a e^a - u_T^- + bv_0(1 - e^a) > 0$ because $2u_a e^a - u_T^- > 0$ and $bv_0(1 - e^a) > 0$, where $0 < a < b < 1$ and $v_0 < 0$. So $\delta_{max} \geq \delta_{max1} > 0$. Now we have

$$\begin{aligned} E &= (u_2^+(\delta_{max}))^2 - 2u_2^+(\delta_{max})f(v_a) \\ &= u_2^+(\delta_{max})(u_2^+(\delta_{max}) - 2u_a) \\ &= u_2^+(\delta_{max})\left(\frac{u_T^- + \delta_{max} - bv_0}{e^a} + bv_0 - 2u_a\right), \end{aligned} \tag{4.59}$$

where $\frac{u_T^- + \delta_{max} - bv_0}{e^a} > 0$, $bv_0 < 0$ and $-2u_a < 0$. Thus

$$\begin{aligned} E &\geq u_2^+(\delta_{max}) \left(\frac{u_T^- + \delta_{max1} - bv_0}{e^a} + bv_0 - 2u_a \right) \\ &= u_2^+(\delta_{max}) \left(\frac{u_T^- + 2u_a e^a + bv_0 - bv_0 e^a - u_T^- - bv_0}{e^a} + bv_0 - 2u_a \right) \\ &= u_2^+(\delta_{max}) \left(\frac{u_T^- + 2u_a e^a + bv_0 - bv_0 e^a - u_T^- - bv_0 + bv_0 e^a - 2u_a e^a}{e^a} \right) \\ &= 0. \end{aligned} \tag{4.60}$$

Now take $\delta_{max} = \delta_{max1} = 2u_a e^a - u_T^- + bv_0(1 - e^a)$. Then the minimum $E = u_2^+(\delta_{max})(u_2^+(\delta_{max}) - 2u_a) = 0 \Rightarrow u_2^+(\delta_{max}) = 2u_a$. Next

$$\begin{aligned} F &= a^2(\Delta v)^2 + (f(v_a))^2 - 2a\Delta v f(v_a) - 2a\Delta v u_2^+(\delta_{max}) + 4abv_a\Delta v \\ &= a^2(\Delta v)^2 + (u_a)^2 - 2a\Delta v u_a - 2a\Delta v u_2^+(\delta_{max}) + 4abv_a\Delta v \\ &= a^2(\Delta v)^2 + u_a \left(u_a - 2a\Delta v - 2a\Delta v \frac{u_2^+(\delta_{max})}{u_a} + 4a\Delta v \frac{bv_a}{u_a} \right) \\ &= a^2(\Delta v)^2 + u_a \left(u_a - 2a\Delta v - 2a\Delta v \frac{2u_a}{u_a} + 4a\Delta v \frac{bv_a}{u_a} \right) \\ &= a^2(\Delta v)^2 + u_a \left(u_a - a\Delta v \left(2 + 2 \cdot 2 - 4\frac{bv_a}{u_a} \right) \right), \end{aligned} \tag{4.61}$$

where

$$\begin{aligned} 0 < a\Delta v &= a(v_2^-(\delta_{max}) - v_a) \\ &= a\left(-5\sqrt{u_T^- + \delta_{max} - u_a} + v_a + \epsilon G - v_a \right) \\ &= a\left(-5\sqrt{u_T^- + \delta_{max} - u_a} + \epsilon G \right) \\ &= a\left(\epsilon G - 5\sqrt{u_T^- + \delta_{max} - u_a} \right). \end{aligned} \tag{4.62}$$

Since $\frac{1}{a} \geq \epsilon G$, we have

$$
\begin{aligned}
&\frac{1}{a} \geq \epsilon G \\
\Rightarrow &\frac{1}{a} - \epsilon G \geq 0 > -5\sqrt{u_T^- + \delta_{max} - u_a} \\
\Rightarrow &\frac{1}{a} - \epsilon G > -5\sqrt{u_T^- + \delta_{max} - u_a} \\
&\Leftrightarrow \frac{1}{a} > \epsilon G - 5\sqrt{u_T^- + \delta_{max} - u_a} \\
&\Leftrightarrow 1 > a\left(\epsilon G - 5\sqrt{u_T^- + \delta_{max} - u_a}\right) \\
\Leftrightarrow &\, 0 < a\Delta v < 1.
\end{aligned} \tag{4.63}
$$

Since $0 < b < 1$, $v_a < 0$ and $u_a > 0$, we have $\frac{bv_a}{u_a} < 0$. Now we take a minimum F

$$
\begin{aligned}
F &= a^2(\Delta v)^2 + u_a\left(u_a - a\Delta v\left(2 + 2\cdot 2 - 4\frac{bv_a}{u_a}\right)\right) \\
F &> a^2(\Delta v)^2 + u_a\left(u_a - 1\cdot\left(2 + 2\cdot 2 - \frac{4\cdot 1\cdot v_a}{u_a}\right)\right) \\
&= a^2(\Delta v)^2 + u_a\left(u_a - \left(6 - \frac{4v_a}{u_a}\right)\right) \\
&= a^2(\Delta v)^2 + u_a\left(u_a - 6 + \frac{4v_a}{u_a}\right),
\end{aligned} \tag{4.64}
$$

where $a^2(\Delta v)^2 > 0$, $u_a > 0$, $-6 < 0$ and $\frac{4v_a}{u_a} < 0$. Clearly, $u_a > 3 + \sqrt{9 - 4v_a}$. Let $q(u_a) = u_a - 6 + \frac{4v_a}{u_a}$. Then

$$
\begin{aligned}
q(u_a) &> 3 + \sqrt{9 - 4v_a} - 6 + \frac{4v_a}{3 + \sqrt{9 - 4v_a}} \\
&= \sqrt{9 - 4v_a} - 3 + \frac{4v_a}{3 + \sqrt{9 - 4v_a}} \\
&= \frac{(\sqrt{9 - 4v_a} + 3)(\sqrt{9 - 4v_a} - 3)}{\sqrt{9 - 4v_a} + 3} + \frac{4v_a}{3 + \sqrt{9 - 4v_a}} \\
&= \frac{9 - 4v_a - 9 + 4v_a}{3 + \sqrt{9 - 4v_a}} \\
&= 0.
\end{aligned} \tag{4.65}
$$

So $F > 0$. Therefore, $Y_1^2 - 4Y_2 = E + F > 0$. If we fix $\delta_{max1} = 2u_a e^a - u_T^- + bv_0(1 - e^a) >$

0, then u_b is a real constant with respect to the fixed δ_{max1}.

(b) If $u_a \in \left[\frac{-Y_1-\sqrt{Y_1^2-4Y_2}}{2}, \frac{-Y_1+\sqrt{Y_1^2-4Y_2}}{2}\right]$ from (4.56), then the flow is in a vertical direction at (v_a, u_a) so that $Q(v_a) < 0$. So $u_a \notin \left[\frac{-Y_1-\sqrt{Y_1^2-4Y_2}}{2}, \frac{-Y_1+\sqrt{Y_1^2-4Y_2}}{2}\right]$. Now

$$\begin{aligned} u_b - u_a &= \frac{-Y_1 + \sqrt{Y_1^2 - 4Y_2}}{2} - u_a \\ &= \frac{-Y_1 + \sqrt{Y_1^2 - 4Y_2}}{2} - \frac{2u_a}{2} \\ &= \frac{-Y_1 - 2u_a + \sqrt{Y_1^2 - 4Y_2}}{2} \\ &= \frac{f(v_a) + u_2^+(\delta_{max}) - a\Delta v - 2u_a + \sqrt{Y_1^2 - 4Y_2}}{2} \\ &= \frac{u_a + 2u_a - a\Delta v - 2u_a + \sqrt{Y_1^2 - 4Y_2}}{2} \\ &= \frac{u_a - a\Delta v + \sqrt{Y_1^2 - 4Y_2}}{2} \\ &\geq \frac{u_a - 1 + \sqrt{Y_1^2 - 4Y_2}}{2} > 0, \end{aligned} \tag{4.66}$$

where $\sqrt{Y_1^2 - 4Y_2} > 0$ and $u_a - 1 > 0$ see (4.11). Therefore $u_b > u_a$.

□

Now we keep u_b fixed in the following. Next, we want to show that $Q(v_2^-(\delta_{max})) > 0$ by choosing a δ_{max}.

4.2.4.4.4 Choosing a δ_{max} for $Q(v_2^-(\delta_{max}))$: Now let $v = v_2^-(\delta_{max})$ in (4.52), we want $Q(v_2^-(\delta_{max})) > 0$, which is equivalent to

$$\frac{abv_2^-(\delta_{max}) - au_2^+(\delta_{max})}{f(v_2^-(\delta_{max})) - u_2^+(\delta_{max})} < \frac{u_2^+(\delta_{max}) - u_b}{v_2^-(\delta_{max}) - v_a}. \tag{4.67}$$

Let $P(v_2^-, u_2^+; \delta_{max}) = \frac{abv_2^-(\delta_{max}) - au_2^+(\delta_{max})}{f(v_2^-(\delta_{max})) - u_2^+(\delta_{max})} - \frac{u_2^+(\delta_{max}) - u_b}{v_2^-(\delta_{max}) - v_a}$. We want $P(v_2^-, u_2^+; \delta_{max}) < 0$.

Claim 2. *For $0 < a < b < 1$, $v_a < 0$ and $v_0 < 0$, we take $\delta_{max} \geq 2u_a e^a - u_T^- + bv_0(1 - e^a)$. If $v_2^-(\delta_{max}) \geq \frac{b-5}{0.08}$, then $\frac{dP}{d\delta_{max}} < 0$.*

Proof. Let $\delta_{max1} = 2u_a e^a - u_T^- + bv_0(1 - e^a)$. Firstly, we check $v_2^-(\delta_{max})$ is defined. $v_2^-(\delta_{max1}) = -5\sqrt{u_T^- + \delta_{max1} - u_a} + v_a + \epsilon G = -5\sqrt{u_a(2e^a - 1) + bv_0(1 - e^a)}$ $+ v_a + \epsilon G$. $u_a(2e^a - 1) > 0$ and $bv_0(1 - e^a) > 0$, so $v_2^-(\delta_{max})$ is defined. $\frac{dP}{d\delta_{max}} = \frac{\partial P}{\partial v_2^-(\delta_{max})}\frac{\partial v_2^-(\delta_{max})}{\partial \delta_{max}} + \frac{\partial P}{\partial u_2^+(\delta_{max})}\frac{\partial u_2^+(\delta_{max})}{\partial \delta_{max}}$. We know that $\frac{\partial v_2^-(\delta_{max})}{\partial \delta_{max}} < 0$ by Lemma 2 and $\frac{\partial u_2^+(\delta_{max})}{\partial \delta_{max}} > 0$ by Lemma 1. Now

$$\frac{\partial P}{\partial v_2^-(\delta_{max})} = \frac{(f(v_2^-(\delta_{max})) - u_2^+(\delta_{max}))ab - a(bv_2^-(\delta_{max}) - u_2^+(\delta_{max}))f'(v_2^-(\delta_{max}))}{(f(v_2^-(\delta_{max})) - u_2^+(\delta_{max}))^2} + \frac{u_2^+(\delta_{max}) - u_b}{(v_2^-(\delta_{max}) - v_a)^2}. \tag{4.68}$$

$a\left(f'(v_2^-(\delta_{max}))(u_2^+(\delta_{max}) - bv_2^-(\delta_{max})) - b(u_2^+(\delta_{max}) - f(v_2^-(\delta_{max}))\right) > 0$, where $bv_2^-(\delta_{max}) < 0 < f(v_2^-(\delta_{max}))$ and $f'(v_2^-(\delta_{max})) = 0.08v_2^-(\delta_{max}) + 5 \geq 0.08 \cdot \frac{b-5}{0.08} + 5 = b - 5 + 5 = b$. Clearly, $u_2^+(\delta_{max}) - u_b > 0$. So $\frac{\partial P}{\partial v_2^-(\delta_{max})} > 0$.

$$\frac{\partial P}{\partial u_2^+(\delta_{max})} = \frac{(f(v_2^-(\delta_{max})) - u_2^+(\delta_{max}))(-a) - a(bv_2^-(\delta_{max}) - u_2^+(\delta_{max}))(-1)}{(f(v_2^-(\delta_{max})) - u_2^+(\delta_{max}))^2} + \frac{-1}{v_2^-(\delta_{max}) - v_a}. \tag{4.69}$$

$v_2^-(\delta_{max}) - v_a > 0$, so $\frac{-1}{v_2^-(\delta_{max}) - v_a} < 0$. $a(u_2^+(\delta_{max}) - f(v_2^-(\delta_{max})) + bv_2^-(\delta_{max}) - u_2^+(\delta_{max})) = a(bv_2^-(\delta_{max}) - f(v_2^-(\delta_{max}))) < 0$ because $bv_2^-(\delta_{max}) < 0$ and $f(v_2^-(\delta_{max}) > 0$. So $\frac{\partial P}{\partial u_2^+(\delta_{max})} < 0$. Therefore, $\frac{dP}{d\delta_{max}} < 0$.

□

Choosing a δ_{max} such that $P(v_2^-, u_2^+; \delta_{max}) < 0$: Firstly, we want to show that there must exist a δ_{max} such that $P(v_2^-, u_2^+; \delta_{max}) < 0$. We know that $\frac{\partial v_2^-(\delta_{max})}{\partial \delta_{max}} < 0$ by Lemma 2 and $\frac{\partial u_2^+(\delta_{max})}{\partial \delta_{max}} > 0$ by Lemma 1, then $u_2^+(\delta_{max}) - u_b > 0$ is increasing

and $v_2^-(\delta_{max}) - v_a > 0$ is decreasing as δ_{max} increases. Thus, $K = \frac{u_2^+(\delta_{max})-u_b}{v_2^-(\delta_{max})-v_a} \to +\infty$ as $v_2^-(\delta_{max}) \to v_a$. However, $\frac{du}{dv}|_{u=u_2^+(\delta_{max}),v=v_2^-(\delta_{max})} > 0$ in the region C and $|\frac{dv}{dt}|_{v=v_2^-(\delta_{max})}| > |\frac{du}{dt}|_{u=u_2^+(\delta_{max})}|$ as long as δ_{max} is sufficiently large, so $\frac{du}{dv}|_{u=u_2^+(\delta_{max}),v=v_2^-(\delta_{max})} \nrightarrow +\infty$ as $v_2^-(\delta_{max}) \to v_a$. Hence, $P(v_2^-, u_2^+; \delta_{max}) = \frac{abv_2^-(\delta_{max})-au_2^+(\delta_{max})}{f(v_2^-(\delta_{max}))-u_2^+(\delta_{max})} - \frac{u_2^+(\delta_{max})-u_b}{v_2^-(\delta_{max})-v_a} = \frac{du}{dv}|_{u=u_2^+(\delta_{max}),v=v_2^-(\delta_{max})} - K < 0$ as $K \to +\infty$ and $\frac{du}{dv}|_{u=u_2^+(\delta_{max}),v=v_2^-(\delta_{max})} \nrightarrow +\infty$ when $v_2^-(\delta_{max}) \to v_a$, which implies that there must exist a δ_{max} such that $P(v_2^-, u_2^+; \delta_{max}) < 0$.

Secondly, since $\frac{dP}{d\delta_{max}} < 0$, we just need to find a δ_{max} to ensure that $P(v_2^-, u_2^+; \delta_{max}) < 0$, because any δ that is greater than δ_{max} will make it better. We want $P(v_2^-, u_2^+; \delta_{max}) = \frac{abv_2^-(\delta_{max})-au_2^+(\delta_{max})}{f(v_2^-(\delta_{max}))-u_2^+(\delta_{max})} - \frac{u_2^+(\delta_{max})-u_b}{v_2^-(\delta_{max})-v_a} < 0$, which is equivalent to

$$
\begin{aligned}
&\frac{abv_2^-(\delta_{max}) - au_2^+(\delta_{max})}{f(v_2^-(\delta_{max})) - u_2^+(\delta_{max})} < \frac{u_2^+(\delta_{max}) - u_b}{v_2^-(\delta_{max}) - v_a} \\
\Leftrightarrow\ & (abv_2^-(\delta_{max}) - au_2^+(\delta_{max}))(v_2^-(\delta_{max}) - v_a) > (u_2^+(\delta_{max}) - u_b)(f(v_2^-(\delta_{max})) - u_2^+(\delta_{max})) \\
\Leftrightarrow\ & \frac{(abv_2^-(\delta_{max}) - au_2^+(\delta_{max}))(v_2^-(\delta_{max}) - v_a)}{u_2^+(\delta_{max}) - u_b} > f(v_2^-(\delta_{max})) - u_2^+(\delta_{max}) \\
\Leftrightarrow\ & \frac{-a(u_2^+(\delta_{max}) - bv_2^-(\delta_{max}))(v_2^-(\delta_{max}) - v_a)}{u_2^+(\delta_{max}) - u_b} > f(v_2^-(\delta_{max})) - u_2^+(\delta_{max}) \\
\Leftrightarrow\ & \frac{-(v_2^-(\delta_{max}) - v_a)}{u_2^+(\delta_{max}) - u_b} > \frac{f(v_2^-(\delta_{max})) - u_2^+(\delta_{max})}{a(u_2^+(\delta_{max}) - bv_2^-(\delta_{max}))} \\
\Leftrightarrow\ & \frac{u_2^+(\delta_{max})}{a(u_2^+(\delta_{max}) - bv_2^-(\delta_{max}))} - \frac{v_2^-(\delta_{max}) - v_a}{u_2^+(\delta_{max}) - u_b} > \frac{f(v_2^-(\delta_{max}))}{a(u_2^+(\delta_{max}) - bv_2^-(\delta_{max}))},
\end{aligned}
\tag{4.70}
$$

where $u_2^+(\delta_{max}) > 0$, $a(u_2^+(\delta_{max}) - bv_2^-(\delta_{max})) > 0$, $v_2^-(\delta_{max}) - v_a > 0$, $u_2^+(\delta_{max}) - u_b > 0$ and $f(v_2^-(\delta_{max})) > 0$. It is very difficult to find the solution for δ_{max} directly, so we need to make another estimation for P. Let $P_1 = \frac{u_2^+(\delta_{max})}{a(u_2^+(\delta_{max})-bv_2^-(\delta_{max}))} - \frac{v_2^-(\delta_{max})-v_a}{u_2^+(\delta_{max})-u_b}$ and $P_2 = \frac{f(v_2^-(\delta_{max}))}{a(u_2^+(\delta_{max})-bv_2^-(\delta_{max}))}$. We want to find a lower bound of P_1, say P_1^- and an upper bound of P_2, say P_2^+ such that $P_1 > P_1^- \geq P_2^+ > P_2$ by choosing a δ_{max}. Both P_1^- and P_2^+ are estimations, so we probably can not get a small δ_{max}, but it still satisfy our goal if $\delta_{max} < u_2^+ - u_a$ so that $\psi'(u_0) < -1$ on a subinterval of $[u_T, u_T + \delta]$,

where $\psi(u_0)$ is defined in equation (4.32). We will verify this by the typical parameter values later. Recall that $\frac{\partial v_2^-(\delta_{max})}{\partial \delta_{max}} < 0$ by Lemma 2 and $\frac{\partial u_2^+(\delta_{max})}{\partial \delta_{max}} > 0$ by Lemma 1. So

$$\begin{aligned} P_1 = \frac{u_2^+(\delta_{max})}{a(u_2^+(\delta_{max}) - bv_2^-(\delta_{max}))} - \frac{v_2^-(\delta_{max}) - v_a}{u_2^+(\delta_{max}) - u_b} > \\ \frac{u_2^+}{a(u_2^+(\delta_{max}) - bv_2^-(\delta_{max}))} - \frac{v_2^- - v_a}{u_2^+ - u_b} = P_1^-, \end{aligned} \tag{4.71}$$

because $\frac{u_2^+}{a(u_2^+(\delta_{max}) - bv_2^-(\delta_{max}))} < \frac{u_2^+(\delta_{max})}{a(u_2^+(\delta_{max}) - bv_2^-(\delta_{max}))}$ and $\frac{v_2^- - v_a}{u_2^+ - u_b} > \frac{v_2^-(\delta_{max}) - v_a}{u_2^+(\delta_{max}) - u_b}$, where $v_2^- - v_a > v_2^-(\delta_{max}) - v_a$ and $u_2^+ - u_b < u_2^+(\delta_{max}) - u_b$. Next

$$P_2^+ = \frac{f(v_2^-)}{a(u_2^+ - bv_2^-)} > \frac{f(v_2^-(\delta_{max}))}{a(u_2^+(\delta_{max}) - bv_2^-(\delta_{max}))} = P_2, \tag{4.72}$$

because $f(v_2^-) > f(v_2^-(\delta_{max}))$ and $a(u_2^+ - bv_2^-) < a(u_2^+(\delta_{max}) - bv_2^-(\delta_{max}))$. We choose a δ_{max} so that

$$P_1^- = \frac{u_2^+}{a(u_2^+(\delta_{max}) - bv_2^-(\delta_{max}))} - \frac{v_2^- - v_a}{u_2^+ - u_b} \geq \frac{f(v_2^-)}{a(u_2^+ - bv_2^-)} = P_2^+. \tag{4.73}$$

Now we solve for δ_{max} by

$$\frac{u_2^+}{a(u_2^+(\delta_{max}) - bv_2^-(\delta_{max}))} - \frac{v_2^- - v_a}{u_2^+ - u_b} \geq \frac{f(v_2^-)}{a(u_2^+ - bv_2^-)}, \tag{4.74}$$

where $v_2^-(\delta_{max})$, $u_2^+(\delta_{max})$, v_2^-, u_2^+ are given by the equation (4.39),(4.41),(4.50),(4.51). $f(v_2^-) = 0.04(v_2^-)^2 + 5v_2^- + 140 + I$ and u_b is a real constant with respect to the fixed $\delta_{max1} = 2u_a e^a - u_T^- + bv_0(1 - e^a)$. Let $J_1 = \frac{f(v_2^-)}{a(u_2^+ - bv_2^-)} + \frac{v_2^- - v_a}{u_2^+ - u_b} > 0$. Then we have

$$\begin{aligned} &\frac{u_2^+}{a(u_2^+(\delta_{max}) - bv_2^-(\delta_{max}))} \geq J_1 \\ &\Leftrightarrow u_2^+(\delta_{max}) - bv_2^-(\delta_{max}) \leq \frac{u_2^+}{aJ_1} \end{aligned} \tag{4.75}$$

Let $J_2 = \frac{u_2^+}{aJ_1}$. We have

$$\begin{aligned} & J_2 \geq u_2^+(\delta_{max}) - bv_2^-(\delta_{max}) \\ \Leftrightarrow\ & J_2 \geq \frac{u_T^- + \delta_{max} - bv_0}{e^a} + bv_0 - b\left(-5\sqrt{u_T^- + \delta_{max} - u_a} + v_a + \epsilon G\right) \\ \Leftrightarrow\ & J_2 \geq u_T^- e^{-a} + e^{-a}\delta_{max} - bv_0 e^{-a} + bv_0 + 5b\sqrt{u_T^- + \delta_{max} - u_a} - b(v_a + \epsilon G) \\ \Leftrightarrow\ & 5b\sqrt{u_T^- + \delta_{max} - u_a} \leq J_2 - u_T^- e^{-a} - e^{-a}\delta_{max} + bv_0 e^{-a} - bv_0 + b(v_a + \epsilon G) \end{aligned} \tag{4.76}$$

Let $J_3 = J_2 - u_T^- e^{-a} + bv_0 e^{-a} - bv_0 + b(v_a + \epsilon G)$. Thus

$$5b\sqrt{u_T^- + \delta_{max} - u_a} \leq J_3 - e^{-a}\delta_{max} \tag{4.77}$$

We know that there must exist a δ_{max} to satisfy the inequality. Then

$$\begin{aligned} \Rightarrow & \left(5b\sqrt{u_T^- + \delta_{max} - u_a}\right)^2 \leq \left(J_3 - e^{-a}\delta_{max}\right)^2 \\ \Rightarrow & 25b^2(u_T^- + \delta_{max} - u_a) \leq J_3^2 - 2J_3 e^{-a}\delta_{max} + e^{-2a}\delta_{max}^2. \end{aligned} \tag{4.78}$$

It gives a quadratic equation of δ_{max}, which is

$$e^{-2a}\delta_{max}^2 - 2J_3 e^{-a}\delta_{max} - 25b^2\delta_{max} + J_3^2 - 25b^2(u_T^- - u_a) \geq 0 \tag{4.79}$$

$$\Leftrightarrow e^{-2a}\delta_{max}^2 - (2J_3 e^{-a} + 25b^2)\delta_{max} + J_3^2 - 25b^2(u_T^- - u_a) \geq 0 \tag{4.80}$$

$$\Leftrightarrow \delta_{max} \in \left(-\infty, \frac{-J_5 - \sqrt{J_5^2 - 4J_4J_6}}{2J_4}\right] \bigcup \left[\frac{-J_5 + \sqrt{J_5^2 - 4J_4J_6}}{2J_4}, +\infty\right). \tag{4.81}$$

where $J_4 = e^{-2a}$, $J_5 = -(2J_3 e^{-a} + 25b^2)$ and $J_6 = J_3^2 - 25b^2(u_T^- - u_a)$. Clearly, $-\infty < \frac{-J_5 - \sqrt{J_5^2 - 4J_4J_6}}{2J_4} < \frac{-J_5 + \sqrt{J_5^2 - 4J_4J_6}}{2J_4} < +\infty$. We pick

$$\delta_{max} = \frac{-J_5 + \sqrt{J_5^2 - 4J_4J_6}}{2J_4}. \tag{4.82}$$

If δ_{max} is a complex number, then (4.80) holds for any δ_{max} because $e^{-2a} > 0$. Let $\delta_{max2} = \frac{-J_5+\sqrt{J_5^2-4J_4J_6}}{2J_4}$. If δ_{max} is a real number, then we take $\delta_{max} \geq \delta_{max2}$ to ensure that $P_1^- \geq P_2^+$ so that $P_1 > P_2$, which means $P(v_2^-, u_2^+; \delta_{max}) < 0$. Therefore, we choose $\delta_{max} \geq \delta_{max2}$ to ensure that $Q(v_2^-(\delta_{max})) > 0$.

To sum up: We take $\delta_{max} \geq \max(\delta_{max1}, \delta_{max2})$ to ensure that $Q(v_a) \geq 0$ by choosing a minimum real constant $u_b(\delta_{max}) > u_a$ and $Q(v_2^-(\delta_{max})) > 0$ by choosing a δ_{max}, which gives $Q(v) > 0 \ \forall v \in (v_a, v_2^-(\delta_{max})]$.

4.2.4.4.5 Verifying the estimation by the typical parameter values

: Now we verify the estimation by applying the typical parameter values $a = 0.02$, $b = 0.2$, $v_0 = c = -65$, $v_s = 30$, $I = 40$, $\epsilon = 3$, $G = 15$, the delay time τ=1ms [8][10] and $v_a = -62.5$, $u_a = 23.75$ from (4.11). Then we have

$$u_T^- \approx 44.57, \quad \frac{1}{a} = 50 > 45 = \epsilon G, \quad \delta_{max1} = 2u_a e^a - u_T^- + bv_0(1 - e^a) \approx 4.15, \tag{4.83}$$

$$u_a = 23.75 > 22.29 = \max(19.09, 22.29) \approx \max(3 + \sqrt{9 - 4v_a}, \frac{u_T^-}{2}), \tag{4.84}$$

$$v_2^- = -5\sqrt{u_T^- - u_a} + v_a + \epsilon G \approx -40.32, \quad u_2^+ = \frac{u_T^- - bv_0}{e^a} + bv_0 \approx 43.43, \tag{4.85}$$

$$v_2^-(\delta_{max1}) = -5\sqrt{u_T^- + \delta_{max1} - u_a} + v_a + \epsilon G \approx -42.49, \tag{4.86}$$

$$u_2^+(\delta_{max1}) = \frac{u_T^- + \delta_{max1} - bv_0}{e^a} + bv_0 \approx 47.5, \quad u_b(\delta_{max1}) \approx 24.39 > 23.75 = u_a, \tag{4.87}$$

so the result of Claim 1 holds. Hence, $Q(v_a) \geq 0$ by choosing a minimum real constant $u_b(\delta_{max}) > u_a$, where $\delta_{max} \geq \delta_{max1}$. Also

$$v_2^-(\delta_{max1}) \approx -42.49 > -60 = \frac{b-5}{0.08}, \tag{4.88}$$

so the result of Claim 2 holds, then $\frac{dP}{d\delta_{max}} < 0$, where $\delta_{max} \geq \delta_{max1}$. Now

$$J_1 \approx 43.34,\ J_2 \approx 50.11,\ J_3 \approx 3.18,\ J_4 \approx 0.96,\ J_5 \approx -7.23,\ J_6 \approx -10.72, \tag{4.89}$$

$$\delta_{max2} = \frac{-J_5 + \sqrt{J_5^2 - 4J_4J_6}}{2J_4} \approx 8.8,\ v_2^-(\delta_{max2}) \approx -44.71, \tag{4.90}$$

$$u_2^+(\delta_{max2}) \approx 52.06,\ f(v_2^-(\delta_{max2})) \approx 36.41,\ u_b(\delta_{max2}) \approx 24.22 > 23.75 = u_a, \tag{4.91}$$

so $P(v_2^-, u_2^+; \delta_{max2}) \approx -1.49 < 0$. Hence, $Q(v_2^-(\delta_{max})) > 0$, where $\delta_{max} \geq \delta_{max2}$. Finally, we take

$$\delta_{max} \geq \max(\delta_{max1}, \delta_{max2}) \approx \max(4.15, 8.8) = 8.8 \tag{4.92}$$

to ensure that $Q(v) > 0\ \forall v \in (v_a, v_2^-(\delta_{max})]$. In fact, if we take $\delta_{max} = \delta_{max1} \approx 4.15$, then $P(v_2^-, u_2^+; \delta_{max1}) \approx -1.01 < 0$. However, we just need $P(v_2^-, u_2^+; \delta_{max}) < 0$, so δ_{max1} is already more than necessary. This is because we made estimations for both P_1^- and P_2^+ in the estimating P so that the error of the estimation has become larger. If we take $\delta_{max} = 1$, then $P(v_2^-, u_2^+; \delta_{max}) \approx -0.37 < 0$, so numerically the $\delta < 1 = \delta_{max}$.

4.2.4.4.6 $\psi'(u_0) < -1$ on a subinterval of $[u_T, u_T + \delta]$, where $\psi(u_0)$ is defined in equation (4.32) : Clearly, $\delta_{max} > \delta$, so $\delta < 8.8$. According to Lemma 6, if u_0 is increased by δ from u_T on the reset line $v = v_0$, then the trajectory from (v_2, u_2) to (v_s, u_3) crosses the vertex (v_a, u_a) of the parabola $F_v = 0$ (see Figure 4.15). Let $\Delta u_2 = u_a - u_2^+$ and $\Delta u_0 = u_T + \delta - u_T = \delta$. We have

$$\frac{\Delta u_2}{\Delta u_0} = \frac{u_a - u_2^+}{\delta} \approx \frac{23.75 - 43.43}{8.8} < -2.24 < -1. \tag{4.93}$$

Then the trajectories starting from (v_2^-, u_2^+) and (v_a, u_a) go to (v_s, u_3) and $(v_s, \tilde{u}_3)$ respectively on the spiking line $v = v_s$ along the Izhikevich flow (see Figure 4.17).

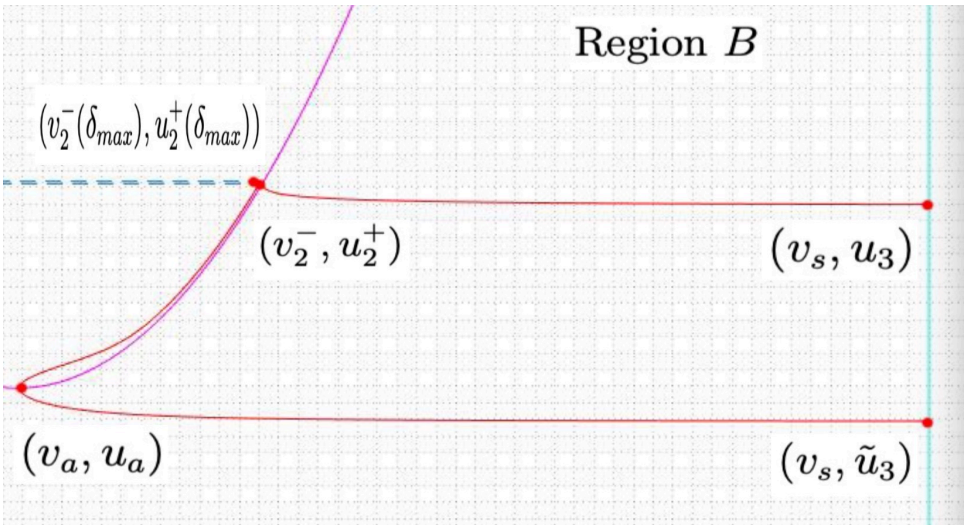

Figure 4.17: The gap between u_3 and $\tilde{u}_3$ is very large after the two trajectories go to the spiking line $v = v_s$ along the Izhikevich flow.

In the region B, we have $\frac{du}{dv} = \frac{a(bv-u)}{0.04v^2+5v+140+I-u} < 0$ with $a = 0.02$, $b = 0.2$ and $I = 40$. Recall that we have a better but complicated lower bound of v_1 from Step I, which is

$$\tilde{v}_1^- = \frac{\left|\frac{v_0+62.5+\alpha}{v_0+62.5-\alpha}\right| e^{\frac{-2\tau\alpha}{25}}(62.5-\alpha) + 62.5 + \alpha}{-\left(1 + \left|\frac{v_0+62.5+\alpha}{v_0+62.5-\alpha}\right| e^{\frac{-2\tau\alpha}{25}}\right)} \approx -80.09, \tag{4.94}$$

where $\alpha = 5\sqrt{u_T^- - u_a} > 0$. $\tilde{v}_2^- = \tilde{v}_1^- + \epsilon G \approx -35.09$. Now we replace v_2^- by the better lower bound $\tilde{v}_2^-$ to estimate u_3. Then

$$\begin{aligned} u_3 &\approx u_2^+ + \int_{\tilde{v}_2^-}^{v_s} \frac{a(bv - u_2^+)}{0.04v^2 + 5v + 140 + I - u_2^+} dv \\ &\approx 43.43 + \int_{-35.09}^{30} \frac{0.02(0.2v - 43.43)}{0.04v^2 + 5v + 140 + 40 - 43.43} dv \\ &\approx 43.43 - 0.94 \\ &\approx 42.49. \end{aligned} \tag{4.95}$$

Since $\frac{du}{dv} < 0$ in the region B, we have $\tilde{u}_3 < u_a$. Let $\Delta u_3 = \tilde{u}_3 - u_3$. Thus

$$\frac{\Delta u_3}{\Delta u_0} = \frac{\tilde{u}_3 - u_3}{\delta} < \frac{u_a - u_3}{\delta} \approx \frac{23.75 - 42.49}{8.8} < -2.13 < -1, \tag{4.96}$$

which means $\frac{\Delta\psi(u_0)}{\Delta u_0} < -2.13 < -1$. Then there must $\exists$ a subinterval of $[u_T, u_T + \delta]$ on which $\frac{d\psi(u_0)}{du_0} < -1$. Therefore, $\psi'(u_0) < -1$ on a subinterval of $[u_T, u_T + \delta]$.

4.2.4.4.7 $u_T + \delta < u_{\star\star\star}$: $u_T + \delta = u_T^- + \delta_{max} \approx 44.57 + 8.8 = 53.37$. $u_2^+(\delta_{max}) = u_1^+(\delta_{max}) = 0.04v^2 + 5v + 140 + I$, where $u_2^+(\delta_{max}) = u_1^+(\delta_{max}) \approx 52.06$ and $I = 40$. Thus, $v = -89.1$ or $v = -35.9$. Clearly, $(v = -89.1, u_1^+(\delta_{max}) = 52.06)$ is on the left branch of the v-nullcline. Now

$$\tilde{v}_1^-(\delta_{max}) = \frac{\left|\frac{v_0+62.5+\alpha}{v_0+62.5-\alpha}\right| e^{\frac{-2\tau\alpha}{25}}(62.5 - \alpha) + 62.5 + \alpha}{-\left(1 + \left|\frac{v_0+62.5+\alpha}{v_0+62.5-\alpha}\right| e^{\frac{-2\tau\alpha}{25}}\right)} \approx -85.02, \tag{4.97}$$

where $\alpha = 5\sqrt{u_T^- + \delta_{max} - u_a} > 0$. $v = -89.1 < -85.02 = \tilde{v}_1^-(\delta_{max})$, so $(\tilde{v}_1^-(\delta_{max}), u_1^+(\delta_{max}))$ is in the region A. Therefore, $u_T + \delta = u_T^- + \delta_{max} < u_{\star\star\star}$.

4.2.4.5 Case 2b: $u_0 \in (u_T + \delta, +\infty)$

If $u_0 \in (u_T + \delta, +\infty)$, then the trajectory from u_0 along Step III of the trajectory from (v_2, u_2) to (v_s, u_3) crosses the left branch of the parabola $F_v = 0$. In other words, the trajectory will go to the recovery phase after Step II (see Figure 4.18).

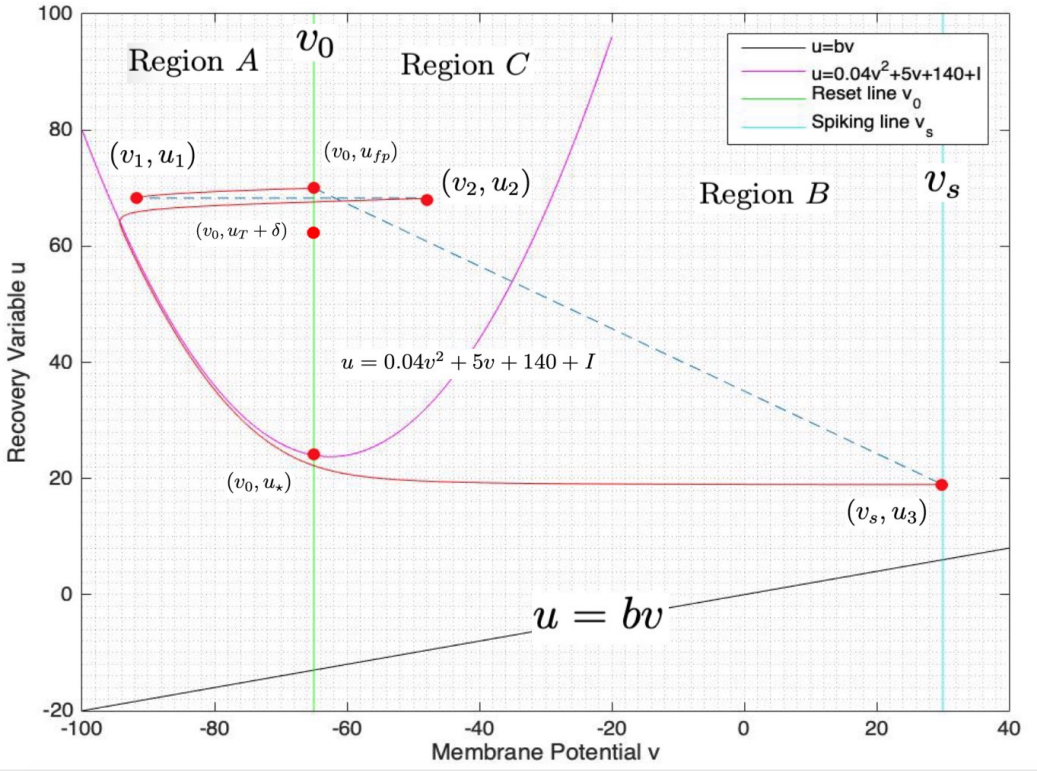

Figure 4.18: All trajectories starting from $u_0 \in (u_T + \delta, +\infty)$ go to the recovery phase after Step II.

Here are three comments in relation to $u_0 \in (u_T + \delta, +\infty)$.

(i) The typical parameter value d in the neuroscience behavior: Since all trajectories go to the recovery phase after Step II, then they all reach the spiking line $v = v_s$ along the Izhikevich flow under the v-nullcline. Clearly, $u_a > u_3$. Thus, if there $\exists$ a fixed point of Φ, such that $u_{fp} \in (u_T + \delta, +\infty)$, then $d > u_T + \delta - u_a = u_T^- + \delta_{max} - u_a \approx 44.57 + 8.8 - 23.75 \approx 29.62$ so that $u_{fp} = \Phi(u_{fp})$. However, Izhikevich [8], Modolo and colleagues [10] have suggested that d should between -21 and 8. Therefore, $d > 29.62$ is not a valid neuroscience parameter, but mathematically d can be very large.

(ii) The differences between two models: The differences between the single-neuron Izhikevich model and our model are Step I and Step II. More precisely, the differences depend on the "jump". If (v_2, u_2) can cross the right branch of the v-

nullcline by the "jump", then we get one spike after the trajectory reaches the spiking line $v = v_s$ along the Izhikevich flow. By repeating this process, we probably obtain a bursting behavior, then we say that this "jump" is effective because it does change the qualitative behaviour from the original Izhikevich model. In other words, for $u_0 \in (u_T + \delta, +\infty)$, the (v_2, u_2) still stays above the v-nullcline after the "jump". Then the trajectory will go to the recovery phase (cross the left branch of the v-nullcline) along the Izhikevich flow. The "jump" does not change the mechanism from the original Izhikevich model, so we say that this "jump" is ineffective. Therefore, for $u_0 \in (u_T + \delta, +\infty)$, where the "jump" is ineffective, our model has exactly the same qualitative behaviour as the Izhikevich model after Step II.

(iii) $-1 < \psi'(u_0) < 0$: In order to study the properties of the fixed point $u_{fp} \in (u_T + \delta, +\infty)$ when it exists (large d), we need to understand the motion of all trajectories that go to the recovery phase after Step II.

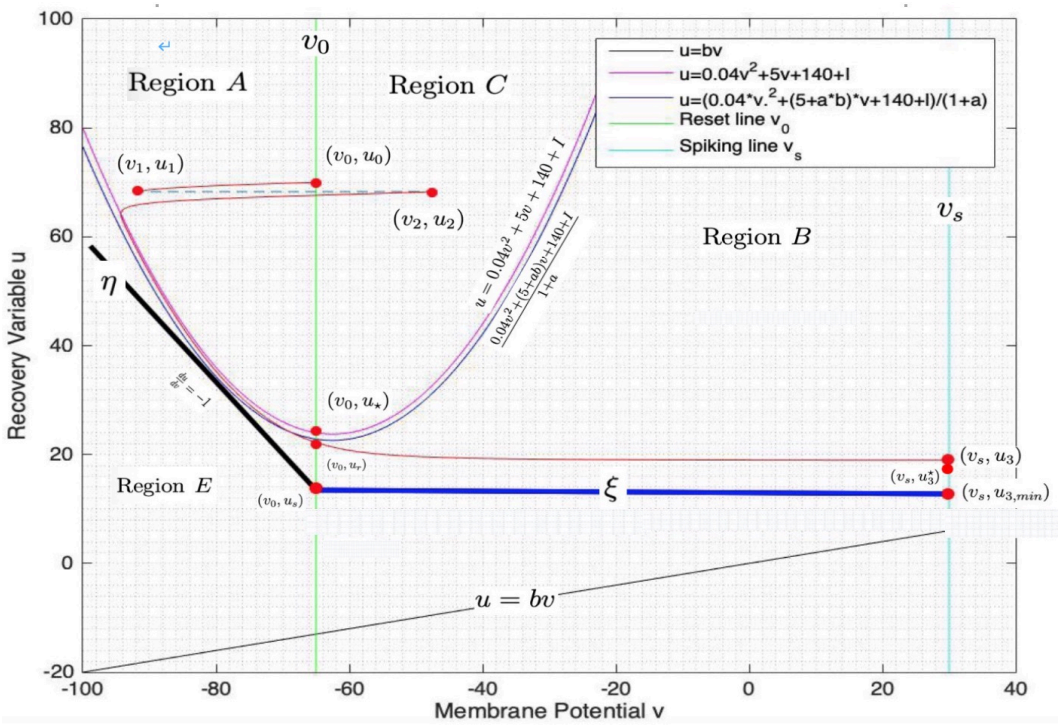

Figure 4.19: All trajectories below $\xi(t)$ backwards in time from (v_s, u_3) cannot go above of the parabola $F_v = 0$.

Let (v_0, u_r) be the intersection between the trajectory from (v_2, u_2) to (v_s, u_3) and the reset line $v = v_0$ in the region B. Let $u = f_s(v)$ be the curve on which $\frac{du}{dv} = -1$ for the Izhikevich flow. This can be derived as follows:

$$\begin{aligned} \frac{du}{dv} = \frac{\frac{du}{dt}}{\frac{dv}{dt}} &= -1, \\ \Leftrightarrow -\frac{du}{dt} &= \frac{dv}{dt}, \\ \Leftrightarrow -(abv - au) &= 0.04v^2 + 5v + 140 + I - u, \\ \Leftrightarrow (1+a)u &= 0.04v^2 + (5+ab)v + 140 + I, \\ \Leftrightarrow u &= \frac{0.04v^2 + (5+ab)v + 140 + I}{1+a}, \end{aligned} \tag{4.98}$$

where a, b and I are positive constants. The $f_s(v) = \frac{0.04v^2+(5+ab)v+140+I}{1+a}$. Clearly, $f_s(v) = \frac{0.04v^2+(5+ab)v+140+I}{1+a} < 0.04v^2 + 5v + 140 + I = f(v)$. Let η be the line tangent to $f_s(v)$ with slope $\frac{du}{dv} = -1$. Let (v_0, u_s) be the intersection between η and the reset line $v = v_0$. Let $\xi(t)$ be the trajectory from (v_0, u_s) to $(v_s, u_{3,min})$ on the spiking line $v = v_s$ along the Izhikevich flow. Let region $E = \{(v, u) | bv_s < u < \eta, v < v_0\}$ (see Figure 4.19). Assume $u_3 \leq u_{3,min}$, then the Izhikevich trajectory from (v_0, u_r) to (v_s, u_3) must be below $\xi(t)$ by the uniqueness theorem for ODEs. So, $u_r \leq u_s$. Also, because $\frac{dv}{dt} > -\frac{du}{dt}$ in the region E, the trajectory reaching (v_0, u_r) can not cross η at an earlier time. Therefore, the trajectory backwards in time from (v_s, u_3) can not go above the parabola $F_v = 0$. So $\lim_{t \to -\infty} v(t) = -\infty$. In other words, if we consider the flow from (v_2, u_2) when $u_0 > u_T + \delta$, then $u_3 = \Phi_3(v_2, u_2) > u_{3,min}$ because the flow backwards from $(v_s, u_{3,min})$ must come from $v = -\infty$. Now

$$\frac{du_3}{du_0} = \frac{d\Phi_3}{dv_2}\frac{dv_2}{du_0} + \frac{d\Phi_3}{du_2}\frac{du_2}{du_0} < 0, \tag{4.99}$$

where $\frac{d\Phi_3}{dv_2} > 0$ and $\frac{d\Phi_3}{du_2} < 0$ by the uniqueness theorem for ODEs, $\frac{dv_2}{du_0} < 0$ by Lemma

2 and $\frac{du_2}{du_0} > 0$ by Lemma 1. So $u_3(u_0)$ is a monotonically decreasing function as $u_0 \in (u_T + \delta, +\infty)$ increases. However, since we know that $u_3 = \Phi_3(v_2, u_2) > u_{3,min}$, we have $\lim_{u_0 \to +\infty} u_3 \geq u_{3,min}$, which implies that u_3 is bounded by $u_{3,min}$. Thus, there must $\exists$ a lower bound of u_3, say $u_3^\star$ such that $\lim_{u_0 \to +\infty} u_3 = u_3^\star \geq u_{3,min}$ by the Bolzano-Weierstrass theorem. Therefore, we have $\lim_{u_0 \to +\infty} \psi'(u_0) = 0$.
Since $\psi'(u_0) < -1$ on a subinterval of $[u_T, u_T + \delta]$ and $\lim_{u_0 \to +\infty} \psi'(u_0) = 0$ for $u_0 \in (u_T + \delta, +\infty)$, we know that there must $\exists$ a largest value u, say u_c such that $\psi'(u_c) = -1$. Now, we can conclude that $-1 < \psi'(u_0) < 0$ for $u_0 \in (u_c, +\infty)$.

4.2.5 Φ_4: $u_3 \mapsto u_4$

Φ_4 is neither an expansion nor a contraction in u. Φ_4 is just an instantaneous reset from (v_s, u_3) to (v_0, u_4), where $u_4 = u_3 + d$ and d is fixed. If Φ_3 is a contraction in u, then the composition of Φ_3 and Φ_4 is also a contraction in u. $\Phi(u_0) = \psi(u_0) + d$, where $\psi(u_0)$ is independent of d.

To sum up, for $u_0 \in (u_{\star\star}, u_T) \cup (u_c, +\infty)$, $\psi(u_0)$ is a contraction in u, so $\Phi(u_0)$ is also a contraction in u. Thus, $-1 < (\Phi_4 \circ \Phi_3 \circ \Phi_2 \circ \Phi_1(u_0))' < 1$, which means $-1 < \Phi'(u_0) < 1$. For $u_0 \in [u_T, u_T + \delta]$, $\psi'(u_0) < -1$ on a subinterval of $[u_T, u_T + \delta]$, so $\Phi'(u_0) < -1$ on a subinterval of $[u_T, u_T + \delta]$.

4.3 The fixed point of Φ

4.3.1 The existence and uniqueness of the fixed point

In order to know if neuron interaction can cause bursting behavior, we need to investigate the fixed point of Φ because Φ has a tonic firing behavior if the fixed point is stable and Φ perhaps has a bursting behavior if the fixed point is unstable.

Definition 8. *Let $d_{\star\star} > 0$ be such that $\Phi_4(u_3) = u_{\star\star}$, where $u_3 = \Phi_3 \circ \Phi_2 \circ \Phi_1(u_{\star\star})$, which means $u_4 = u_3 + d_{\star\star} = u_{\star\star}$. This choice makes $u_{\star\star}$ the fixed point of Φ.*

Lemma 7. *If $d > d_{\star\star}$, then $\Phi(u_{\star\star}) > u_{\star\star}$.*

Proof. Obviously, according to definition 8, if $d > d_{\star\star}$, then $d > u_{\star\star} - u_3 \Rightarrow \Phi(u_{\star\star}) > u_{\star\star}$. □

Lemma 8. *Given a fixed d, if $u_0 > \max(u_T + \delta, u_a + d)$, then $\Phi(u_0) < u_0$.*

Proof. First suppose $d < u_T + \delta - u_a$. If $u_0 > u_T + \delta$, then $u_3 < u_a$, so $u_4 < u_a + d < u_T + \delta < u_0 \Rightarrow \Phi(u_0) < u_0$ for all $u_0 \in (u_T + \delta, +\infty)$. Now suppose $d \geq u_T + \delta - u_a$. If $u_0 > u_a + d \geq u_T + \delta$, then $u_3 < u_a$, so $u_4 < u_a + d < u_0 \Rightarrow \Phi(u_0) < u_0$ for all $u_0 \in (u_a + d, +\infty)$. □

Theorem 1. *There exists a unique fixed point $u_{fp} \in (u_{\star\star}, +\infty)$ such that $\Phi(u_{fp}) = u_{fp}$, if*

1, $\Phi(u) < u$ for $u \in [\max(u_T + \delta, u_a + d), +\infty)$,

2, d is sufficiently large such that $\Phi(u_{\star\star}) > u_{\star\star}$, and

3, $\Phi'(u) < 1$ $\forall u \in (u_{\star\star}, +\infty)$.

Proof. $\Phi(u)$ is a continuous function with $\Phi(u_{\star\star}) > u_{\star\star}$ and $\Phi(u) < u$ for $u \in [\max(u_T+\delta, u_a+d), +\infty)$, so there must exist at least one fixed point $u_{fp} \in (u_{\star\star}, +\infty)$ such that $\Phi(u_{fp}) = u_{fp}$. Moreover, assume $\exists$ two fixed points, then one of them has $\Phi'(u) \geq 1$, which contradicts assumption 3. Therefore, there exists a unique fixed point $u_{fp} \in (u_{\star\star}, +\infty)$ such that $\Phi(u_{fp}) = u_{fp}$ (see Figure 4.20). □

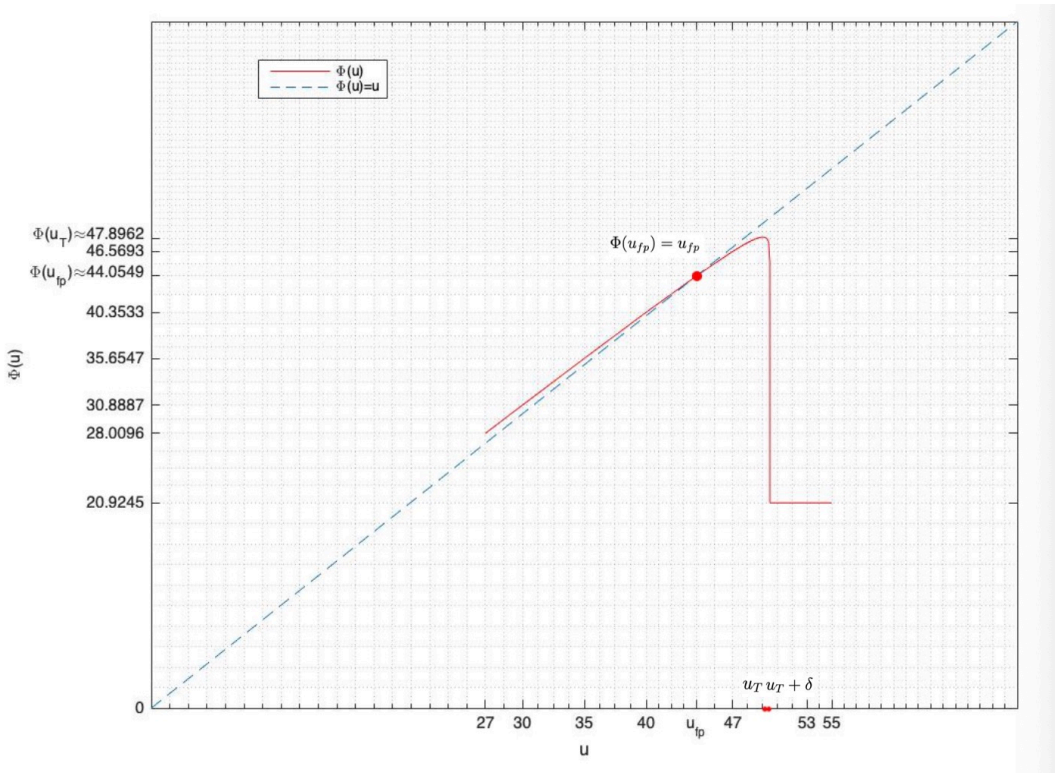

Figure 4.20: When $d = 2$, $\Phi(u_{fp}) = u_{fp} \approx 44.0549 \in (u_{\star\star}, u_T)$, where $u_{\star\star} \approx 24.84$ and $u_T \approx 49.73$. The fixed point is stable because $0 < \Phi'(u_{fp}) < 1$.

4.3.2 The stability of the fixed point

For $u_{fp} \in (u_{\star\star}, u_T) \cup (u_c, +\infty)$, we have $-1 < \Phi'(u_{fp}) < 1$, so u_{fp} is a stable fixed point. We have $\Phi'(u_{fp}) < -1$ on a subinterval of $[u_T, u_T + \delta]$, so u_{fp} is the unstable fixed point on a subinterval of $[u_T, u_T + \delta]$. Therefore, Φ probably has a bursting behavior on a subinterval of $[u_T, u_T + \delta]$. We will discuss this in more detail in the next section.

4.4 Bifurcation

4.4.1 The location of the fixed point

Now we apply the typical parameter values $a = 0.02$, $b = 0.2$, $v_0 = c = -65$, $v_s = 30$, $I = 40$, $\epsilon = 3$, $G = 15$, the delay time τ=1ms [8][10] in the numerical simulations.

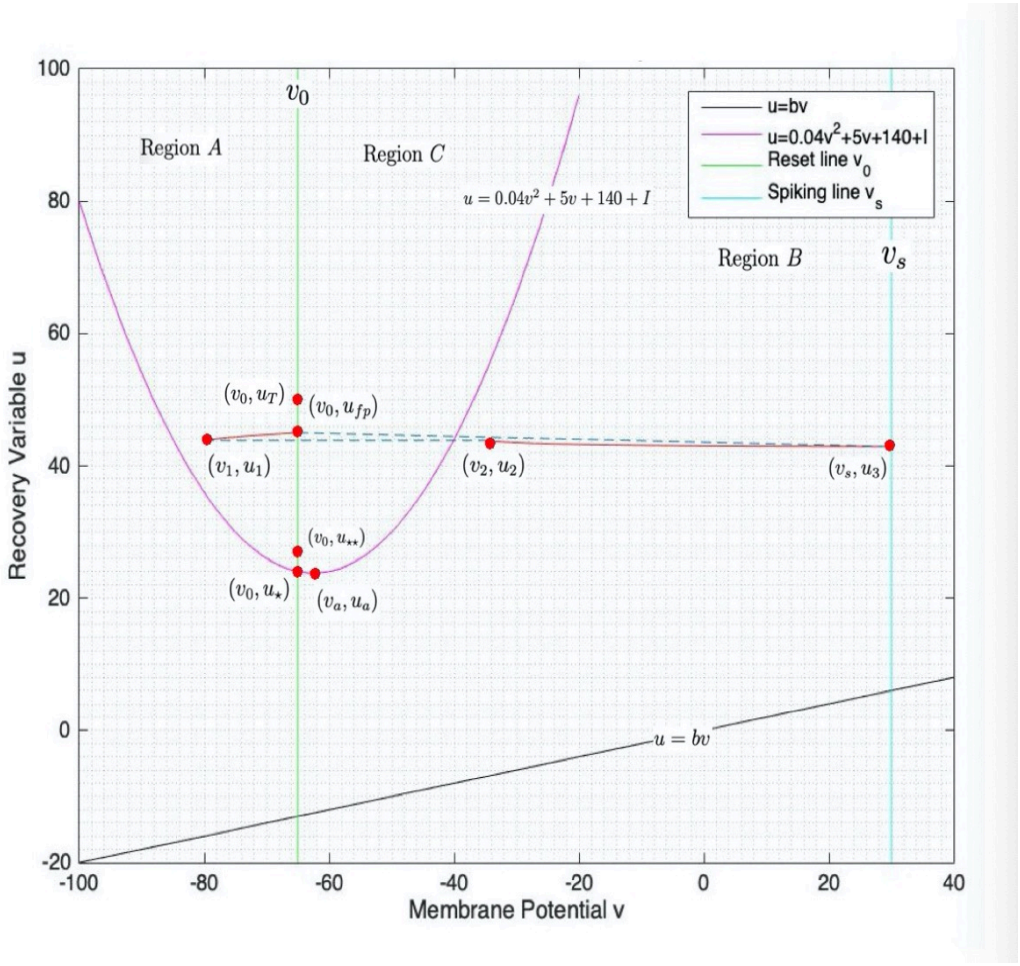

Figure 4.21: Stable periodic solution corresponding to the fixed point of Φ for $0.9096 < d < 3.8361$.

If $0.9096 < d < 3.8361$, where $d = 0.9096 = d_{\star\star}$ (see definition 8) and $d = 3.8361$ is such that $\Phi(u_T) = u_T$, then we have a unique fixed point u_{fp} such that $\Phi(u_{fp}) = u_{fp} \in (u_{\star\star}, u_T)$ (see Figure 4.21), where $u_{\star\star} \approx 24.84$ and $u_T \approx 49.73$. The fixed

point and the corresponding periodic orbit are stable. Note that if $d < 5.9155$ then a trajectory starting in the recovery phase (left branch of the v-nullcline) will spike more than once before arriving in $\mathcal{D}$ after which it converges to the periodic orbit. If $3.8361 \leq d \leq 30.6717$, where $d = 30.6717$ is such that $\Phi(u_T + \delta) = u_T + \delta$, then we have a unique fixed point u_{fp} such that $\Phi(u_{fp}) = u_{fp} \in [u_T, u_T + \delta]$ (see Figure 4.22), where $u_T + \delta \approx 50.003$. For most of this range of d, the fixed point of Φ, and the corresponding periodic orbit, will be unstable because $\Phi'(u_{fp}) < -1$. If $30.6717 < d < +\infty$, we have a unique fixed point u_{fp} such that $\Phi(u_{fp}) = u_{fp} \in (u_T + \delta, +\infty)$ (see Figures 4.23 and 4.24).

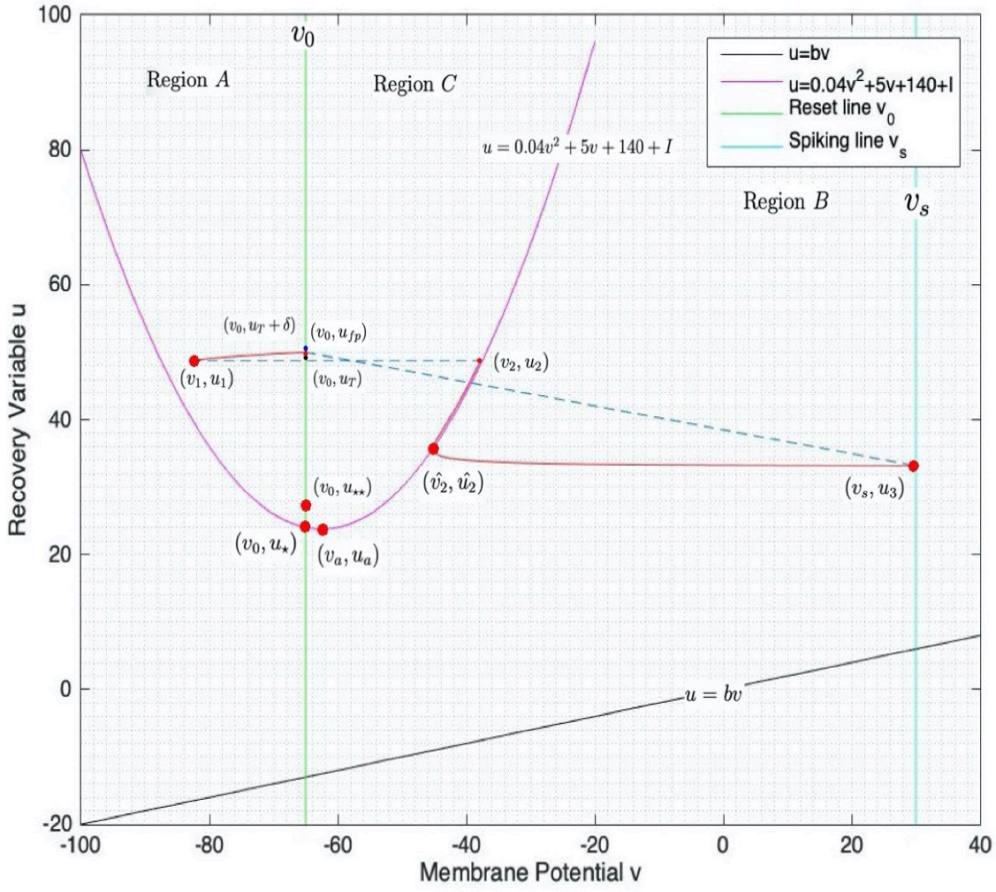

Figure 4.22: Periodic orbit corresponding to the fixed point of Φ for $3.8361 \leq d \leq 30.6717$.

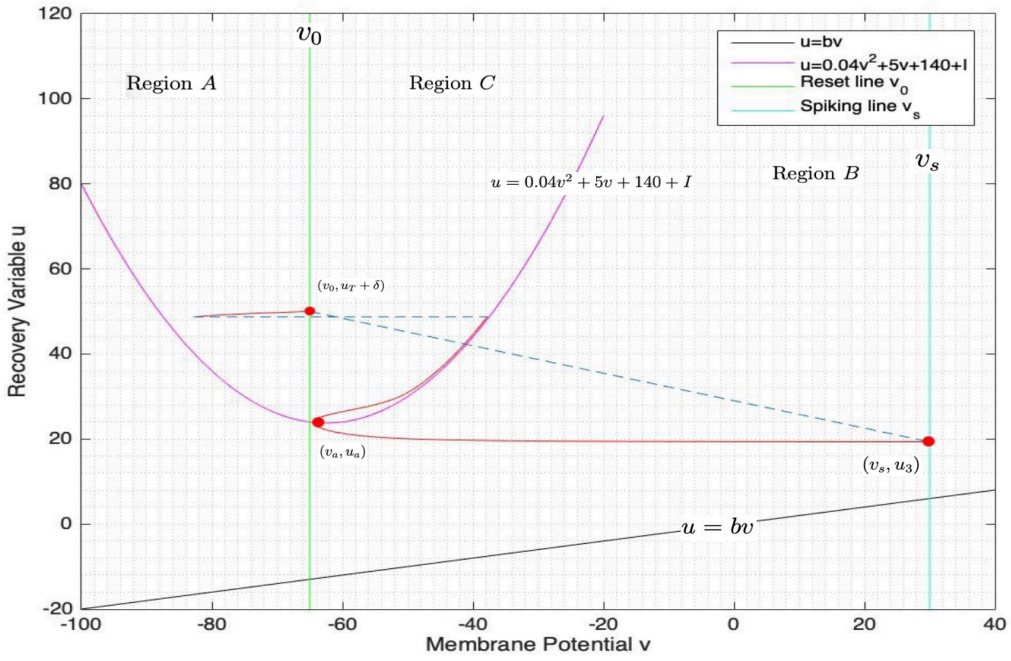

Figure 4.23: Periodic orbit corresponding to the fixed point of Φ for $d = 30.6717$. Here, the fixed point is at $u_T + \delta$ and the trajectory passes through the vertex of the v-nullcline.

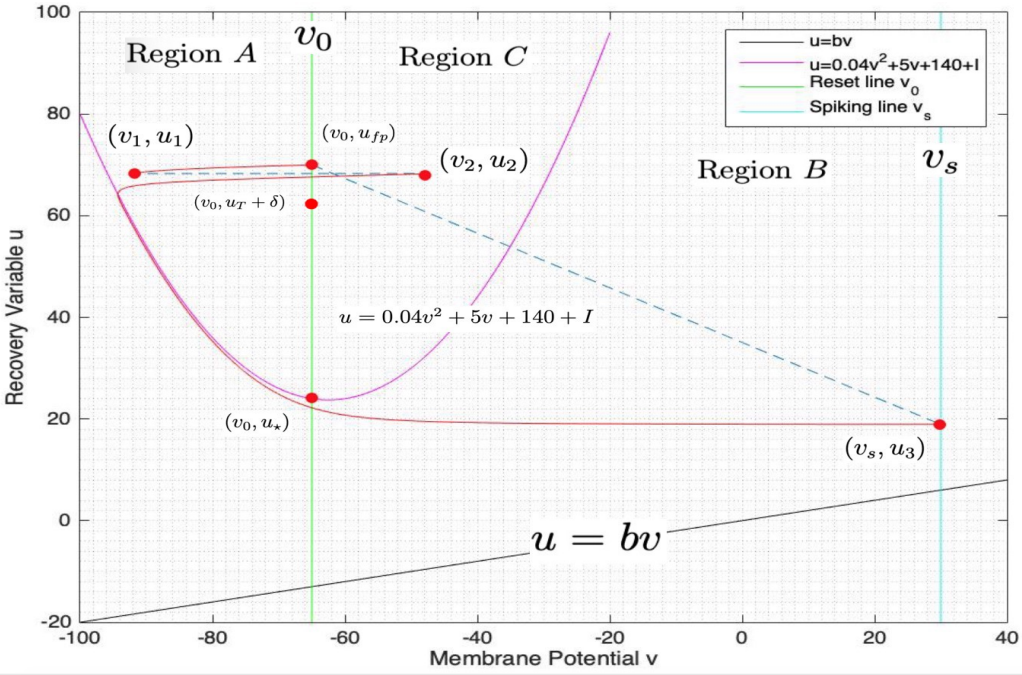

Figure 4.24: Stable periodic orbit corresponding to the fixed point of Φ for $30.6717 < d < +\infty$.

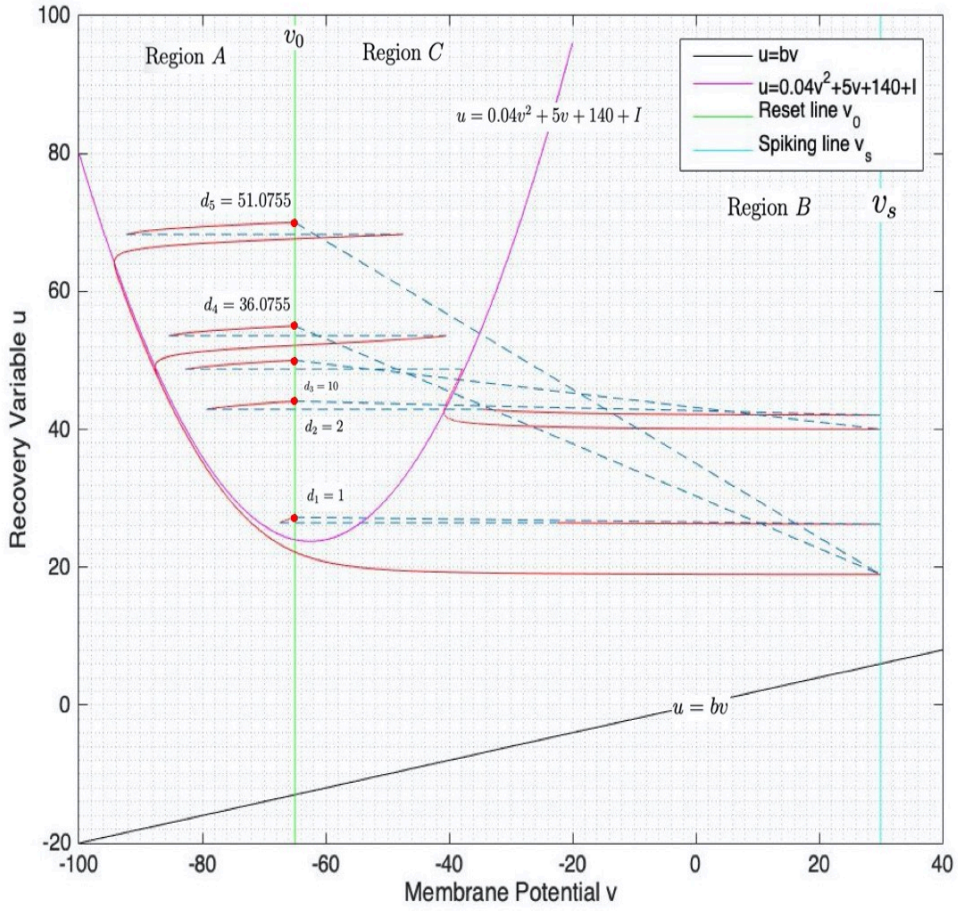

Figure 4.25: Periodic orbits corresponding to the fixed point of Φ for $d_1 = 1$, $d_2 = 2$, $d_3 = 10$, $d_4 = 36.0755$ and $d_5 = 51.0755$. The fixed point increases as d increases.

Figure 4.25 shows that the locations of the fixed points with different d. We can see that $u_{fp}(d_1) < u_{fp}(d_2) < u_{fp}(d_3) < u_{fp}(d_4) < u_{fp}(d_5)$ as $d_1 < d_2 < d_3 < d_4 < d_5$, which must be the case because $\Phi'(u_{fp}) < 1$ for $u_{fp} \in (u_{\star\star}, +\infty)$. Since $\Phi(u_{fp}) = \psi(u_{fp}) + d$, we know that the location of the fixed point depends on d, but the stability of the fixed point does not depend directly on d (only because the location changes).

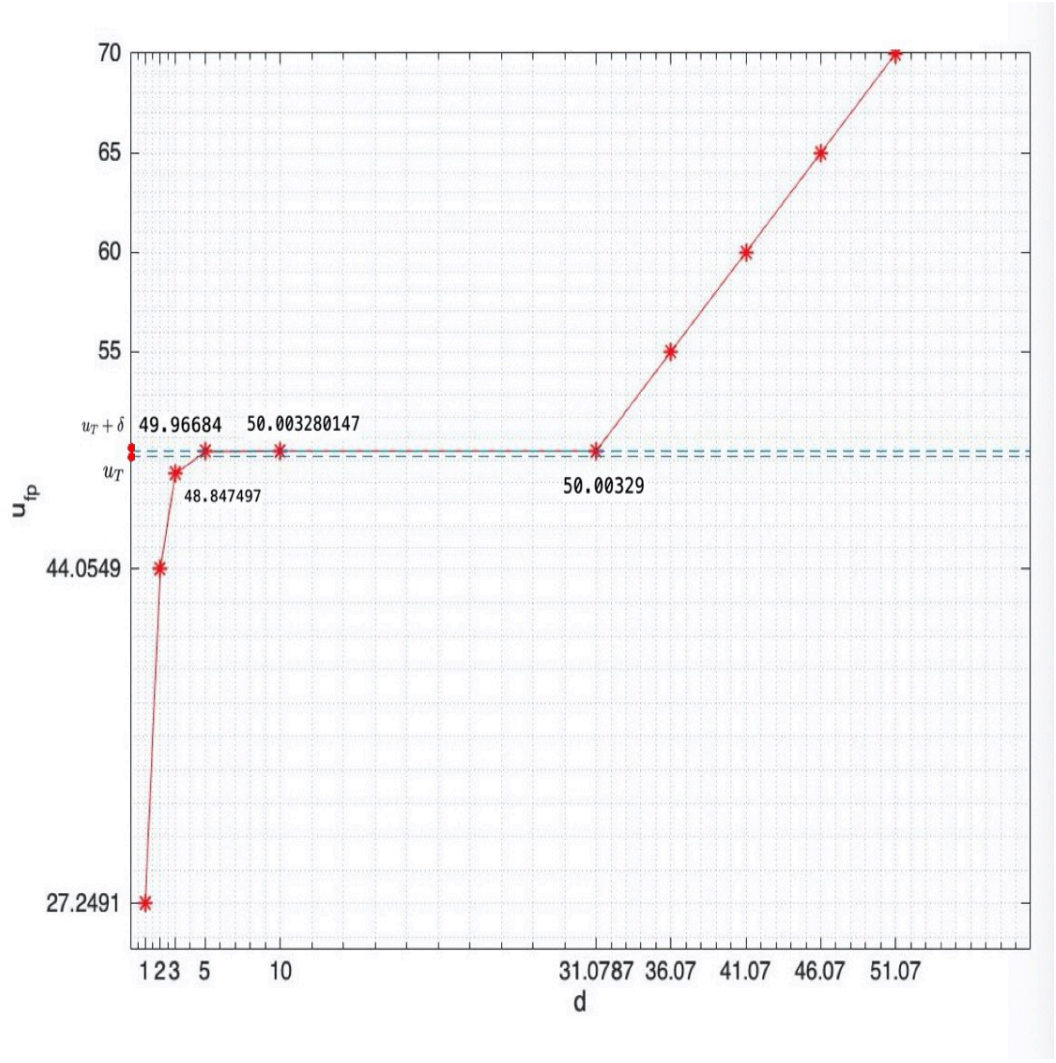

Figure 4.26: The unique fixed point of Φ as a function of d. d must have a very large increment in order for $u_{fp} \in [u_T, u_T + \delta]$ to have a slight increment.

In Figure 4.26, we can see that for $u_{fp} \in (u_{\star\star}, u_T)$, a small increase in d can lead a big increase in u_{fp}, thus $u'_{fp}(d) \gg 1$. On the contrary, in order to have an extremely slight increase in $u_{fp} \in [u_T, u_T + \delta]$, d must have a very large increase, then $0 < u'_{fp}(d) \ll 1$. If $u_{fp} \in (u_T + \delta, +\infty)$, then $0 < u'_{fp}(d) < 1$ but close to 1.

4.4.2 Bifurcation parameter

Now we want to know how d as a bifurcation parameter affects the fixed point and dynamics of Φ as d increases. Firstly, d must be large enough such that $\Phi(u_{\star\star}) > u_{\star\star}$, then we choose a small d ($d = 2$) [8], a medium d ($d = 6$) [10] and a large d ($d = 36$).

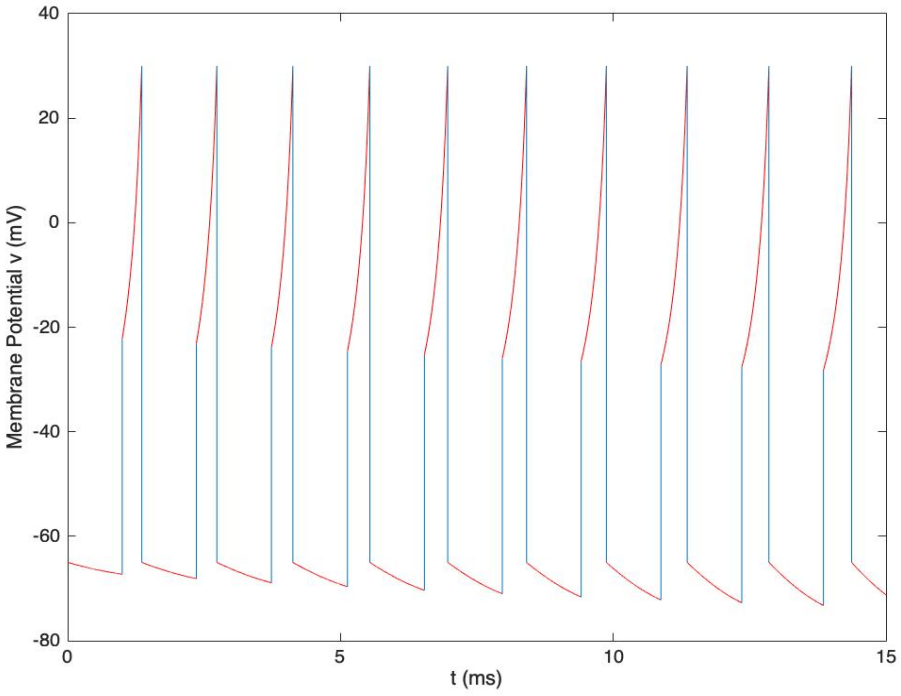

Figure 4.27: When $d = 2$, the behavior is a fast tonic firing with infinite number of spikes per burst (*i.e.*, no recovery phase between spikes).

Case 1: $d = 2$ (see Figures 4.20 and 4.27). We know that $0 < \Phi'(u_{fp}) < 1$ as $u_{fp} \in (u_{\star\star}, u_T)$, since $u_{fp} < u_T$, we have that the Φ map stops at the stable fixed point u_{fp} and the behavior is a fast tonic firing with infinite number of spikes per burst. There is no recovery phase in the Φ map between spikes.

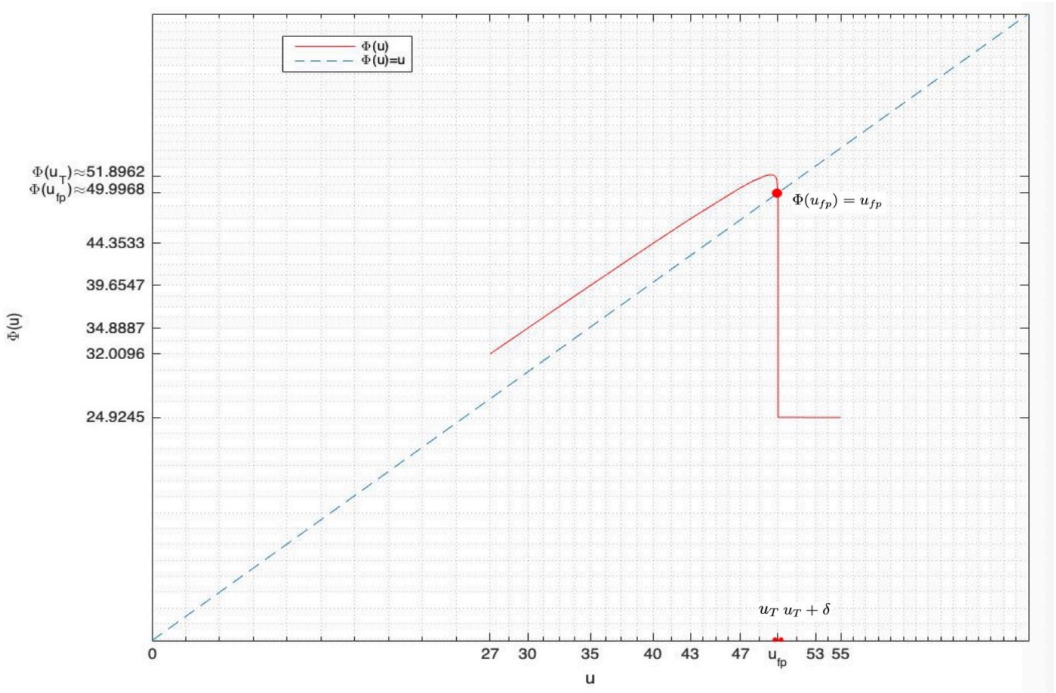

Figure 4.28: When $d = 6$, $\Phi(u_{fp}) = u_{fp} \approx 49.9968 \in [u_T, u_T + \delta]$, where $u_T \approx 49.73$ and $u_T + \delta \approx 50.003$. $\Phi'(u_{fp}) < -1$, so the fixed point is unstable.

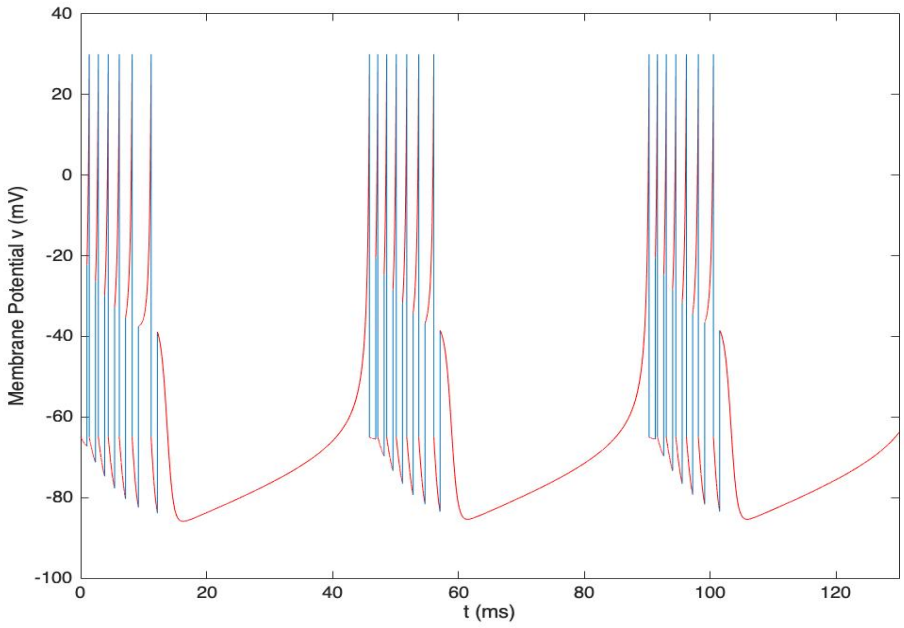

Figure 4.29: When $d = 6$, the behavior is a bursting with 7 spikes per burst.

Case 2: $d = 6$ (see Figures 4.28 and 4.29). For $u_{fp} \in [u_T, u_T+\delta]$, we have $\Phi'(u_{fp}) < -1$ on a subinterval of $[u_T, u_T+\delta]$, so the fixed point in this subinterval is unstable. Thus the behavior is a bursting with k spikes per burst, where $1 < k < \infty$.

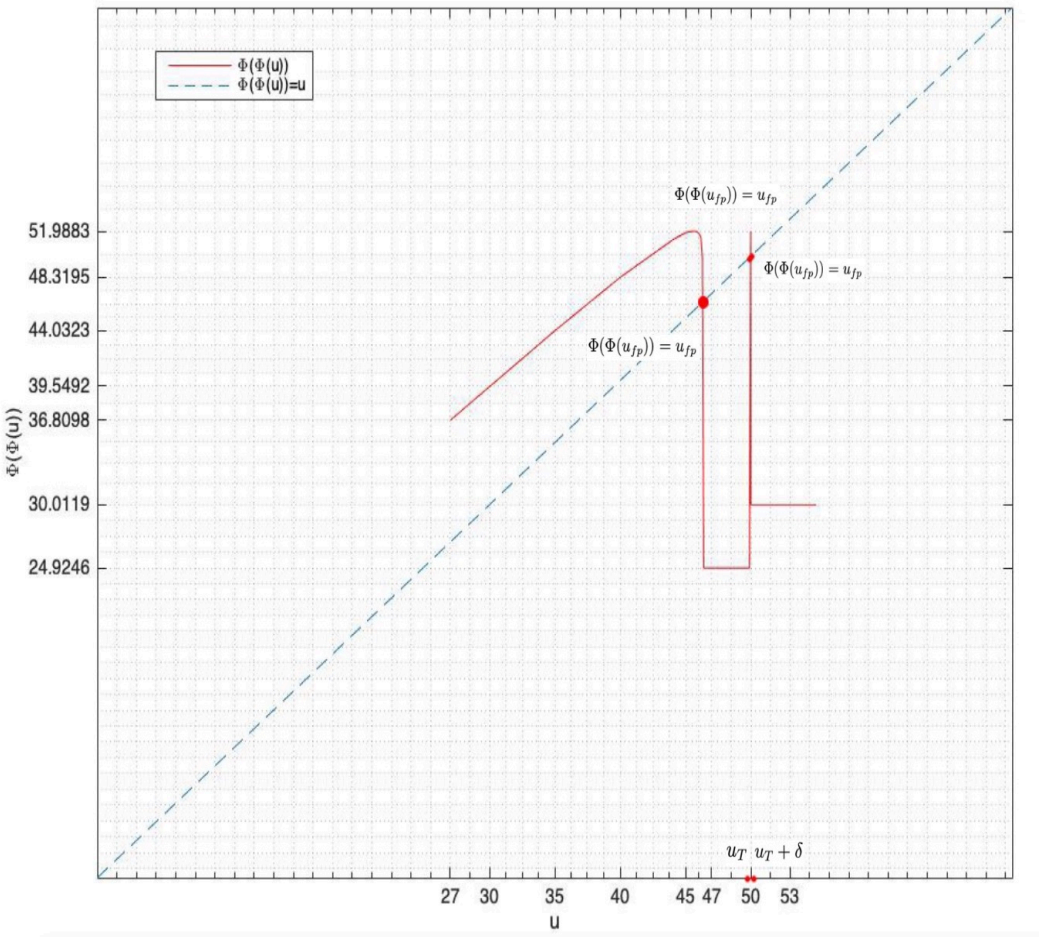

Figure 4.30: The $\Phi(\Phi(u))$ map has three fixed points (all unstable) with $d = 6$.

Now, in order to find the type of bifurcation, we are looking for the $\Phi(\Phi(u))$ map (see Figures 4.30 and 4.31). The second-iterate map $\Phi(\Phi(u)) \equiv \Phi^2(u)$ has three fixed points. The fixed point in the Φ map is unstable with $d = 6$ and the three fixed points in the $\Phi(\Phi(u))$ map are also unstable. Actually, since $0 < \Phi'(u_{fp}) < 1$ for $u_{fp} \in (u_{\star\star}, u_T)$ and $\Phi'(u_{fp}) < -1$ on a subinterval of $[u_T, u_T + \delta]$, we must have $\Phi'(u_{fp}) = -1$ for some $u_{fp} \in [u_T, u_T + \delta]$ and immediately after this value of d, there

exist two stable fixed points and one unstable fixed point in the $\Phi(\Phi(u))$ map. The resulting bifurcation is called a flip bifurcation. Immediately past the flip bifurcation, $\exists$ a stable period-2 orbit of the Φ map, but for a very small range of d, since Φ is so steep, there will be a sequence of further bifurcations and complex behavior but still in a very small range of d[19].

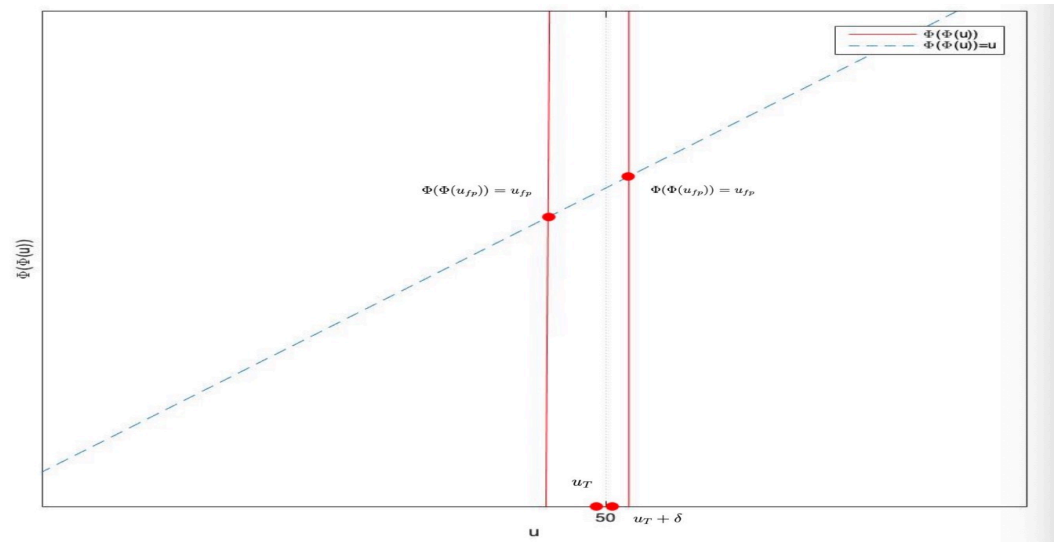

Figure 4.31: The two fixed points in the $\Phi(\Phi(u))$ map when $d = 6$ are very close each other.

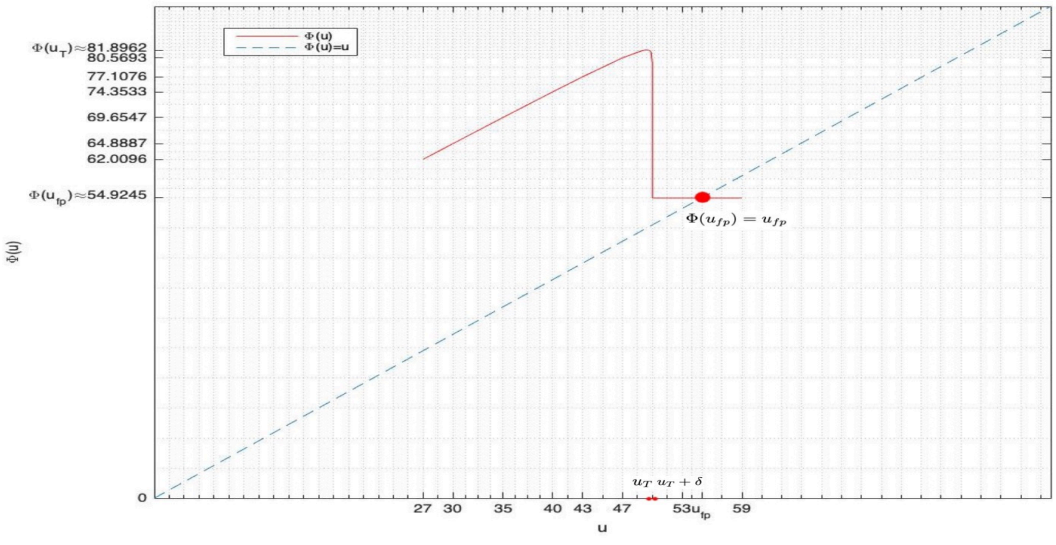

Figure 4.32: When $d = 36$, $\Phi(u_{fp}) = u_{fp} \approx 54.9245 \in (u_T + \delta, +\infty)$, where $u_T + \delta \approx 50.003$. The fixed point is stable because $-1 < \Phi'(u_{fp}) < 0$.

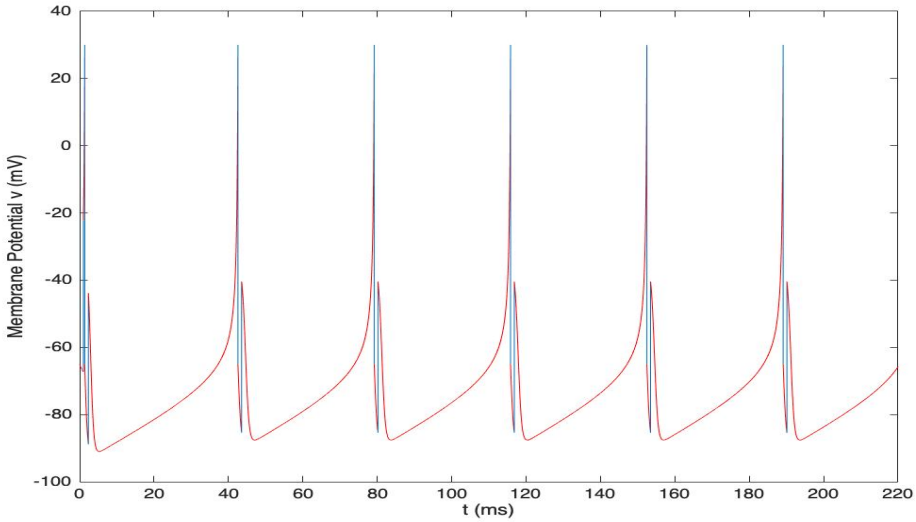

Figure 4.33: When $d = 36$, the Φ map contains the recovery phase. The behavior is a slow tonic firing with one spike per burst (*i.e.*, only one spike occurs between recovery phases).

Case 3: $d = 36$ (see Figures 4.32 and 4.33). Clearly, we can see that $u_T < u_c < u_T + \delta$ in the Figure because $\Phi'(u_{fp})$ is almost 0 for $u_{fp} \in (u_T + \delta, +\infty)$. Thus, $-1 < \Phi'(u_{fp}) < 0$ as $u_{fp} \in (u_c, +\infty)$, so the fixed point $u_{fp} > u_c$ is stable. Since the Φ map contains the recovery phase, we have that the behavior is a slow tonic firing with one spike per burst (*i.e.*, only one spike occurs between recovery phases).

Therefore, we can conclude that if $u_{fp} \in (u_{\star\star}, u_T)$, then the behavior is a fast tonic firing (with infinite number of spikes per burst). If u_{fp} is on a subinterval of $[u_T, u_T + \delta]$, then the behavior is a bursting with k spikes per burst, where $1 < k < \infty$. If $u_{fp} \in (u_c, +\infty)$, then the behavior is a slow tonic firing (with one spike per burst). The unique fixed point u_{fp} changes from stable to unstable and then returns to stable again as $u_{fp} \in (u_{\star\star}, +\infty)$ increases. Then how does the k change when d increases?

4.4.3 The number of spikes in the bursting behavior

For both of the cases below, we define d_i such that (d_{i+1}, d_i) has i spikes per burst, where i=1,2,3... and let $d_1 = \infty$.

4.4.3.1 Case 1: $a \to 0$ and $\tau = 0$

First, we analyze a simpler situation where we can do exact calculations.

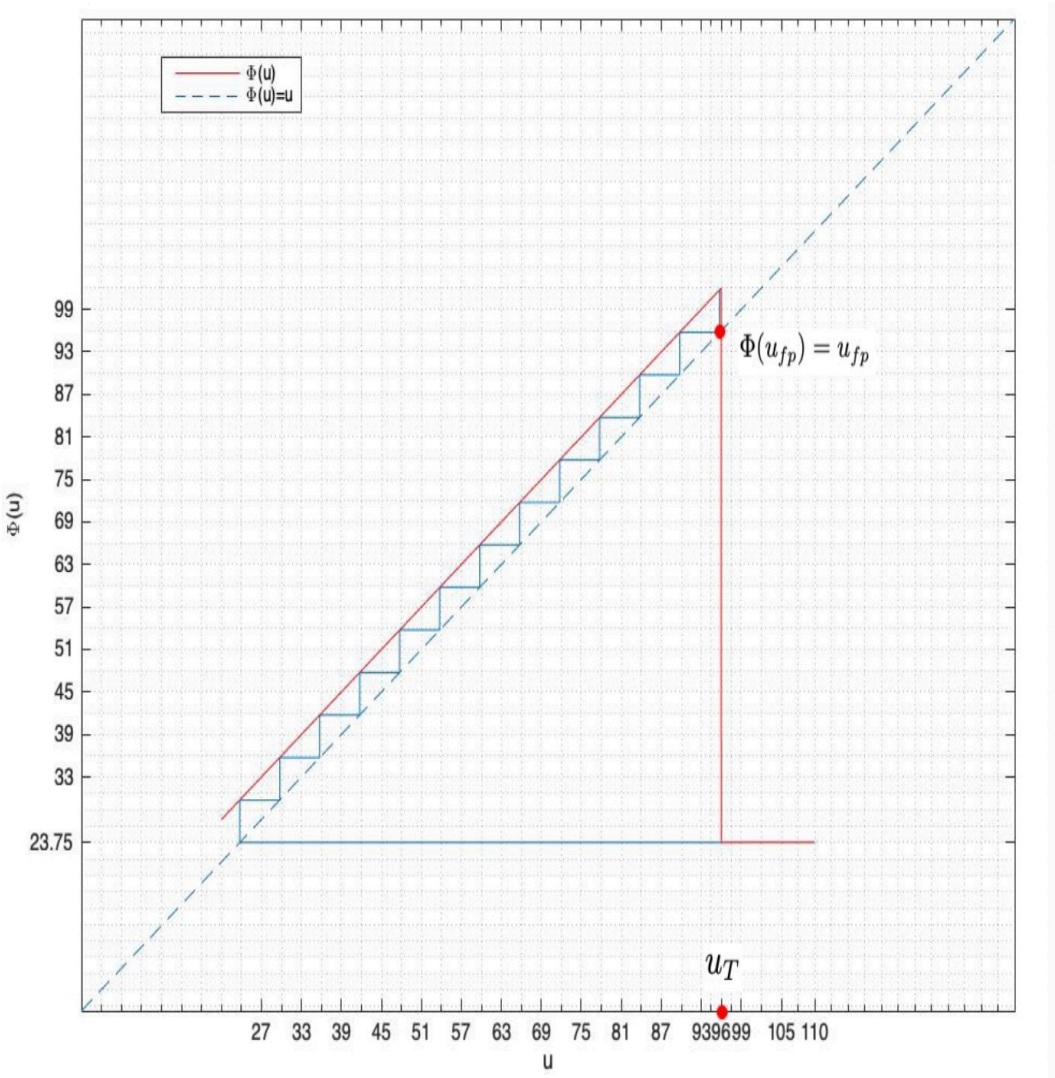

Figure 4.34: When $d = 6$, $a \to 0$ and $\tau = 0$, then $NS = 13$.

This is an easy case because we do not need to worry about the drops in u, so we can count the number of spikes per burst theoretically. Let NS=number of spikes per burst. The delay time $\tau = 0$, so the trajectory "jumps" at the beginning. Effectively, the reset line is shifted to the right by ϵG. Thus, $u_T = 0.04(v_0 + \epsilon G)^2 + 5(v_0 + \epsilon G) + 140 + I$. By applying the typical parameter values $v_0 = -65$, $I = 40$, $\epsilon = 3$ and $G = 15$, we get $u_T = 96$. Since $a \to 0$, we have $u_T = u_3$ and the trajectory does not drop until u_T. For counting NS, we have $NS = \lceil \frac{u_T - u_a}{d} \rceil$ as $a \to 0$ (see Figure 4.34). Clearly, $\lim_{d \to 0} \lceil \frac{u_T - u_a}{d} \rceil \to +\infty$ and $NS = \lceil \frac{u_T - u_a}{d} \rceil = 1$ for $d \geq u_T - u_a$, where u_T and u_a are fixed. Therefore, $NS(d)$ is non-increasing (i.e., if $d_2 > d_1$, then $NS(d_2) \leq NS(d_1)$). Moreover, we have $[d_2, d_1) = [u_T - u_a, \infty) = [72.25, \infty)$, which means if $d \in [d_2, d_1) = [72.25, \infty)$, then $NS = 1$. We have $NS = 2$ for $d \in [d_3, d_2) = [\frac{u_T - u_a}{2}, u_T - u_a) = [36.125, 72.25)$, $NS = 3$ for $d \in [d_4, d_3) = [\frac{u_T - u_a}{3}, \frac{u_T - u_a}{2}) = [24.083, 36.125)$ and $NS = \infty$ for $d = 0$.

4.4.3.2 Case 2: $a = 0.02$ and $\tau = 1$

Now, we return to the original case, and attempt to identify numerically bifurcation points where the number of spikes per burst changes. Although there exists a complex behavior in a tiny range of d_i, it is still a good approximation because Φ is so steep. First, we identify numerically the lowest value of d for which u_{fp} is in $\mathcal{D}$: $d_{\star\star} = 0.9096$ (see definition 8), then d_∞, d_4, d_3, d_2 (see Figures 4.35, 4.36, 4.37, 4.38, 4.39).

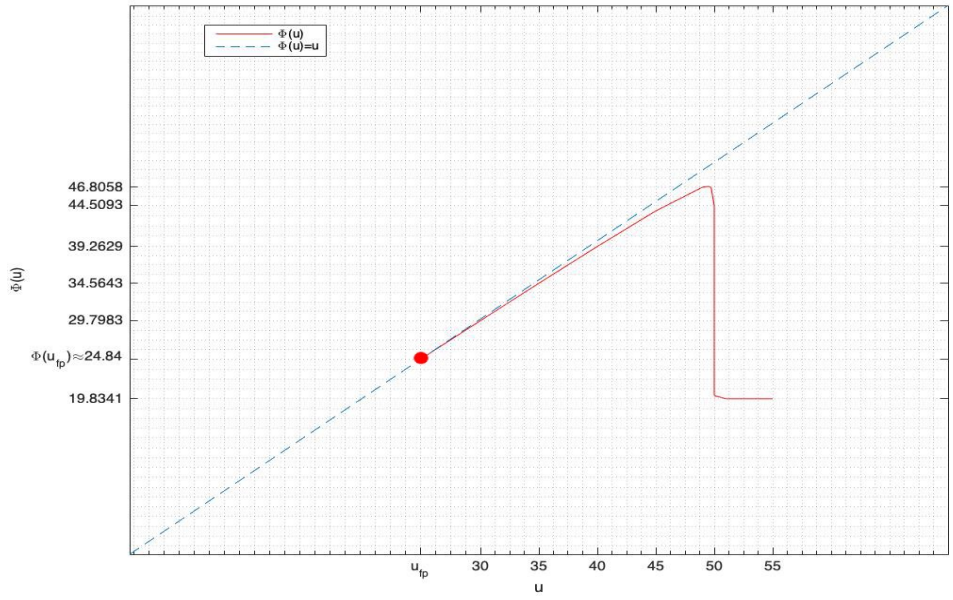

Figure 4.35: $d = 0.9096 = d_{\star\star}$, $u_{fp} = u_{\star\star} \approx 24.84 < u_T$, so the behavior is a fast tonic firing (with infinite number of spikes per burst).

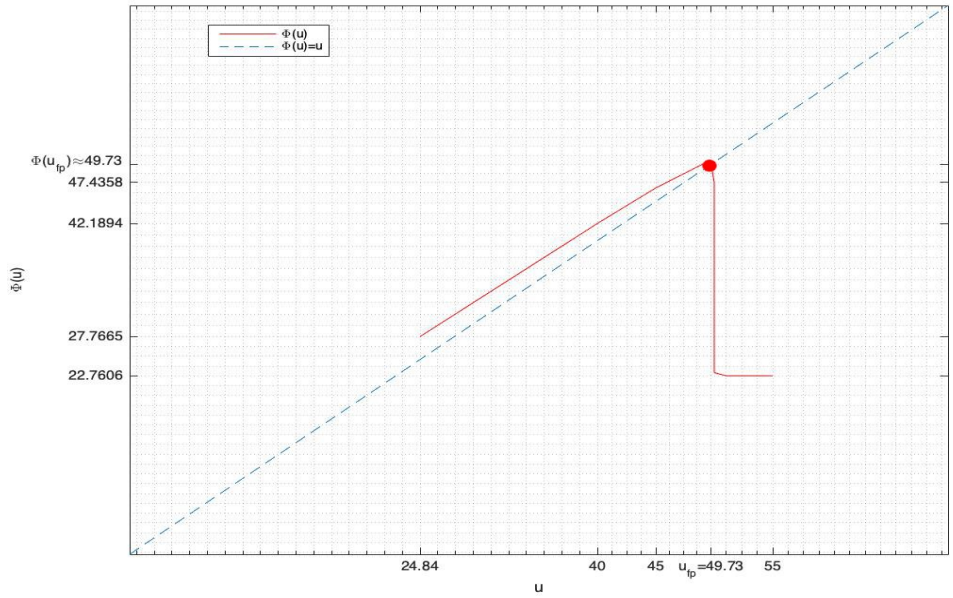

Figure 4.36: $d_\infty = 3.8361$ is the approximate maximum value of d giving ∞ spikes per burst, $u_{fp} \approx u_T \approx 49.73$, so the behavior is also a fast tonic firing (with infinite number of spikes per burst).

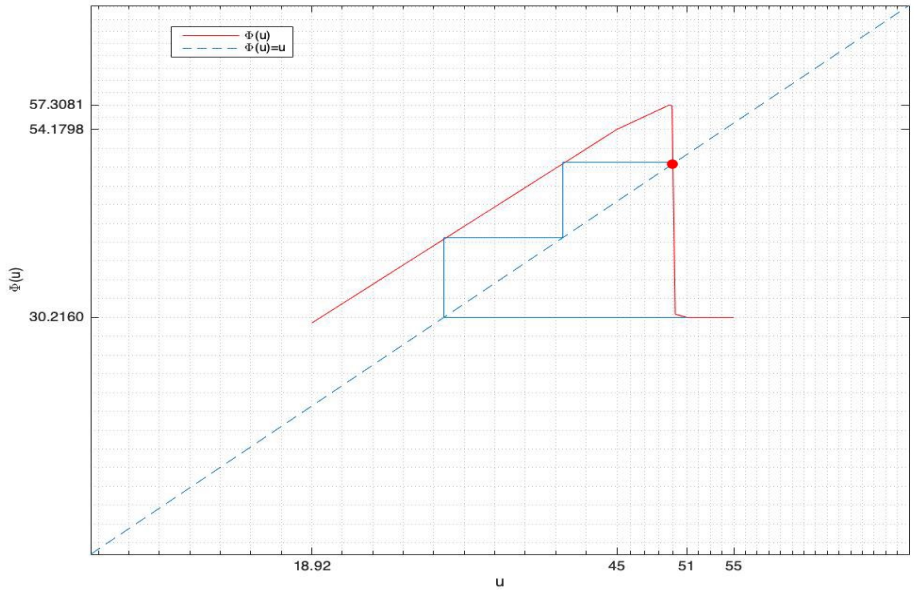

Figure 4.37: $d_4 = 11.2915$ is the approximate minimum value of d giving 3 spikes per burst, $u_{fp} \in [u_T, u_T + \delta]$, so the behavior is a bursting with 3 spikes per burst.

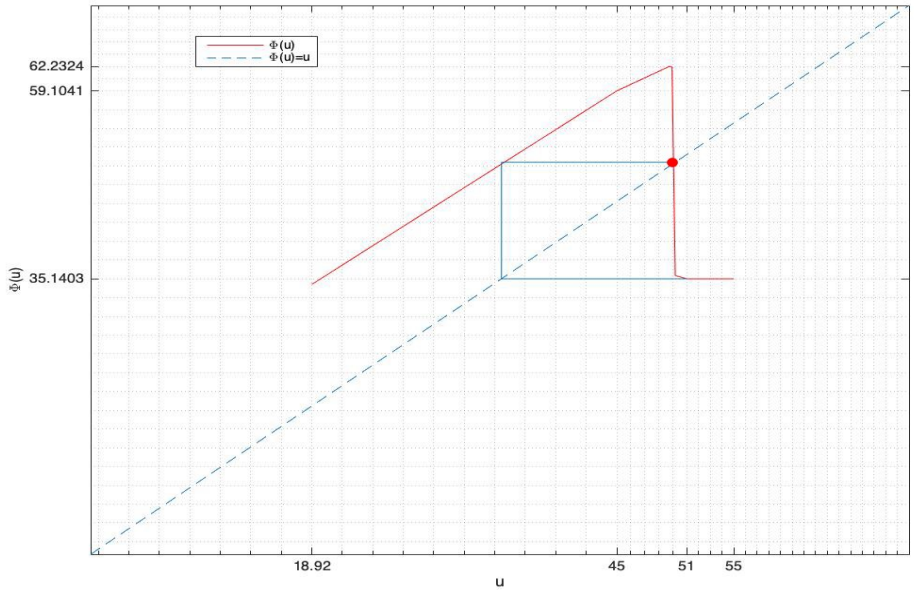

Figure 4.38: $d_3 = 16.2158$, $u_{fp} \in [u_T, u_T + \delta]$, so the behavior is a bursting with 2 spikes per burst.

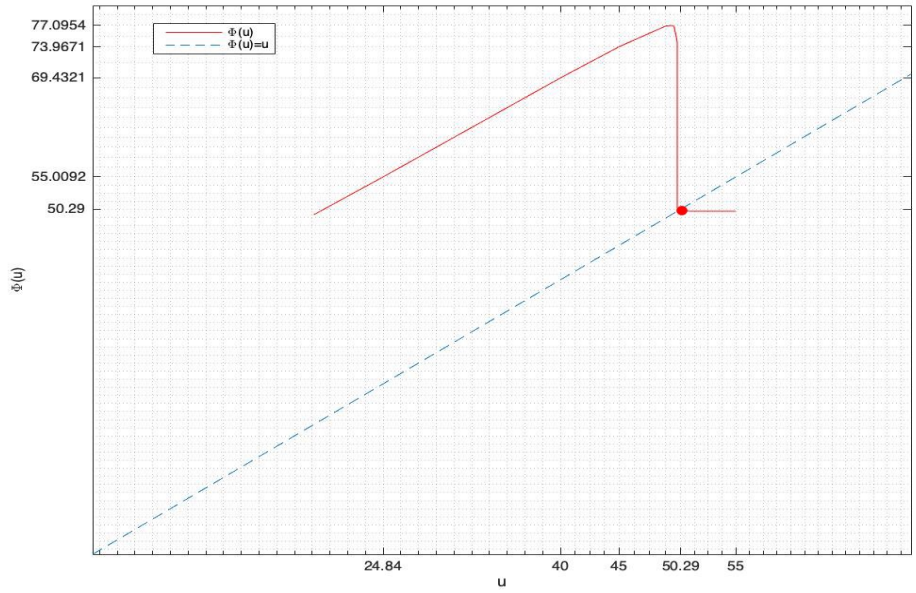

Figure 4.39: $d_2 = 31.0788$, $u_{fp} \approx 50.29 > u_T + \delta \approx 50.003$, so the behavior is a slow tonic firing (with one spike per burst).

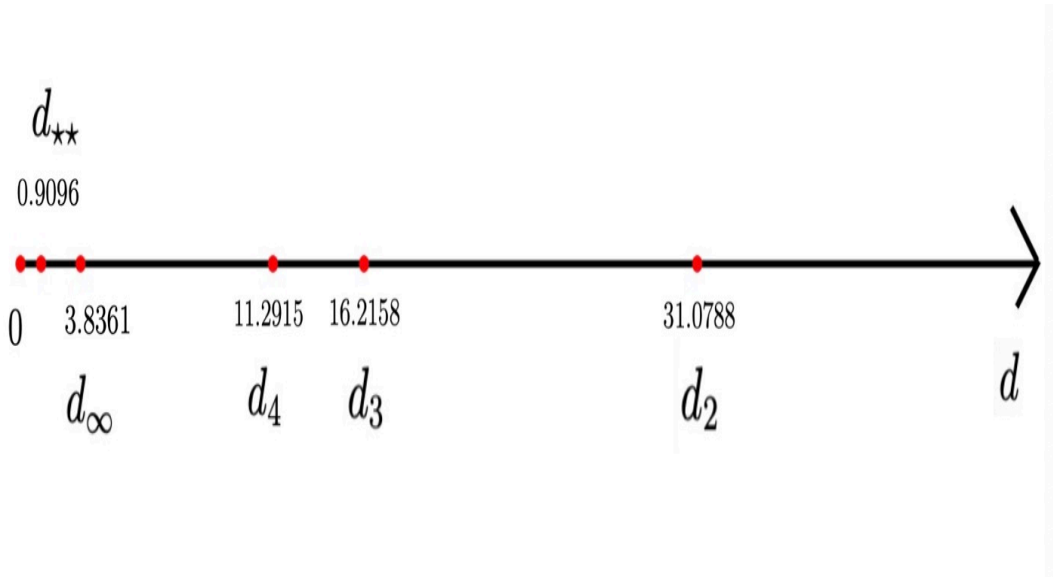

Figure 4.40: NS depends on the range of d.

For case 2, we have $NS = 1$ for $d \in [d_2, d_1) = [31.0788, \infty)$, $NS = 2$ for $d \in [d_3, d_2) = [16.2158, 31.0788)$, $NS = 3$ for $d \in [d_4, d_3) = [11.2915, 16.2158)$ and $NS = \infty$ for

$d \in (d_{\star\star}, d_\infty) = (0.9096, 3.8361)$. To sum up, Table 1 shows that NS increases as d decreases in a similar way but at different values for the two cases.

	d_2	d_3	d_4	d_∞
$a \to 0$, $\tau = 0$	72.25	36.125	24.083	0
$a = 0.02$, $\tau = 1$	31.0788	16.2158	11.2915	3.8361

Table 4.1: Transition points, d_i, between intervals of i and $i-1$ spikes per burst.

Chapter 5

Conclusion

In this thesis we give the Izhikevich model with "jumps" that was obtained by a reduction from the population density equation for the Izhikevich model with a Dirac distribution as an initial condition in the phase space. It is able to reproduce the patten of evolution of the interacting population density equation for the Izhikevich model. We defined a Φ map (the Poincaré map) to analyze this model. We proved that the Φ map has a unique fixed point and $-1 < \Phi'(u_{fp}) < 1$ for $u_{fp} \in (u_{\star\star}, u_T) \cup (u_c, +\infty)$, so u_{fp} is a stable fixed point and $\Phi'(u_{fp}) < -1$ on a subinterval of $[u_T, u_T + \delta]$, so u_{fp} is an unstable fixed point. A stable fixed point of the Poincaré map corresponds to tonic firing of the neuron, either with (slow tonic firing) or without (fast tonic firing) a recovery phase between each spike. When the fixed point is unstable, the uniform tonic firing is unstable.

The numerical simulation confirms that: if $u_{fp} \in (u_{\star\star}, u_T)$, then the behavior is a fast tonic firing (with infinite number of spikes per burst); if u_{fp} is in a sub-interval of $[u_T, u_T + \delta]$, then the behavior is a bursting with k spikes per burst, where $1 < k < \infty$; and if $u_{fp} \in (u_c, +\infty)$, where $u_T < u_c < u_T + \delta$, then the behavior is a slow tonic firing (with one spike per burst). A flip bifurcation occurs where $\Phi'(u_{fp}) = -1$ for some $u_{fp} \in [u_T, u_T + \delta]$, which may leads to a period-doubling cascade and even chaos, but

on a microscopically small interval of the parameter d, before the regular bursting behaviour sets in. NS (number of spikes per burst) increases as d decreases.

This thesis is based on the studies of Modolo, et al. We proved that the reduced model from the population density equation for the Izhikevich model with a Dirac distribution has a bursting behavior. This is an explanation for the numerical results of Modolo, et al, that the neuron interactions cause bursting behavior for the entire population of neurons. Moreover, this mechanism could be relevant to the understanding of tremor oscillations in Parkinson's disease. This study focused on fixed I, ϵ, G, v_0, v_s and Assumption 1 in the theoretical part. Also we fixed the typical parameter values $a = 0.02$, $b = 0.2$, $v_0 = c = -65$, $v_s = 30$, $I = 40$, $\epsilon = 3$, $G = 15$, and the delay time τ=1ms [8] [10] in the numerical simulations. Actually the parameters of the model are of great interest and are key factors in the properties of the fixed point. The mathematical study of variation in parameter values is very rich and would make an interesting topic for future work.

Bibliography

[1] Gillies A and Willshaw D. Models of the subthalamic nucleus: The importance of intranuclear connectivity. *Med Eng Phys*, 26:723–732, 2004.

[2] Omurtag A, Knight BW, and Sirovich L. On the simulation of large populations of neurons. *J Comput Neurosci*, 8:51–63, 2000.

[3] Hodgkin AL and Huxley AF. A quantitative description of membrane current and its application to conduction and excitation in nerve. *J Physiol*, 117:500–544, 1952.

[4] Casti ARR, Omurtag A, Sornborger A, Kaplan E, Knight B, Vitor J, and Sirovich L. A population study of integrate-and-fire-or-burst neurons. *Neural Comput*, 14:957–986, 2002.

[5] Knight BW, Manin D, and Sirovich L. Dynamic models of interacting neuron populations. *in Gerf EC (ed.), Symposium on Robotics and Cybernetics: Computational Engineering in System Applications, Cité Scientifique, Lille, France*, 1996.

[6] Nykamp DQ and Tranchina D. A population density approach that facilitates large-scale modeling of neural networks: Analysis and an application to orientation tuning. *J Comput Neurosci*, 8:19–50, 2000.

[7] E Foxall, R Edwards, S Ibrahim, and P van den Driessche. A contraction argument for two-dimensional spiking neuron models. *SIAM J. Applied Dynamical Systems*, 11:540–566, 2012.

[8] Eugene M Izhikevich. Simple model of spiking neurons. *IEEE Transactions on Neural Networks*, 14:1569–1572, 2003.

[9] Eugene M Izhikevich. *Dynamical Systems in Neuroscience: The Geometry of Excitability and Bursting*. MIT Press, 2010.

[10] Modolo J, Garenne A, Henry J, and Beuter A. Development and validation of a neural population model based on the dynamics of a discontinuous membrane potential neuron model. *J Integr Neurosci*, 6:625–655, 2007.

[11] Modolo J, Henry J, and Beuter A. Dynamics of the subthalamo-pallidal complex in parkinson's disease during deep brain stimulation. *J Biol Phys*, 34:351–366, 2008.

[12] Touboul J and Brette R. Dynamics and bifurcations of the adaptive exponential integrate-and-fire model. *Biol Cybern*, 99:319–334, 2008.

[13] Touboul J and Brette R. Spiking dynamics of bidimensional integrate-and-fire neurons. *SIAM J. Applied Dynamical Systems*, 8:1462–1506, 2009.

[14] Huertas MA and Smith GD. A multivariate population density model of the dlgn/pgn relay. *J Comput Neurosci*, 21:171–189, 2006.

[15] J Modolo, E Mosekilde, and A Beuter. New insights offered by a computational model of deep brain stimulation. *Journal of Physiology-Paris*, 101:56–63, 2007.

[16] Leveque R. *Finite Volumes Methods for Hyperbolic Systems*. Cambridge University Press, 2002.

[17] J Rubin, J Signerska-Rynkowska, J Touboul, and A Vidal. Wild oscillations in a nonlinear neuron model with resets: (i) bursting, spike-adding and chaos. *Discrete and Continuous Dynamical Systems-Series B*, 22:3967–4002, 2017.

[18] J Rubin, J Signerska-Rynkowska, J Touboul, and A Vidal. Wild oscillations in a nonlinear neuron model with resets: (ii) mixed-mode oscillations. *Discrete and Continuous Dynamical Systems-Series B*, 22:4003–4039, 2017.

[19] Strogatz S. *Nonlinear Dynamics And Chaos: With Applications To Physics, Biology, Chemistry, And Engineering.* CRC Press, 2000.

[20] T Wichmann and M DeLong. Deep brain stimulation for neurologic and neuropsychiatric disorders. *Handbook of Behavioral Neuroscience*, 24:971–995, 2016.